

Metop-B GOME Annual In-Flight Performance Report 2014

Doc.No. : EUM/OPS-EPS/REP/14/771772
Issue : v2A
Date : 19 February 2015
WBS/DBS :

EUMETSAT
EUMETSAT-Allee 1, D-64295 Darmstadt, Germany
Tel: +49 6151 807-7
Fax: +49 6151 807 555
<http://www.EUMETSAT.int>

This page intentionally left blank.

Document Change Record

<i>Issue / Revision</i>	<i>Date</i>	<i>Changed Pages / Paragraphs</i>
v1	06 October 2014	First issue
V1C	15 October 2014	Updated draft after internal review
V1D	31 October 2014	Updated following discussion during Annual review 2014
V2	03 February 2015	Final issue
V2A	19 February 2015	Document template updated (no content changes)

Table of Contents

1	Introduction	8
1.1	Purpose and Scope	8
1.2	Document Structure.....	8
1.3	Applicable Documents.....	9
1.4	Reference Documents.....	9
1.5	Additional Information.....	9
1.6	Open Issues.....	9
2	Overview of Instrument Main events	10
2.1	Event Categorisation	10
2.2	Chronology of Main Events	12
2.3	Event Details.....	13
2.3.1	Routine.....	13
2.3.2	External.....	15
3	Operational Availability and Outage Statistics	16
3.1	Instrument Outages	16
3.2	Operative Modes Budget.....	17
4	Anomaly and Non-Conformance Reports	18
4.1	AR and NCR Overview	18
4.2	Anomalies during Idle Mode (AR.13557)	18
4.3	Anomalies during Timeline Execution (AR.13556).....	18
4.4	Signal issue in the measurements used to derive GOME-202 slit function. (AR.14395) ..	19
4.5	Throughput test observation during GOME-2 MetopB SIOV (AR.14439).....	19
4.6	Anomalies During CAL0 Timeline Execution (AR.14442)	19
4.7	Scan-angle dependent offset in reflectivity (AR.14557)	19
4.8	GOME-2 FM2 leakage current increase in band 4 (channel 4) (AR.14946)(AR.15205)...	19
4.9	GOME SU behaviour at static mirror positions (AR.15517)	20
5	Functional Performance Assessment and Trending	21
5.1	Analysis Method description.....	21
5.2	Physical Signature Synopsis	23
5.3	GOM01: HKTM Stability	25
5.3.1	Description.....	25
5.3.2	Analysis.....	25
5.3.3	Interpretation.....	26
5.3.4	Assessment	30
5.4	GOM02: SU Bearings Monitoring	30
5.4.1	Description.....	30
5.4.2	Analysis.....	31
5.4.3	Interpretation.....	32
5.4.4	Related Anomalies.....	35
5.4.5	Assessment	38
5.5	GOM03: HCL and QTH Lamps Monitoring	38
5.5.1	Description.....	38
5.5.2	Analysis.....	38
5.5.3	Interpretation.....	39
5.5.4	Assessment	45
5.6	GOM04: Detector response stability	45
5.6.1	Description.....	45
5.6.2	List of Correlated Events	45
5.6.3	Analysis.....	46
5.6.4	Interpretation.....	46
5.6.5	Assessment	47
5.7	GOM05: Spectral Stability	47
5.7.1	Description.....	47
5.7.2	List of Correlated Events	47
5.7.3	Analysis.....	48

5.7.4	Interpretation.....	49
5.7.5	Assessment.....	53
5.8	GOM06: Throughput Stability.....	54
5.8.1	Description.....	54
5.8.2	List of Correlated Events.....	54
5.8.3	Analysis.....	54
5.8.4	Assessment.....	59
5.9	GOM07: Darksignal.....	60
5.9.1	Description.....	60
5.9.2	List of Correlated Events.....	60
5.9.3	Analysis.....	60
5.9.4	Interpretation.....	61
5.9.5	Assessment.....	68
5.10	Physical Signatures Conclusion.....	69
6	Operational Configuration and Evolution Plan.....	70
6.1	HW Component Configuration.....	70
6.2	Lifetime Limited Items.....	71
6.3	SW Configuration and Evolution Plan.....	72
6.3.1	Timelines and Onboard Tables.....	73
6.4	Operational Documentation Status.....	73
7	Conclusion.....	74

List of Tables

Table 1-1: Open Issue.....	9
Table 2-1: Overview of Significant Events	12
Table 2-2 Moon calibrations during the reporting period	13
Table 2-3 OOP Manoeuvres during the reporting period.....	14
Table 2-4 IP Manoeuvres during the reporting period	14
Table 2-5 Geometric Events during the reporting period.....	15
Table 3-1: Instrument Outage Breakdown	16
Table 4-1: Anomaly and Non-Conformance Report Overview	18
Table 5-1: Physical Signatures Synopsis.....	23
Table 5-2 GOME Wavelength Range per Pixel for all main channels.....	48
Table 5-3: List of Correlated Events	60
Table 5-4 GOME Wavelength Range per Pixel for all main channels.....	61
Table 6-1: HW Component Performance and Configuration.....	70
Table 6-2 GOME-2 Software Versioning	72
Table 6-3: Onboard Tables Configuration.....	73

List of Figures

Figure 3-1: Timelines executed aboard Metop-B 01-Sep-2013 to Aug-31-2014.....	17
Figure 3-2: Timeline status during the reporting period	17
Figure 5-1: Test Unit Breakdown	22
Figure 5-2 GOME ICU Power since launch	26
Figure 5-3 GOME EQ Power since launch	27
Figure 5-4 GOME Optical Bench Temperature since launch	27
Figure 5-5 GOME Optical Bench Temperature comparison with M02	28
Figure 5-6 GOME FPA Detector Temperatures since launch	28
Figure 5-7 GOME FPA Peltier Output since launch	29
Figure 5-8 GOME PMD-s Temperature since launch.....	29
Figure 5-9 GOME Analogue Board Offset (blue) and Gain Value (red) during the reporting period.....	30
Figure 5-10: Typical GOME SU Torque Profile over a 6s 1920km swath scan cycle. Areas in yellow are considered scan extremities and are assessed separately. (Data from Metop-A)	31
Figure 5-11: GOME SU Position Error Evolution since launch.....	33
Figure 5-12: GOME SU Torque Evolution.	34
Figure 5-13: GOME SU monitoring of "high" torque values >20mNm during daily spinning (blue), and max torque value reported (red) with limits (dashed).....	35
Figure 5-14: Comparison of count of torque values >20mNm during spinning, by calendar week, of Metops A and B.	36
Figure 5-15: Maximum duration of torques >20mNm at the start of spinning in seconds.	37
Figure 5-16: Comparison of the maximum torque reported at the start of spinning by M01 and M02, with rolling average.	37
Figure 5-17: GOME HCL Ignition Time since launch.....	39
Figure 5-18: GOME HCL Activation Voltages since launch.....	39
Figure 5-19: Upper panel: Change in instrument throughput around 570 nm for SLS signal. SLS is smoothed with the spectral response function of PMDs in black and with a moving average in blue for main channel data. SLS data for PMD P and S are plotted in red and green respectively. Lower panel: The same but for SMR, WLS and LED.....	40
Figure 5-20 GOME QTH Voltage.....	41
Figure 5-21: GOME WLS to SMR ratio normalised to January 2007 for all Main Channels.	43
Figure 5-22: GOME WLS v SMR Throughput for PMD Channels (Upper pane PMD-P, lower panel PMD-S). Note, the etalon structure for PMD-S is an artefact of an anomaly introduced at the 28 th of November 2012 and resolved at the 21 st December 2012 in the on-ground processing. It can only be resolved by reprocessing of the full archive.	44
Figure 5-23: Time series of PPG standard deviation over the channel in all four main channels (red: channel 1, blue: channel 2, green: channel 3, black: channel 4).....	46

Figure 5-24: Time series of PPG standard deviation over the channel in PMD channels (red: PMD-P, blue: PMD-S).....	47
Figure 5-25: Spectral stability at various wavelengths between November 2012 and October 2013 and for main channels and PMD channels at 275, 309, 310, 330, 380 and 420 nm. The initial step functions are due to thermal environment changes during IOV, the second step function during 2 weeks in March 2013 is due to the darkness-test and the slight thermal environment change then. There is a step function visible at the end of channel 2 starting end of January for both 2013 and 2014 at 330 and 380 nm which is due to changing polynomial solutions in different OB regimes.....	49
Figure 5-26: Same as Figure 5-25 but at 570 and 745 nm.....	50
Figure 5-27 Spectral stability of the co-registration between PMD-P and S in percentage of fractional detector pixel around 311 and 745 nm.....	50
Figure 5-28: Signal strength of 380 nm spectral line.....	51
Figure 5-29: FWHM relative change with respect to November 2012 evaluated from a regular Gaussian fitting of well separated SLS lines. Upper panel shows the results in channel 1 and 2. The lower panel results for channel 3 and 4.....	52
Figure 5-30: Difference of the centre line position with respect to November 2012 evaluated from a regular Gaussian fitting of well separated SLS lines. Upper panel shows the results in channel 1 and 2. The lower panel results for channel 3 and 4.....	53
Figure 5-31: Signal degradation of SMR, SLS, WLS and LED sources at 275 nm in channel 1 (LED at approx. 570 nm) normalised to the 1 st of December 2012.....	55
Figure 5-32: Signal degradation (SMR ratio values; see legend) of GOME-2 FM2 (blue line) and FM3 (red line) over a period of 547 days and after both instruments have been in-orbit for 102 days.....	55
Figure 5-33: Same as Figure 5-32 but for PMD-P (left panel) and PMD-S (right panel) respectively...	56
Figure 5-34: Signal degradation for LED (ratio values; see legend) of GOME-2 FM2 (blue line) and FM3 (red line) over a period of 500 days and after both instruments have been in-orbit for 102 days.....	56
Figure 5-35: Same as Figure 5-34 but for PMD-P (left panel) and PMD-S (right panel) respectively...	57
Figure 5-36: Signal evolution for selected wavelength for GOME-2 Metop-B (solid line) based on version 0.9 of the signal degradation model for Metop-A (dashed line). The projection is based on the signal evolution of the pre Second throughput test period of Metop-A. Left panel: Earthshine signal averaged over all viewing directions. Right panel: Solar mean reference signal. For details see text.....	58
Figure 5-37: Same as Figure 5-36 but for the reflectivity. The dashed line shows the forecasted projection.....	59
Figure 5-38: Band 1A averaged electronic offset (blue dots) and leakage current (green dots).....	61
Figure 5-39: Band 1B averaged electronic offset (blue dots) and leakage current (green dots).....	62
Figure 5-40: Band 2B averaged electronic offset (blue dots) and leakage current (green dots).....	62
Figure 5-41: Band 3 averaged electronic offset (blue dots) and leakage current (green dots).....	63
Figure 5-42: Band 4 averaged electronic offset (blue dots) and leakage current (green dots). The sudden increase and recovery during July/August 2013 and November to January 2013/2014 is covered by AD5. Note the difference in Leakage current scale.....	63
Figure 5-43: PMD-P averaged electronic offset (blue dots) and leakage current (green dots).....	64
Figure 5-44: PMD-S averaged electronic offset (blue dots) and leakage current (green dots).....	64
Figure 5-45: Band 1A averaged noise.....	65
Figure 5-46: Band 1B averaged noise.....	65
Figure 5-47: Band 2B averaged noise.....	66
Figure 5-48: Band 3 averaged noise.....	66
Figure 5-49: Band 4 averaged noise.....	67
Figure 5-50: PMD-P averaged noise. Due to an ingestion problem in the operational database, noise levels before April 2014 are unfortunately not available for PMDs.....	67
Figure 5-51: PMD-S averaged noise. Due to an ingestion problem in the operational database, noise levels before April 2014 are unfortunately not available for PMDs.....	68
Figure 6-1: Life-limited Item Usage to Sep 2014.....	71

1 INTRODUCTION

1.1 Purpose and Scope

After two years of operations, the Metop-B satellite is in a routine operational phase. The health and performance of various functions of each instrument is assessed both to report on the performance during the reporting period and provide indications of degradations which may affect instrument performance with respect to the baseline assumption of a mission duration of 12 years.

By assessment of instrument functional performance, cumulative life limited item usage and instrument outage during the reporting period, these reports are also used to trigger any necessary operational changes, software updates or studies which will be required to maximise instrument performance and life time both for this spacecraft and future recurrent spacecraft.

The main reporting cycle is typically September-August, with a draft version of the report generated in September and reviewed during a formal In-flight performance review held in October. This review includes representatives from EUMETSAT Operations, EUMETSAT Program Development, SSST and Industry or Cooperating Agencies. A shorter mid-term review is also typically held in the Second quarter of the year.

This report covers the period from 2013-09-01 to 2014-09-01.

1.2 Document Structure

This document is structured in eight sections as follows:

- Section 1: General introduction presenting purpose, scope and structure of this document, the list of applicable and reference documents and the open issues contained in this document.
- Section 2: Presentation of all events in the reporting period, according to the four event categories anomaly, routine, operational request and external.
- Section 3: Statistics on the duration and cause of outages and on the operational mode budgets.
- Section 4: Discussion of all open anomaly and non-conformance reports.
- Section 5: Assessment of the in-flight performance, providing sufficient data and analysis as is necessary to conclude on the behaviour and trending over the period of the report.
- Section 6: Operational configuration and evolution plan of hardware, software, documentation, procedures and database. Status of lifetime limited items.
- Section 7: Conclusion summarising the trending results and providing operational recommendation if any.

1.3 Applicable Documents

<i>Number</i>	<i>Document Name</i>	<i>EUMETSAT Reference Number</i>
<i>AD 1</i>	GOME-2 Instrument Operations Manual	MO.MA.ESA.GO.0304
<i>AD 2</i>	GOME-2 Metop-A and Metop-B Tandem Operations and Dark Test - Detailed Proposal	EUM/RSP/TEN/13/692007
<i>AD 3</i>	GOME-2 / Metop-B Product Validation Report	EUM/OPS-EPS/DOC/12/0760
<i>AD 4</i>	EPS Metop-B GOME SIOV Operations Implementation Plan	EUM/OPS-EPS/PLN/11/0273
<i>AD 5</i>	EPS Metop-B GOME-2 Channel 4 Dark Current Increase	EUM/TSS/TEN/13/715650
<i>AD 6</i>	MetOp B GOME 202 Anomaly 15102 (SU torque anomaly)	MO-TN-ESA-GO-1115

1.4 Reference Documents

<i>Number</i>	<i>Document Name</i>	<i>EUMETSAT Reference Number</i>
<i>RD 1</i>	GOME-2 L1 Product Generation Specification	EPS.SYS.SPE.990011,(v.6.1)
<i>RD 2</i>	EPS Metop-B product validation report: GOME-2 level 1	EUM/OPS-EPS/DOC/12/0760
<i>RD 3</i>	GPDU FM3 electrical test report	MO-TR-FIN-GO-647
<i>RD 4</i>	Metop-B / GOME-2 PMD band definitions and PMD calibration	EUM/OPS-EPS/DOC/12/0714

1.5 Additional Information

This report, other reports and additional information are available on the EPS OPS Extranet at <http://www.EUMETSAT.int/OPS-OPS-Extranet/>

1.6 Open Issues

<i>Issue</i>	<i>Section</i>	<i>Description</i>	<i>Due Date</i>	<i>Status</i>
		None		

Table 1-1: Open Issues

2 OVERVIEW OF INSTRUMENT MAIN EVENTS

In this section, the main events that have impacted the instrument over the reporting period are presented. These events are categorised to allow easier assessment of instrument and system performance. Also, instrument and mission outage are distinguished. For the GOME instrument, for example, the instrument is fully recovered after a switch off when the PMD flight line is selected and dale resistor relay disabled. However, the mission outage extends until L1 data dissemination resumes after quality checks have been made.

2.1 Event Categorisation

The events and activities are categorized into four categories. These categories have been further broken down into classes as follows:

Anomaly	This category is for those activities/events that are the result of an instrument-specific anomaly. It is broken down into the following classes:
<i>SEU/MEU</i>	anomalies where the root cause is a single- or multiple-event-upset affecting the software or software registers of the instrument
<i>SET</i>	a single-event-transient affecting the physical state of a relay or other equipment of the instrument
<i>OB Monitoring</i>	anomalies caused by on-board limit exceptions
<i>OG Monitoring</i>	anomalies detected by on-ground monitoring
<i>Software</i>	anomalies caused by incorrect behaviour of the OB software, if not caused by SEU/MEU and SET
<i>Hardware</i>	anomalies caused by unexpected hardware behaviour
<i>Other</i>	anomalies without a clearly identified cause, hardware failures requiring reconfiguration, and anomaly reports raised on unexpected behaviour

Routine	This category is for those activities/events that are of routine nature. It is broken down into the following classes:
<i>OOP</i>	for out-of-plane manoeuvres all instruments must be put into a safe configuration
<i>IP</i>	for in-plane manoeuvres some instruments must be put into a safe configuration in-plane manoeuvre
<i>Calibration</i>	for routine instrument calibration activities
<i>Other</i>	any other routine activities

Operational Requests	This category is for special activities initiated at the request of operational entities, It is broken down into the following classes:
<i>Calibration</i>	requests for special instrument calibration activities
<i>SW Maintenance</i>	requests for modifications of the onboard software
<i>HW Maintenance</i>	requests for modifications of the onboard hardware
<i>Onboard Tables</i>	requests to update on-board tables to tune instrument performance
<i>Timelines</i>	requests to update operational timelines
<i>Tandem Ops</i>	requests to update onboard sequence or timeline activations to support the two spacecraft working in tandem, with one in a reduced swath-width configuration

External	This category is for those activities/events that are external to the instrument but still have an impact. It is broken down into the following classes:
<i>PL-SOL</i>	PL-SOL is a spacecraft anomaly external to the instrument but still resulting in a switch off of the instrument
<i>PLM</i>	PLM operations or anomalies that cause outages
<i>NIU</i>	NIU operations or anomalies that cause outages, only applicable to NIU instruments
<i>FDS</i>	related to space mechanics events, e.g. ANX, Eclipse, etc.
<i>[Instrument]</i>	related to other instrument, e.g. <i>GOME-2</i> , <i>ASCAT</i> , <i>IASI</i> , etc.
<i>Other</i>	any other external influence

2.2 Chronology of Main Events

This table reports relevant main events during the reporting period.

<i>Date UTC yyyy-mm-dd hh:mm:ss</i>	<i>Category</i>	<i>Event Title</i>	<i>Description</i>	<i>Class</i>	<i>Reference</i>	<i>Instrument Outage</i>	<i>Mission Outage</i>
2013-09-24 08:37:28	Routine	Mooncal	September 2013 Mooncal	Calibration		N/A	N/A
2013-10-28 ... 2014-02-02	Anomaly	Dark signal anomaly	leakage current increase in band 4 (channel 4) -Reoccurrence	Hardware	AR15205	N/A	N/A
2013-10-24 06:39:11	Routine	Mooncal	October 2013 Mooncal	Calibration		N/A	N/A
2013-10-29 07:19:23	External	EUM/OPS/AR/15129	Outage due to SSR LTC_ANALOGUE_VERIFICATION_ERROR	Other	AR15129	nil	03:20:00
2013-11-05 11:32:23	Routine	Out of Plane Manoeuvre	Safing Action: Mirror Parked	OOP	OOP 01	01:41:21	01:41:21
2013-11-22 20:13:10	Routine	Mooncal	November 2013 Mooncal	Calibration		N/A	N/A
2013-12-22 16:31:02	Routine	Mooncal	December 2013 Mooncal	Calibration		N/A	N/A
2014-02-19 11:38:16	Routine	In Plane Manoeuvre	Safing Action: Mirror Parked	IP	IP 06	01:41:21	01:41:21
2014-04-29 11:01:30	Routine	In Plane Manoeuvre	Safing Action: Mirror Parked	IP	IP 07	01:41:22	01:41:22
2014-05-25 13:42:59	Routine	MIAMI Manoeuvre	Safing Action: Mirror Parked	IP	IP 08	01:41:22	01:41:22
2014-07-23 11:39:59	Routine	In Plane Manoeuvre	Safing Action: Mirror Parked	IP	IP 09	01:41:22	01:41:22
2014-06-02 12:06:40	External	EUM/OPS/AR/15532	GEANT and Fibre Link down the same time, data half available due to ADA dump	Other	AR15532	02:30:24	02:30:24
2014-06-10 20:06:00	External	EUM/OPS/AR/15555	CDA1 ACU failure	Other	AR15555	01:42:00	01:42:00
2014-08-15 03:03:41	Routine	Mooncal	August 2014 Mooncal	Calibration		N/A	N/A
2014-08-20...ongoing	Anomaly	Dark signal anomaly	leakage current increase in band 4 (channel 4) -Re-occurrence	Hardware	AR15205	N/A	N/A

Table 2-1: Overview of Significant Events

2.3 Event Details

This section expands on the details of events, especially those which have had an impact on instrument performance.

Note: For the categories Anomaly and Operational Request, there were no outages during the reporting period.

2.3.1 Routine

2.3.1.1 Calibration

Most GOME-2 calibration measurements are handled in the routine cycle of timeline activations and so are not mentioned in this report. The exception to this is the Moon calibration. Whenever an opportunity arises, the scan mirror is directed such that the Moon will enter the field of view so that it can be used as a calibration source. Moon calibrations occur on a synodic period (approximately 29 days) throughout the year, except January-June.

Moon calibrations only ever occur on the dark side of the orbit, so do not result in a mission outage – shortened timelines are used which leave most of the night side of the orbit free. Moon opportunities occur on several successive orbits and so it is not necessary to miss daily calibrations. Also, Moon calibration opportunities are linked to the synodic period, which is nearly at the same frequency as the 412 orbit repeat cycle, so clashes with the monthly calibration sequence are a once per mission event. As a result of this, Moon calibrations have no impact on other aspects of the mission.

The table below indicates the start dates of Moon calibration campaigns during the reporting period.

<i>Date UTC yyyy-mm-dd</i>	<i>Category</i>	<i>Event Title</i>	<i>Description</i>	<i>Class</i>	<i>Instrument Outage</i>	<i>Mission Outage</i>
2013-09-24	Routine	Mooncal	September 2013 Mooncal	Calibration	N/A	N/A
2013-10-24	Routine	Mooncal	October 2013 Mooncal	Calibration	N/A	N/A
2013-11-22	Routine	Mooncal	November 2013 Mooncal	Calibration	N/A	N/A
2013-12-22	Routine	Mooncal	December 2013 Mooncal	Calibration	N/A	N/A
2014-08-15	Routine	Mooncal	August 2014 Mooncal	Calibration	N/A	N/A

Table 2-2 Moon calibrations during the reporting period

2.3.1.2 Out-Of-Plane Manoeuvre

Out-of-plane (OOP) manoeuvres are required in-frequently to maintain the orbit of Metop within the requirements. The current orbit maintenance strategy foresees one OOP manoeuvre at the autumn equinox per year. This may consist of one or two burns and is usually followed by an In-Plane “touch-up” manoeuvre.

Since the start of tandem operations (July 2013), all GOME timelines end with the mirror parked internally (launch position) with all lamps off and the diffuser closed. For the orbit on which the OOP occurs, GOME is safed by simply not issuing a “timeline activate” command, thereby leaving GOME in this configuration. As a result, there is a 1 orbit outage for GOME.

<i>Date UTC yyyy-mm-dd hh:mm:ss</i>	<i>Category</i>	<i>Event Title</i>	<i>Description</i>	<i>Reference</i>	<i>Instrument Outage</i>	<i>Mission Outage</i>
2013-11-05 11:32:23	Routine	Out of Plane Manoeuvre	Safing Action: Mirror Parked	OOP 01	01:41:21	01:41:21

Table 2-3 OOP Manoeuvres during the reporting period

2.3.1.3 In-Plane Manoeuvre

In Plane (IP) manoeuvres are required in-frequently to maintain the Metop ground track, avoid debris in case of conjunction warnings (MIAMI) and to “touch-up” the orbit after an OOP. During the reported period there were six IP manoeuvres performed.

As with the Out Of Plane manoeuvres described above, for the orbit on which the IP occurs, GOME is safed by not issuing a “timeline activate” command. As a result, there is a 1 orbit outage for GOME.

<i>Date UTC yyyy-mm-dd hh:mm:ss</i>	<i>Category</i>	<i>Event Title</i>	<i>Description</i>	<i>Reference</i>	<i>Instrument Outage</i>	<i>Mission Outage</i>
2014-02-19 11:38:16	Routine	In Plane Manoeuvre	Safing Action: Mirror Parked	IP 06	01:41:21	01:41:21
2014-04-29 11:01:30	Routine	In Plane Manoeuvre	Safing Action: Mirror Parked	IP 07	01:41:22	01:41:22
2014-05-25 13:42:59	Routine	MIAMI Manoeuvre	Safing Action: Mirror Parked	IP 08	01:41:22	01:41:22
2014-07-23 11:39:59	Routine	In Plane Manoeuvre	Safing Action: Mirror Parked	IP 09	01:41:22	01:41:22

Table 2-4 IP Manoeuvres during the reporting period

2.3.2 External

This category is for those activities/events that are external to the instrument but still have an impact.

2.3.2.1 PL-SOL

PL-SOLs cause a switch down of the entire payload module and instruments. During the reporting period, one PL-SOL occurred. The outage for GOME is mainly due to the time required to re-upload software and regain thermal stability.

Note: There were no PL-SOLs during the reporting period.

2.3.2.2 FDS

This category includes events that are due to geometric events. During the reporting period, the only such events were eclipses of the sun by the moon.

<i>Date UTC yyyy-mm-dd hh:mm:ss</i>	<i>Category</i>	<i>Event Title</i>	<i>Description</i>	<i>Class</i>	<i>Instrument Outage</i>	<i>Mission Outage</i>
2013-11-03 10:55:33	External	Sun Eclipse by the Moon	General Temperature Reduction	FDS	none	none
2014-04-29 05:05:20	External	Sun Eclipse by the Moon	General Temperature Reduction	FDS	none	none

Table 2-5 Geometric Events during the reporting period

3 OPERATIONAL AVAILABILITY AND OUTAGE STATISTICS

3.1 Instrument Outages

Table 3-1 details the mission outages in the reporting period.

<i>CAT.</i>	<i>CLASS</i>	<i>Instrument Outage %</i>	<i>Mission</i>	<i>EVENT / DESCRIPTION</i>	<i># OF</i>	<i>CUMULATIVE outage (DAYS)</i>
<i>Anomaly</i>	SEU/MEU	0.00	0.00	None	0	00 days 00:00
	SET	0.00	0.00	None	0	00 days 00:00
	Software	0.00	0.00	None	0	00 days 00:00
	OB Monitoring	0.00	0.00	None	0	00 days 00:00
	OG Monitoring	0.00	0.00	None	0	00 days 00:00
	Other	0.00	0.00	None	0	00 days 00:00
	SUBTOTAL	0.00	0.00		0	00 days 00:00
<i>Routine</i>	Calibration	0.00	0.00	Mooncal does not cause outage	0	00 days 00:00
	OOP	0.02	0.02	Safing action for manoeuvre	1	00 days 01:41
	IP	0.08	0.08	Safing action for manoeuvre	4	00 days 06:45
	Other	0.00	0.00	None	0	00 days 00:00
	SUBTOTAL	0.10	0.10		5	00 days 08:27
<i>Request</i>	Calibration	0.00	0.00	None	0	00 days 00:00
	SW Maintenance	0.00	0.00	None	0	00 days 00:00
	HW Maintenance	0.00	0.00	None	0	00 days 00:00
	Timeline Update	0.00	0.00	None	0	00 days 00:00
	Onboard Table Update	0.00	0.00	None	0	00 days 00:00
	SUBTOTAL	0.00	0.00		0	00 days 00:00
<i>INS</i>	TOTAL	0.10	0.10		5	00 days 08:27
<i>External</i>	PL-SOL	0.00	0.00	None	0	00 days 00:00
	PLM	0.00	0.00	None	0	00 days 00:00
	NIU	0.00	0.00	None	0	00 days 00:00
	Instrument	0.00	0.00	None	0	00 days 00:00
	FDS	0.00	0.00	Sun Eclipse by the Moon	2	00 days 00:00
	Other	0.09	0.09	None	3	00 days 07:32
	SUBTOTAL	0.09	0.09	-	5	00 days 07:32
TOTAL	0.18	0.18		10	00 days 15:59	

Table 3-1: Instrument Outage Breakdown

From Table 3-1, it can be seen that the overall availability of the GOME-2 instrument was over 99%.

3.2 Operative Modes Budget

The only outages during the reporting period were due to manoeuvres or problems external to the instrument. Note that moon calibrations do not cause an outage, nor did the recurrences of the dark current anomaly.

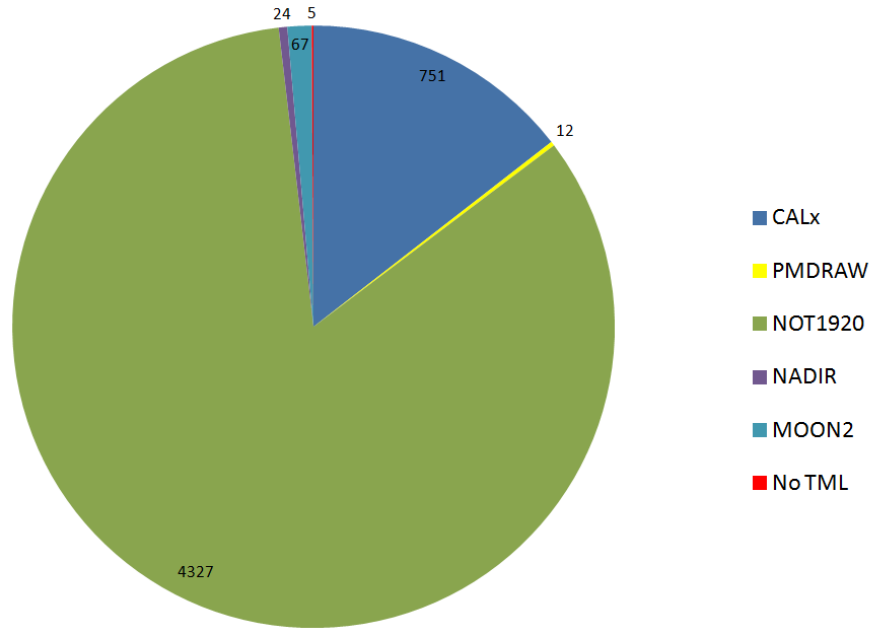


Figure 3-1: Timelines executed aboard Metop-B 01-Sep-2013 to Aug-31-2014

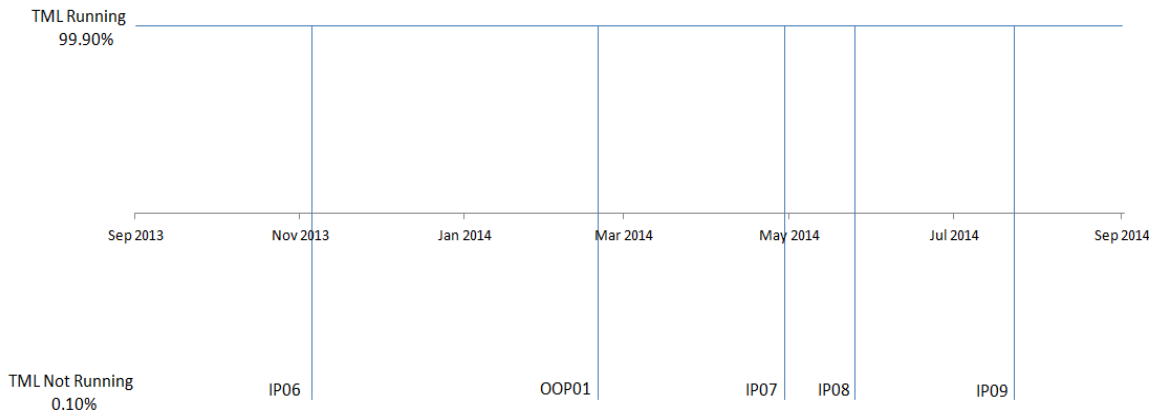


Figure 3-2: Timeline status during the reporting period

4 ANOMALY AND NON-CONFORMANCE REPORTS

This section outlines the status of anomalies and non-conformances relating to the GOME-2 instrument onboard Metop-B. For completeness a description of the anomalies is given even if they are closed.

Note: The list only includes Anomalies related to the GOME-2 instrument itself. In the EUMETSAT anomaly processing tool, there are other anomalies assigned to GOME-2 that actually relate to other items such as the IOM, procedures or timelines.

4.1 AR and NCR Overview

<i>Sect.</i>	<i>Ref</i>	<i>Title</i>	<i>Class</i>	<i>Occurrences in Reporting Period</i>	<i>Disposition</i>
4.2	AR.13557	Anomalies during Idle mode	SW	0	Closed
4.3	AR.13556	Anomalies during timeline execution	HW	0	Closed
4.4	AR.14395	Signal issue in the measurements used to derive GOME-202 slit function	SW	N/A	Closed
4.5	AR.14439	Throughput test observation during GOME-2 MetopB SIOV	HW	On-going	Open
4.6	AR.14442	Anomalies during CAL0 execution	HW	0	Closed
4.7	AR.14557	Scan-angle dependent offset in reflectivity	SW	0	Closed
4.8	AR.14946 AR.15205	GOME-2 FM leakage current increase in band 4 (channel 4)	HW	0 2 (on-going)	Closed Open
0	AR.15517	GOME SU behaviour at static mirror positions	HW	On-going	Open

Table 4-1: Anomaly and Non-Conformance Report Overview

4.2 Anomalies during Idle Mode (AR.13557)

During SSVT, while GOME was in idle mode, the anomaly counter began incrementing due to OOLs on the optical bench temperature. This is due to GOME hovering around the yellow limits in ambient conditions. Once the calibration curves for Metop-C become available (circa 2016) the limits should take this into account.

4.3 Anomalies during Timeline Execution (AR.13556)

Several GOME anomalies were raised during execution of the SIOV Timeline. In particular, a breach of yellow limits on the SU Torque and HCL Lamp Voltage can be noted.

- Regarding the scanner issue, the cause was a degradation of the lubricant distribution which was solved after the full rotation. It is not explicitly recommended in the report having periodical full rotations but it seems that it would help.

- Regarding the lamp issue, Galileo confirm that the behaviour is OK. The FM2 lamp reaches a higher voltage when it works. The Lamp voltage high yellow limit must be raised to 233 V in order to avoid unwanted false alarms during flight operations.

4.4 Signal issue in the measurements used to derive GOME-202 slit function. (AR.14395)

A spurious signal was detected on top of the expected measurements. It is believed to be caused by stray light from the Xenon light source. RAL managed to model the observed additional "ghost" feature in the original key-data as delivered by TNO.

4.5 Throughput test observation during GOME-2 MetopB SIOV (AR.14439)

GOME-2 FM2 on Metop-B appears to currently degrade at an overall similar rate to FM3 on Metop-A at approximately the same lifetime in orbit.

4.6 Anomalies During CAL0 Timeline Execution (AR.14442)

A breach of yellow limits on the Scan unit Torque was received during CAL0 execution. The anomaly was triggered during the first full rotation of the Scan mirror in the CAL0 timeline. Same behaviour was seen during SSVT-5 (AR13556). There are still signs of extra torque at the start of scan cycles - the behaviour has improved over time but is still much worse than M02, and continues to be monitored closely.

4.7 Scan-angle dependent offset in reflectivity (AR.14557)

After the initial validation of calibrated radiances a scan-angle dependent offset has been observed in the reflectivity especially for band 3 (with some potential contributions from band 2b).

4.8 GOME-2 FM2 leakage current increase in band 4 (channel 4) (AR.14946) (AR.15205)

While passing through the south polar radiation belts, GOME experienced a sudden spike in noise accompanied by a step increase in dark (leakage) current. An IDLE-STANDBY-IDLE transition was performed on 17 July 2013, which confirmed the behaviour was not transient. The leakage current behaved erratically for several weeks following the event, including several step changes. It is believed to have been caused by the shorting of a switch in the detector, which then failed in the closed position, sending dark current values back to nominal. For a detailed analysis of the anomaly we refer to AD5.

The anomaly recurred on 28 October 2013, until 2 Feb 2014 (AR.15205) and again on 20 Aug 2014 and continuing until 1 Sep 2014). No mitigating actions were taken on either occasion. This behaviour is now considered to be a feature of the instrument with no impact, but is closely monitored.

4.9 GOME SU behaviour at static mirror positions (AR.15517)

For six of the seven nominal scenarios in which the GOME scan mirror is in a fixed position, the SU reports a non-zero torque. This includes immediately before the start of scanning for each timeline, where the torque values reported are “large” (absolute magnitude $>20\text{mNm}$) and appear to be increasing over time. This is applicable to both Metop A/B, and assumed to also affect Metop-C. In two of the scenarios, the torque profile exhibits a well defined saw-wave pattern.

An explanation for this behaviour has been provided by SSST in the form of MO-TN-ESA-GO-1115 [AD6]. The reported torque is not a direct measurement of torque, but rather the output of a PID algorithm which dictates the input to the 3 motor current drivers. This gives an accurate representation of torque during nominal mirror movements, but not during fixed pointing scenarios. During fixed pointing, the rotor “tends to align with the stator magnetic field; once aligned, no torque is generated, regardless of the current intensity.” The saw-tooth pattern observed at (in particular) the DARKCAL position is a feature of the control system. Note that although no mirror position error is reported in TLM, that used by the position controller has a higher resolution and the “torque” values reported can be explained by deviations of mirror position smaller than would be visible in TLM.

5 FUNCTIONAL PERFORMANCE ASSESSMENT AND TRENDING

5.1 Analysis Method description

Instruments are monitored per **physical signature** to which indicators are assigned to reflect its performance and trending.

A **physical signature** is a sub-set of correlated parameters which describes a vital function of the instrument or a particular observed behaviour. These signatures are interpreted and then apportioned to the instrument **component**, and a status is assigned (ref. to test coverage matrix in annex A

A function is provided by a set of instrument **components generally** linked to the instrument subsystem.

For each **component**, several *test units* are created. A unit test can cover anything from simple trending of a group of parameters and inspection of the average, standard deviation etc., to performing detailed analysis on a particular set of parameters to determine the state of a particular component (e.g. principle component analysis, derived parameter calculations, comparison of a group of parameters against another group etc.), and raise **indicators**.

Indicators are then monitored on different timescale, then apportioned to the instrument component. Some additional physical signature may also be performed under certain specific conditions (e.g. troubleshooting, to analyse decontamination etc.), while others are performed routinely.

For all physical signatures the immediate and lasting effects of system level events (PL-SOL, OOP) or instrument events (anomalies, operating strategy changes) will be identified and discussed.

Trends indicating a long term change of physical signature will be identified, discussed and compared against the operating limits. Nevertheless, it must be noted that even if the analysis is based on these observations, all parameters remain available for troubleshooting or deeper analysis.

In the plots contained in the following sections the following colour convention applies:

- 1) *Graphs with three coloured lines (Black/Blue/Magenta)*: The black line represents the orbital averages of the parameter, while the blue and the magenta lines represent respectively the minimum and maximum on the orbit.
- 2) *Graphs with a single blue line*: The red line represents the value of that parameter.
- 3) *Graphs with multiple coloured lines (other colours, red, green, blue)*: As specified in the plot labels.

This colour convention is applicable to the plots produced for all the physical signatures.

Plots are either covering the reporting period, the entire time since the instrument has been declared operational or a shorter time period related to a specific event.

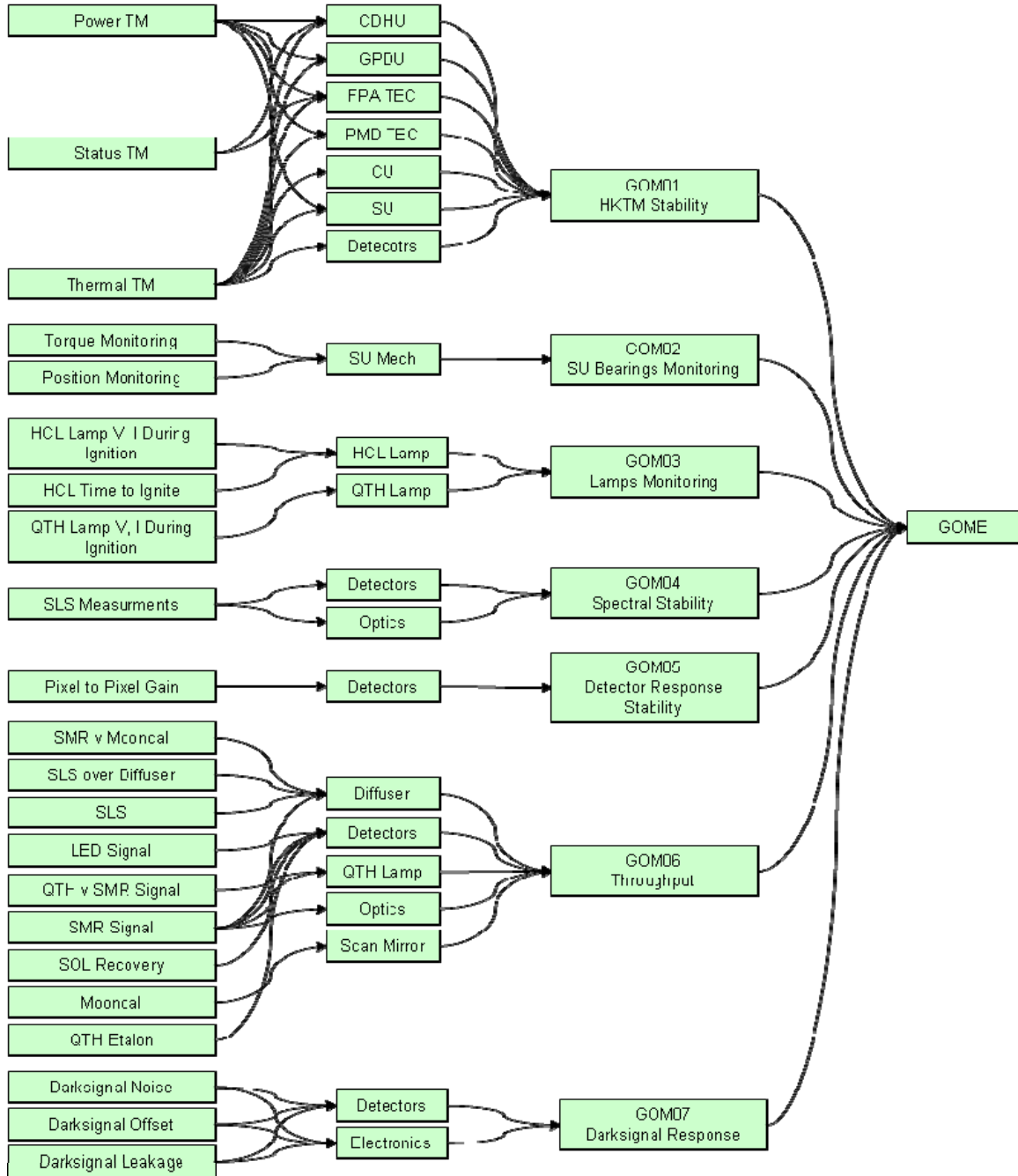


Figure 5-1: Test Unit Breakdown

5.2 Physical Signature Synopsis

Section	PS	Title	Component	Status	Trend	Conclusion
5.3	GOM01	HKTM stability	Functional health and trending analysis (including SVM/PLM TM correlation, ageing factors, etc) covering below aspects: <ul style="list-style-type: none"> • Thermal HKTM stability (detector cooler) • Power HKTM stability (GPDU, CDHU) • Software stability (type 14 entries) 	GREEN	⇒	GOME Healthy
5.4	GOM02	SU Bearings Monitoring	<ul style="list-style-type: none"> • Torque monitoring • Position Error monitoring 	GREEN	⇓	Mechanism Healthy, although torque profile becoming more noisy. Spinning on each Metop recommended
5.5	GOM03	HCL and QTH Lamps Monitoring	<ul style="list-style-type: none"> • HCL Output and Electrical Stability • QTH Output and Electrical Stability 	GREEN	⇒	QTH Lamp Blackening possible, but does not look serious HCL Lamp Output Stability Questionable No signs of HCL LVM or similar. Usage of lamps indicates plenty of life remains
5.6	GOM04	Spectral Stability	Stability of Spectral Calibration	GREEN	⇒	Some correlation with known events, but well within specs.
5.7	GOM05	Detector response stability	Pixel to Pixel Gain	GREEN	⇒	
5.8	GOM06	Throughput Stability	Overall throughput assessment based on the below analysis <ul style="list-style-type: none"> • SLS, SMR Throughput • Earthshine • WLS Etalon Monitoring • WLS vs. SMR • SLS vs. SLS Over Diffuser • SMR vs. Mooncal 	GREEN	⇓	Throughput falling in line with Metop-A
5.9	GOM07	Darksignal	Measure stability of Darksignal corrections <ul style="list-style-type: none"> • Offset • Leakage • Noise 	GREEN	⇒	Channel 2B data missing, requires L0-1B reprocessing. Separation of Offset and leakage not available Some seasonal variation in mean dark signal evident. Anomaly due to failed switch now considered a feature of this model with no impact.

Table 5-1: Physical Signatures Synopsis

Status definition	
Status Colour	Status Meaning
BRIGHT GREEN	Fully Operational
LIGHT GREEN	Fully Operational, but not in use, redundancy available
YELLOW	Operational with Limitations
ORANGE	Operational with Degraded Performance
LIGHT ORANGE	Not Operational with Degraded Performance
RED	Not Operational
GREY	Not applicable
BLANK	No status reported

Trend arrow definition	
Trend Arrow	Trend Meaning (trend, not the consequences)
⇒	no negative trend, i.e. stable
↘	negative trend within expectations
↗	positive trend within expectations
⇓	negative trend above expectations
⇑	positive trend above expectations
	no trend reported

Trend definition	
Trend Colour	Trend Meaning
GREEN	any trend (if there is any) will have no impact before end of assumed mission life at current rates
YELLOW	any trend will lead to a change of status before the end of assumed mission life at current rates
ORANGE	any trend will lead to a change of status within the next year at the current rates
RED	any trend will impact ability to perform EOL operations within the next year at the current rates
BLANK	No trend reported

5.3 GOM01: HKT M Stability

5.3.1 Description

This physical signature reflects the main housekeeping functions of the instrument, as follows:

- FPA, PMDs thermal management;
- Power conditioning;
- Housekeeping and science data management;
- The optical bench structure.

The health assessment of GPDU, CDHU electronics is performed by measuring voltage, current, power according to status of equipment.

To assess the health of detector coolers the following temperatures are monitored:

- FPA temps should be within 0.2 degrees of target temp and vary less than 0.25 degrees per orbit.
- PMD temps should be around 230 K on the flight line, varying with Pre-disperser Prism Temp.
- PMD s/p temperature gradient must be monitored since the signal ratio is used in the derivation of polarisation correction for the main channels.

The monitoring of equipment, e.g., problems with switching failures, latch-ups, etc. is detected through the Type 14 Entries. The trending is performed through evolution of consumed power, considering the ageing and seasonal evolution

5.3.2 Analysis

The long term behaviour of several HK parameters has been analyzed in order to identify and justify:

- Expected transients and discontinuities correlated to instrument /satellite and external events or operations.
- Trends or evolutions that can be correlated to other parameters/phenomena discovered on-board or on-ground, and that can be used as input for the discussion regarding the durability (or residual reliability) of the instrument with regard to the planned operational life.
- Any kind of unexpected behaviour and its correlation with regard to other parameters/phenomena.

Hereafter we report a summary of the observations made and a selection of the plots where the evidences of such phenomena are evident and from which such features can be completely described and discussed. Furthermore, plots indicating HK Stability are presented in weekly extranet reports, so only some representative examples are included here.

The orbital averages are used to generate statistics on the min, mean and max where valid HKT is available.

1. The correlation between mean temperature values across the instrument is checked.
2. Unusual behaviour is cross checked against instrument/satellite events

3. The overall trend of the temperatures and voltages across the reporting period is considered in order to decide whether or not the temperature is likely to exceed the parameter limits in the next 5-10 years.

5.3.3 Interpretation

All the observed parameters show a good stability over the reported period. The only noticeable variations are those due to seasonal effects.

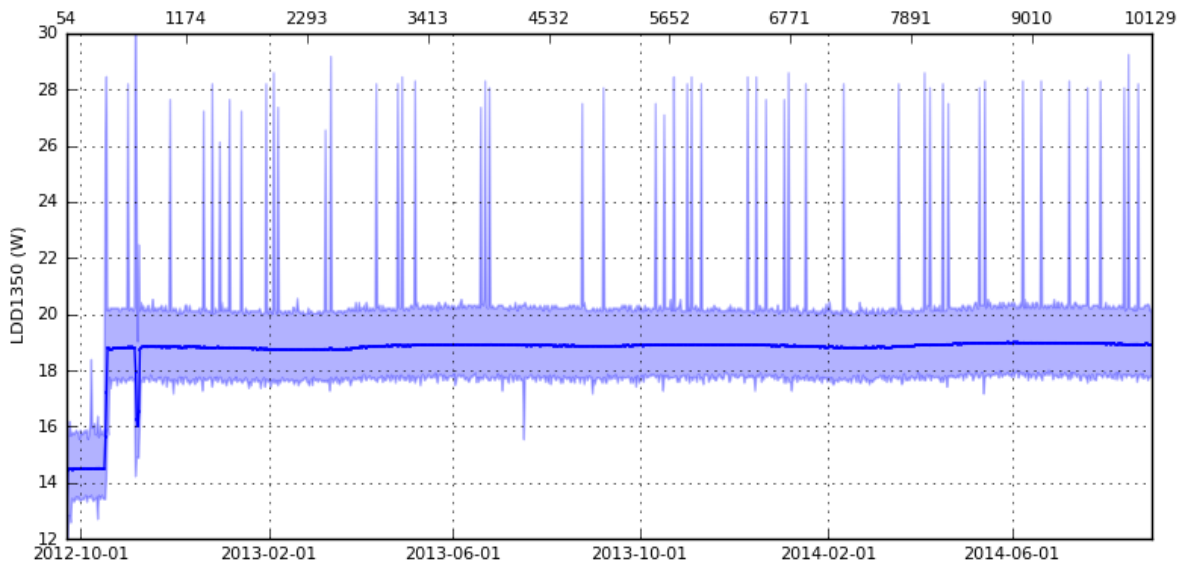


Figure 5-2 GOME ICU Power since launch

Figure 5-2 shows stable ICU Power consumption during the reporting period. Spikes in the ICU Power are due to Telemetry sampling being coincident with shutter movements, which are powered by the ICU. Lower values coincide with known activities such as the IDLE-STANDBY-IDLE transition on 17 July 2013 due to AR14946, but no such events have occurred during the reporting period.

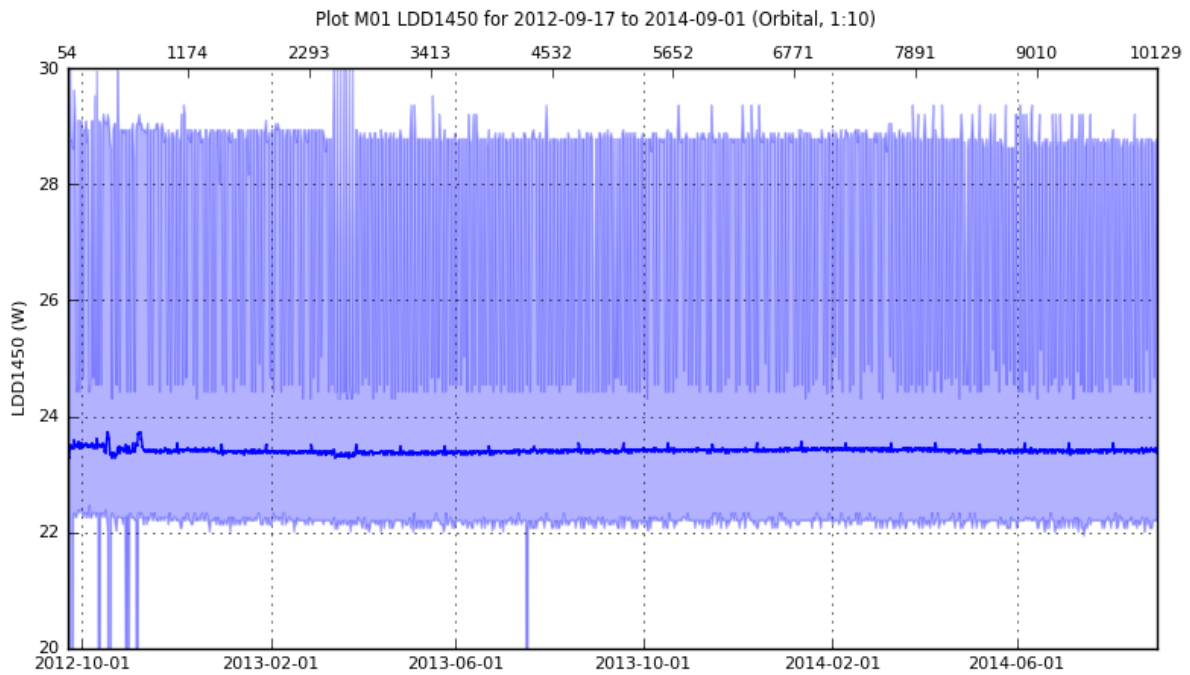


Figure 5-3 GOME EQ Power since launch

Figure 5-3 shows that the EQ Power has been relatively stable during the reporting period.

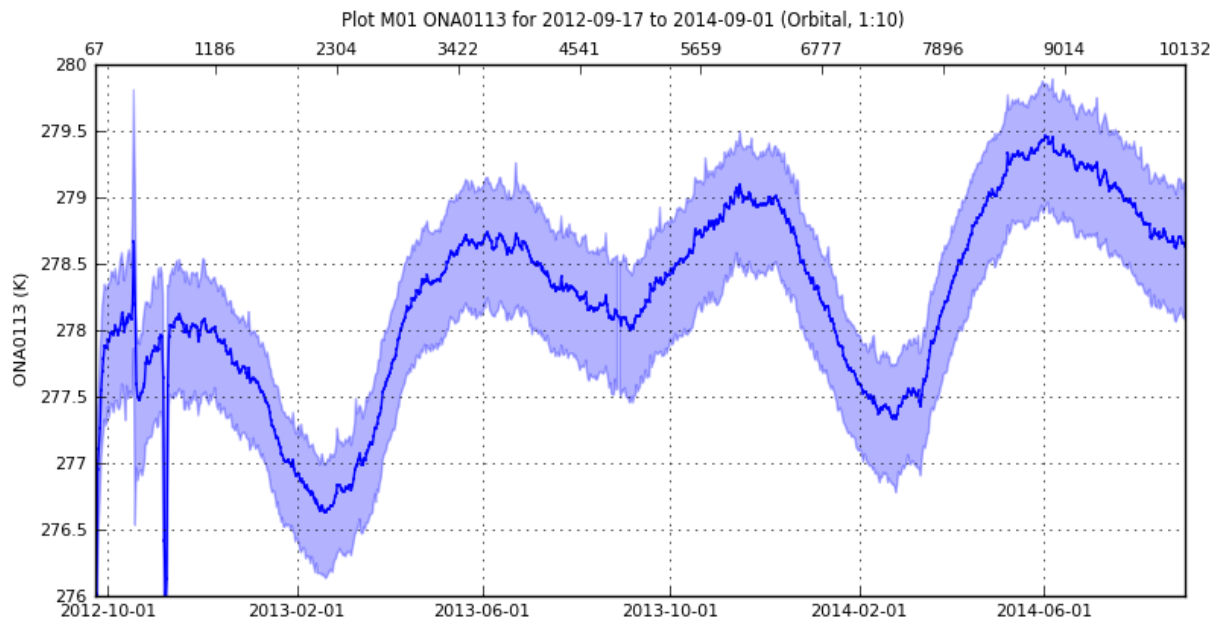


Figure 5-4 GOME Optical Bench Temperature since launch

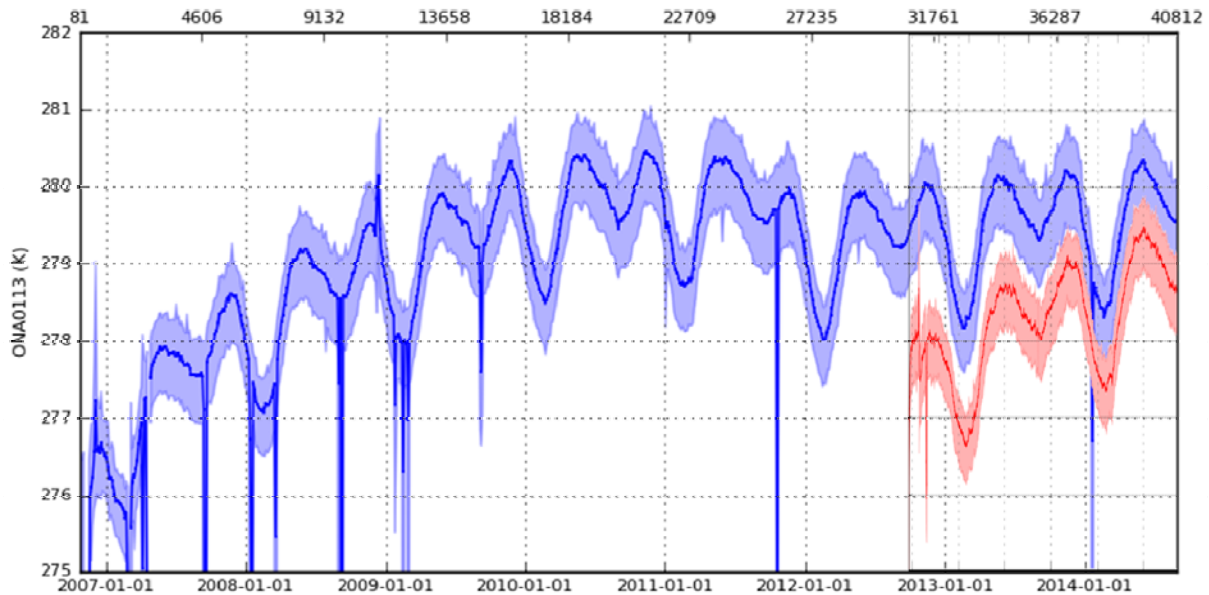


Figure 5-5 GOME Optical Bench Temperature comparison with M02

Figure 5-4 shows that the Optical Bench Temperature has been following the expected seasonal trend during the reporting period. All deviations from this trend are explained by known events. A full comparison of the M01 OB temperature with that of M02 is provided in Figure 5-5, from which it can be seen that the seasonal trend closely matches that of M02, and the temperature ranges are converging.

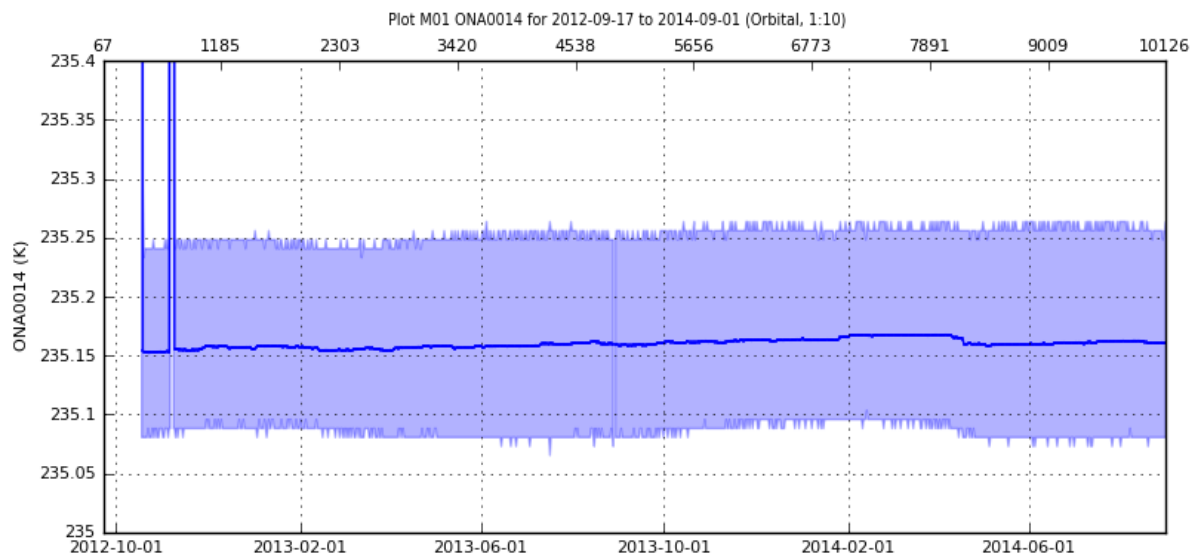


Figure 5-6 GOME FPA Detector Temperatures since launch

Figure 5-6 shows FPA 1 detector Temperature 1, which is representative of the other FPA thermistors. From this figure, it can be seen that the temperatures are stable under nominal conditions. All deviations from $235.3 \pm 1K$ are well understood and due to known events.

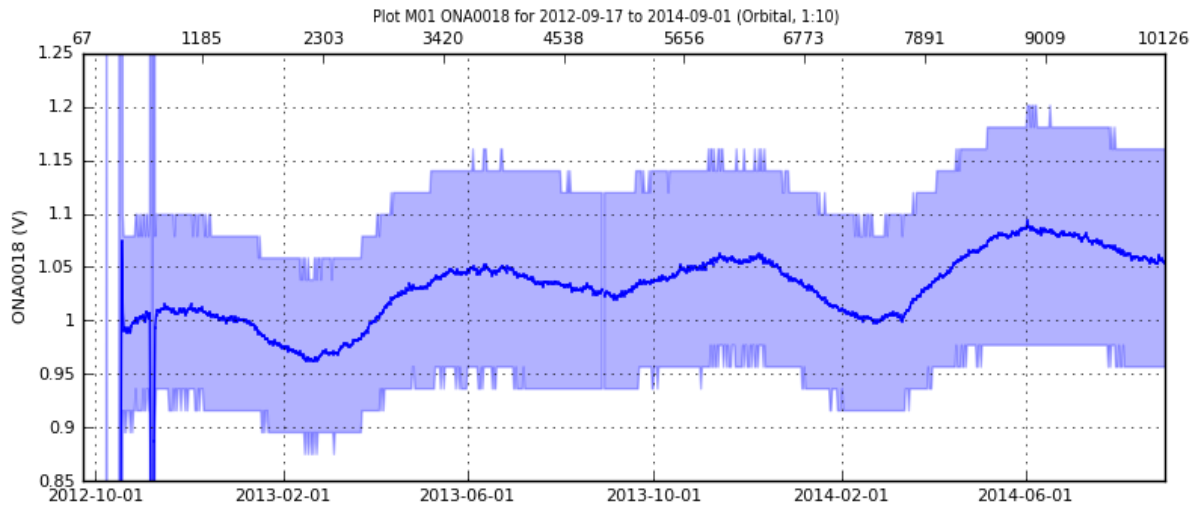


Figure 5-7 GOME FPA Peltier Output since launch

Figure 5-7 shows FPA 1 Peltier Output, which is representative of the output of the other FPA Peltier Loops. From this figure, it can be seen that the output is consistent with other GOME temperatures.

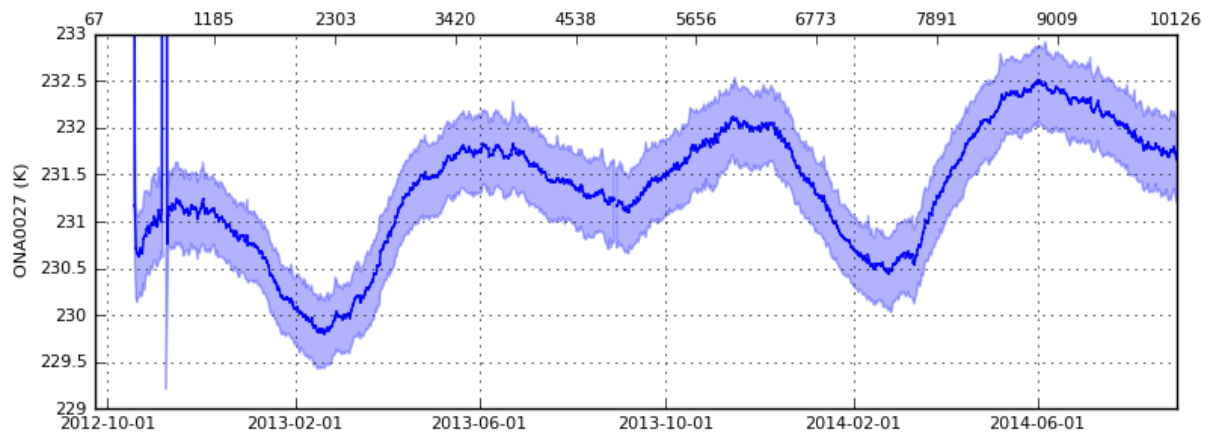


Figure 5-8 GOME PMD-s Temperature since launch

Figure 5-8 shows PMD-s temperature, which is close to that of the PMD-p temperature. From this figure, it can be seen that the trend is consistent with other GOME temperatures.

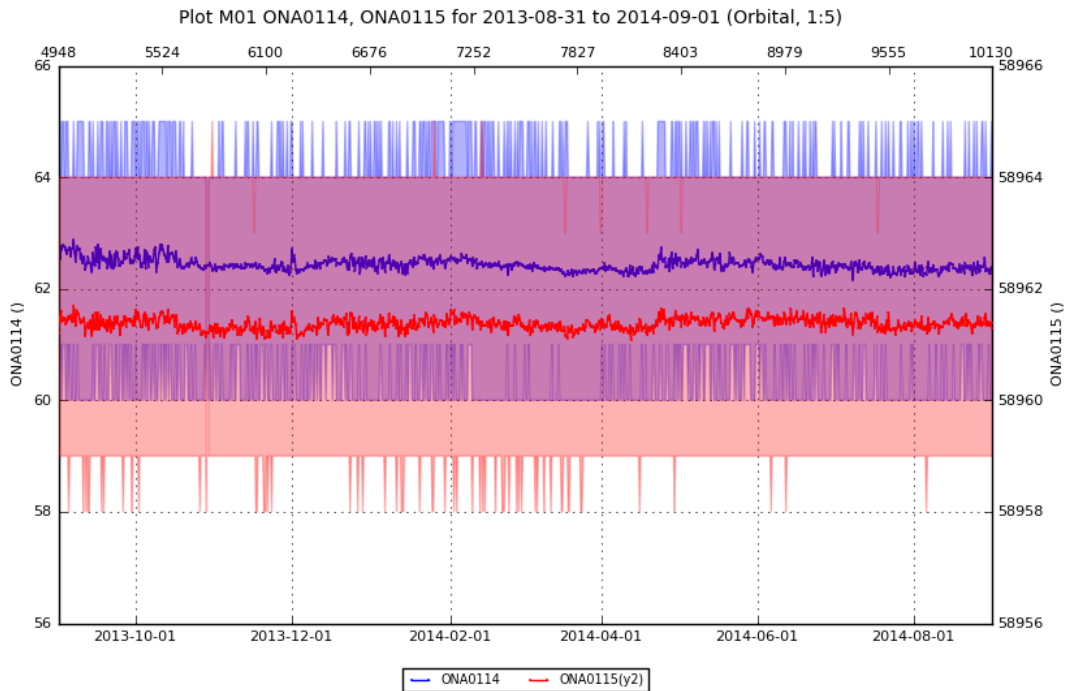


Figure 5-9 GOME Analogue Board Offset (blue) and Gain Value (red) during the reporting period

Figure 5-9 shows the Analogue Offset and Gain Value. From this figure, it can be seen that the both values are stable.

5.3.4 Assessment

All the observed parameters are well within specification range. This clearly shows that the functional performances status of the instrument does not raise any particular concern to date.

Temperatures are behaving in line with those over the satellite as a whole showing seasonal, diurnal and orbital variations. There are no indications of any trends which may limit the lifetime of the instrument within the timeframe of 2024.

5.4 GOM02: SU Bearings Monitoring

5.4.1 Description

During scanning, the GOME Scan Mirror is controlled by means of on-board lookup tables to achieve a 1920 km Earth Curvature Corrected scan. These lookup tables contain a list of target positions at certain intervals within the scan profile. The Mirror position is measured and control loops calculate the required motor drive current based on the difference between the target and actual mirror positions. The motor drive current is what is actually being measured during torque monitoring.

The Scan Unit bearings and races are lead lubricated. It is known that constant forwards and backwards scanning without making complete rotations can result in this lubricant becoming unevenly distributed along the races. This can lead to large position errors due to accumulation of lead hills on some parts of the races and depletion on other parts of the races. This can ultimately result in the mirror occasionally sticking and even damage to the races and bearings. Permanent failure of the scanning mechanism would result in a loss of the mission, so monitoring the health of the bearings is essential.

This Physical Signature is intended to measure the performance of the GOME Scan Unit in terms of pointing accuracy and the torque required to drive the mirror.

5.4.2 Analysis

The GOME Scan Mirror Torque is telemetered in such a way in Science Data Packets that after 16 complete scans, it is possible to construct a single pseudo 171Hz sampling torque profile. By constructing a torque profile of a 1920 km scan from near BOL and using this as a reference, it is possible to compare all subsequent 1920 km scan torque profiles and thus monitor the evolution of the torque profile.

The absolute difference between each point on the torque profile being measured and the reference profile is calculated and averaged over the whole profile. This is repeated for all 1920 km swath profiles in a day and then the average result determined.

By looking at individual torque profiles, it was noticed that the evolution of the torque profile at the extremities of the scan was different to that of the main part of the forward scan and fly-back, so these have been separated as illustrated in Figure 5-10

Scan mirror position is monitored in exactly the same way, although with less temporal resolution since it is only possible to construct position profiles at 10.66 Hz resolution.

To capture the maximum errors in position and torque, the orbital maximum torque is presented (this is assumed to be a spike at one of the scan cycle extremities). For position, the daily maximum deviation from the reference is displayed.

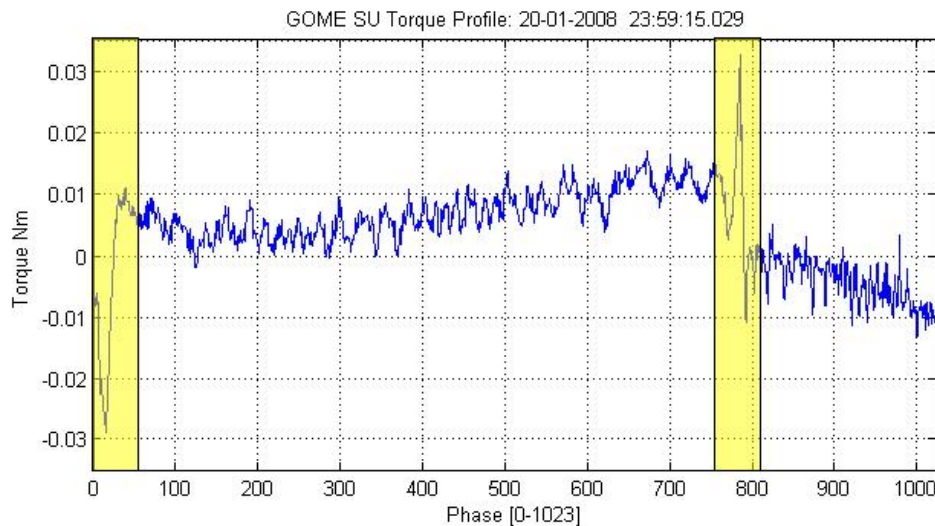
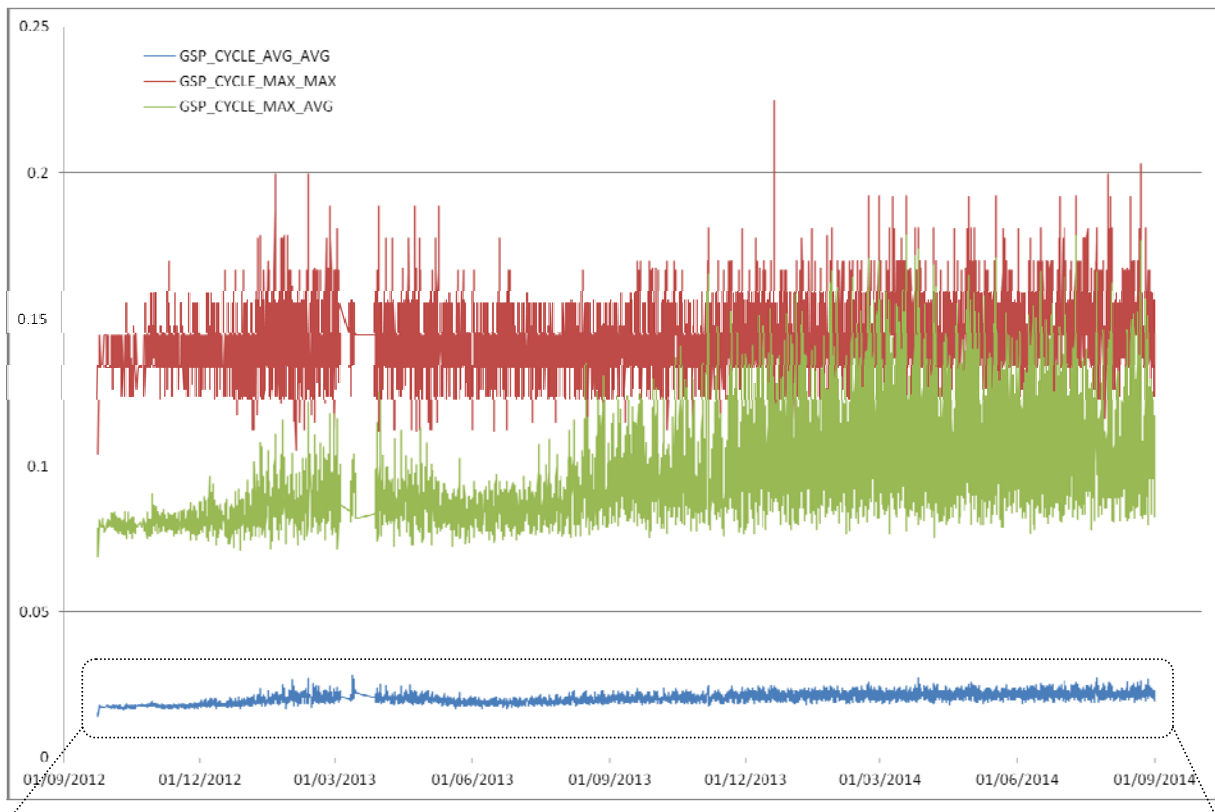


Figure 5-10: Typical GOME SU Torque Profile over a 6s 1920km swath scan cycle. Areas in yellow are considered scan extremities and are assessed separately. (Data from Metop-A)

Due to the fact that the Scan Unit mechanism has exhibited a worsening trend on Metop-A for which mitigating action was taken to rectify, a complete history of the evolution is presented here.

5.4.3 Interpretation

Figure 5-11 shows the position error evolution. The blue line is the average error in position (compared with reference profile) over the entire scan cycle (left axis) and the red line represents the maximum position error (right axis).



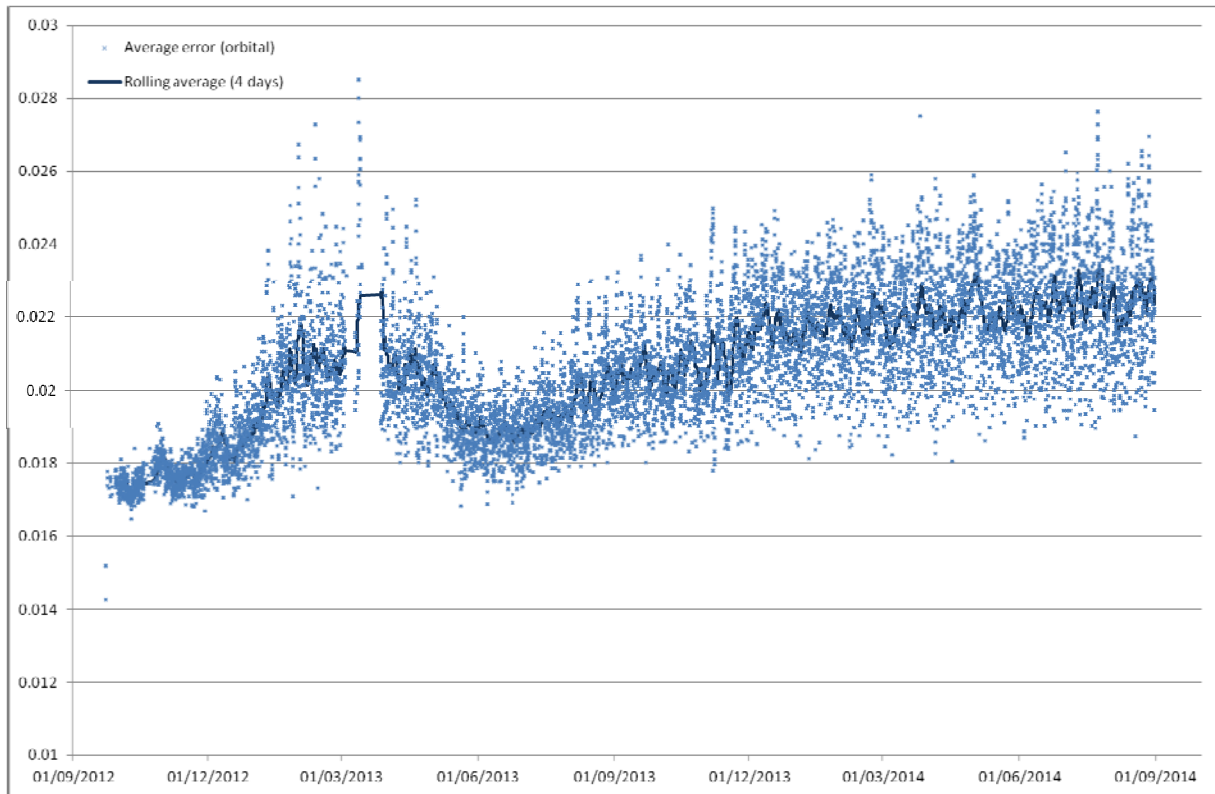


Figure 5-11: GOME SU Position Error Evolution since launch.

Figure 5-11 shows the average SU position error (blue), the orbital maximum (red) and the average maximum per cycle (green). From this it can be seen that position error has been relatively stable throughout the reporting period. However, there was a noticeable increase (~10%) of the average in Nov-Dec 2013, with a similar absolute increase in the maximum. The average maximum has become noisier since launch, showing there are now an increased number of cycles per orbit which experience deviations comparable to the maximum reported values. Similarly, the rolling average shows there is a slightly positive trend, but there is nothing apparent which would cause concern at this time.

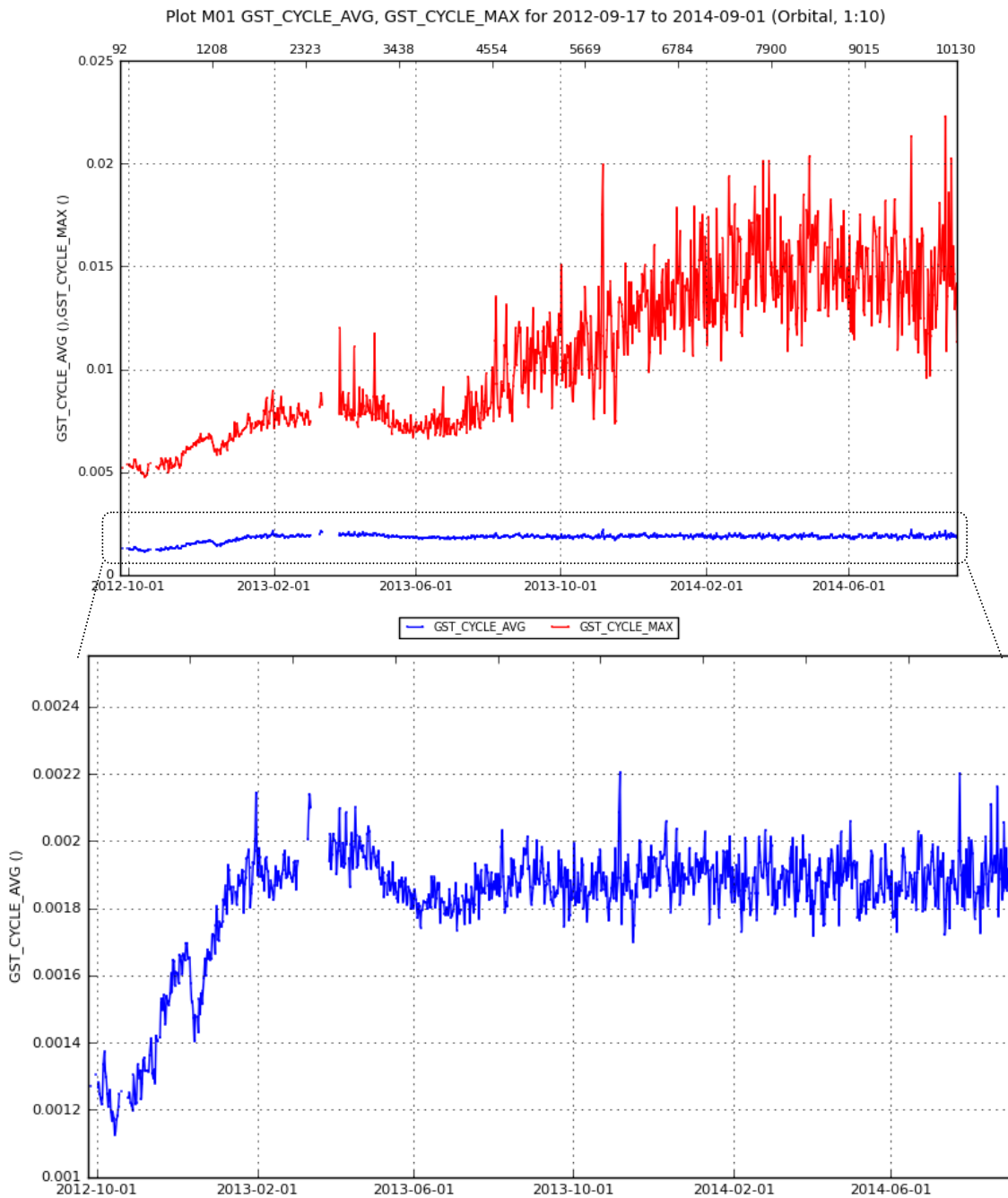


Figure 5-12: GOME SU Torque Evolution.

Figure 5-12 shows the average error in SU torque with respect to the reference profile over the entire cycle. The gaps are caused by testing a different (960km) swath width prior to tandem operations, and the darkness test in which no timelines were executing. From this plot it can be seen the average deviation is very stable. The maximum deviation rose steadily from mid-2013 to early 2014, as is expected in line with the rise in position error, but now appears to be relatively stable.

5.4.4 Related Anomalies

On a number of occasions near BOL, the SU Torque went beyond the yellow limits and triggered anomalies (ref AR13556, AR13557, AR14442). These events were caused by degradations of the lubricant distribution, which is understood and was fixed by performing a full rotation of the scan mirror. Such a rotation is performed daily, as routine maintenance of the instrument. However, these incidents are masked in the trending plots above, but can be highlighted by extracting the total number of TLM values beyond nominal limits during the daily spinning as shown in Figure 5-13.

From Figure 5-13, it is clear that there was a significant improvement from BOL, until roughly the start of the current reporting period (Sep 2013). Throughout the majority of the reporting period, both the maximum (absolute) reported torque and count of high torque values were increasing. Both have been improving since July, but will need to be closely monitored as the rolling average highlights this trend clearly alternates but has been trending upwards. For reference, the “red” limit of $\pm 56\text{mNm}$ and “yellow” limit of $\pm 35\text{mNm}$ are show as dashed red and green lines respectively. A comparison with M02 throughout the life of M01 is also provided in Figure 5-14, from which it can clearly be seen that M02 is much more stable than M01, which has been trending upwards since late 2013.

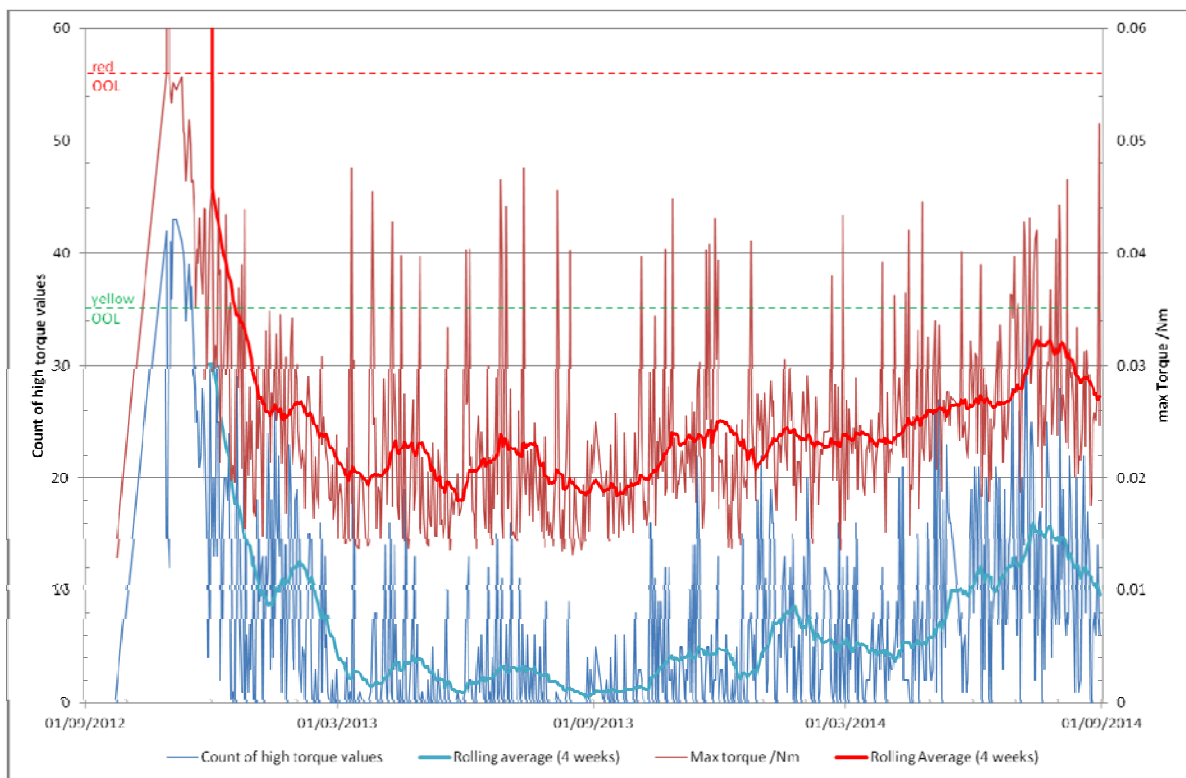


Figure 5-13: GOME SU monitoring of “high” torque values $>20\text{mNm}$ during daily spinning (blue), and max torque value reported (red) with limits (dashed).

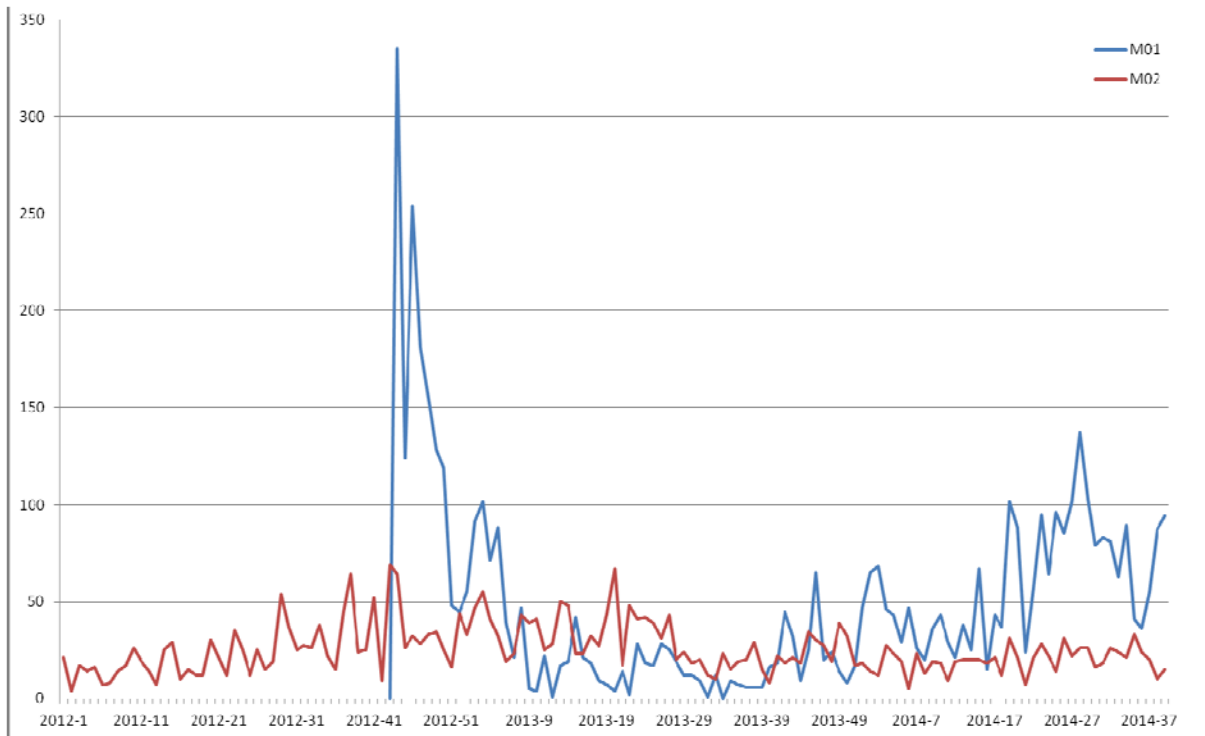


Figure 5-14: Comparison of count of torque values >20mNm during spinning, by calendar week, of Metops A and B.

It should be noted that, although the yellow limit is commonly reached, and the red limit is now being approached, the maximum values are transient peaks and do not result in anomalies being raised by the onboard monitoring. However, the maximum duration in which high (greater than 20 mNm) torques are exhibited does closely follow the above two factors, as shown in Figure 5-15. A comparison of the maximum torque reported on each spacecraft, by calendar week for aesthetics, is given in Figure 5-16. From this it can be seen that the maximum torque values reported by M01 and M02 are noisy but directly comparable, but that while M02 is stable, M01 appears to be showing an rising trend.

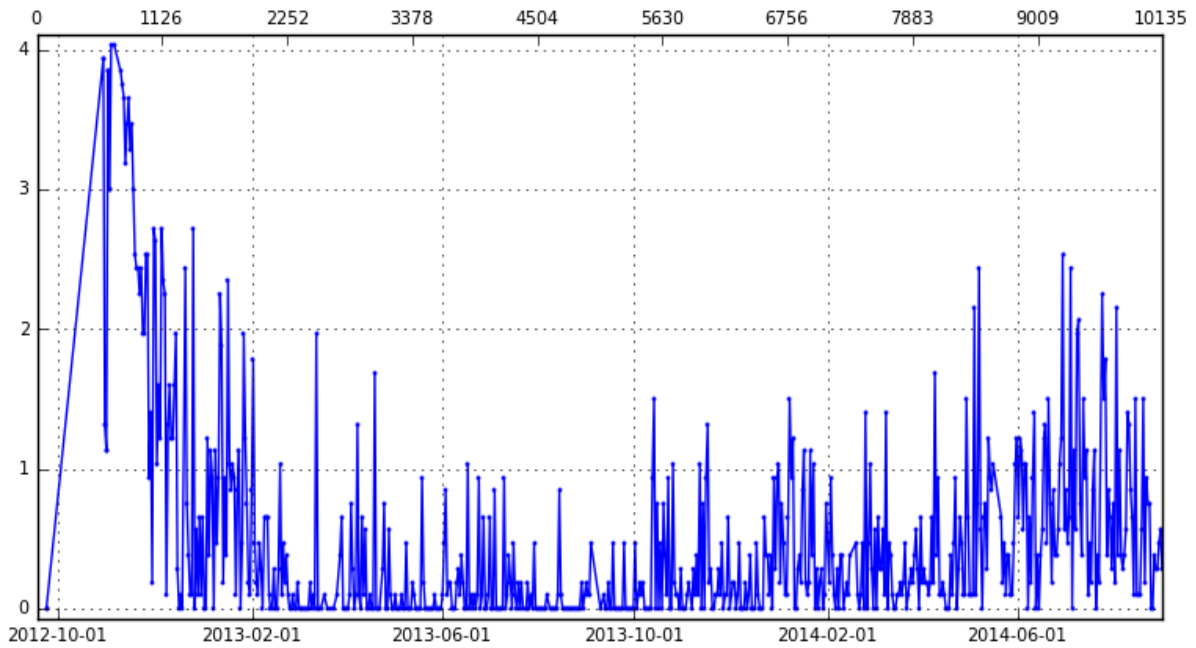


Figure 5-15: Maximum duration of torques >20mNm at the start of spinning in seconds.

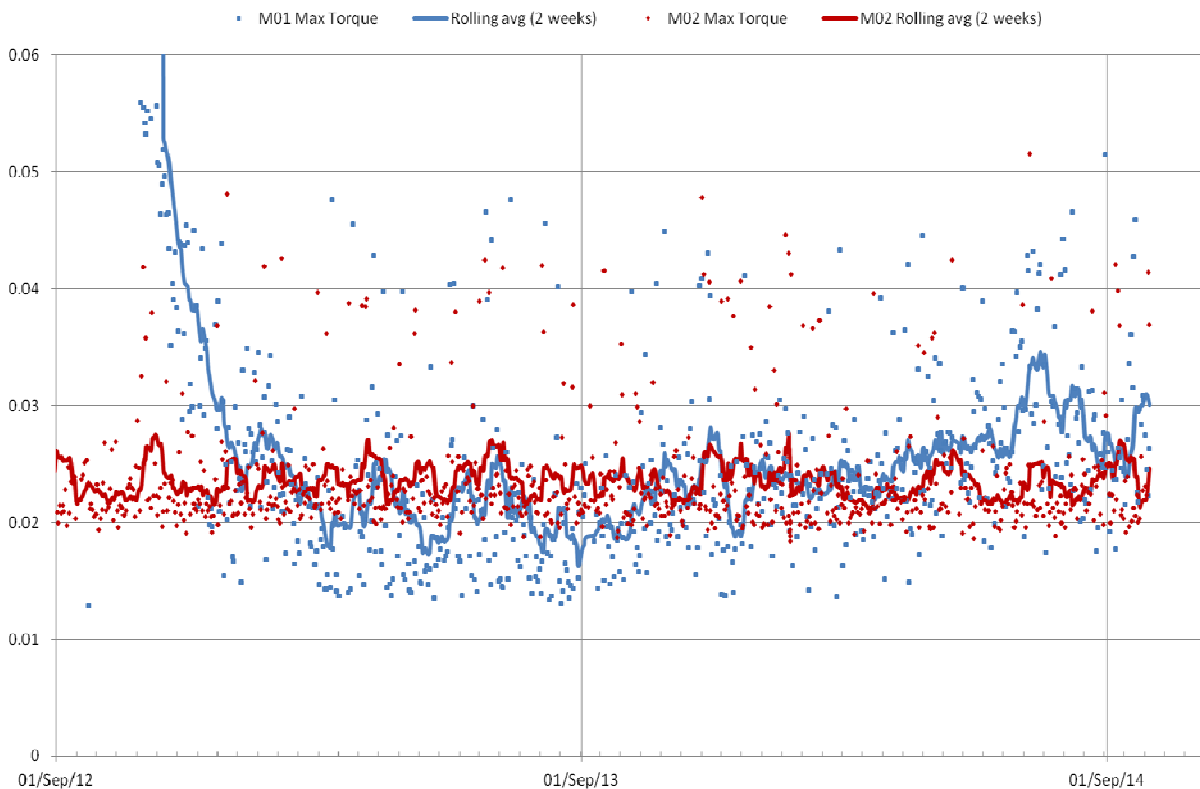


Figure 5-16: Comparison of the maximum torque reported at the start of spinning by M01 and M02, with rolling average.

5.4.5 Assessment

From the attached plots, it can be seen that the regular daily has a beneficial effect on the noise in the position and torque. Since regular spinning began, the noises in the torque and position profiles have followed similar patterns.

In both cases, the profiles during the main part of the scan and flyback appear to be reasonably stable. There is still plenty of torque margin and the Line of Sight Requirement of ± 0.0645 degrees is only breached at the turn-around points. There is plenty of margin for the main part of the profile, however the trend needs to be closely monitored as it has proved to be very non-linear on Metop-A. Similarly, the behaviour at the start of the daily spinning activity will continue to be closely monitored.

ESA tribology experts will perform a deeper analysis of these results to determine whether it is possible to make any predictions on evolution or recommend a different spinning strategy.

5.5 GOM03: HCL and QTH Lamps Monitoring

5.5.1 Description

The HCL lamp can be monitored for changes in ignition time by taking the difference between the time at which the voltage ramp begins and the time that current begins to flow for each lamp ignition. During each lamp ignition, the voltage profile can also be monitored to look for signs of unusual behaviour. The throughput as monitored by HCL lamp measurements when compared to SMR measurements can also act as an indicator of lamp health.

QTH Lamp voltage monitoring can show signs of filament thinning. Also, throughput of the lamp compared to that of SMR can reveal blackening of the QTH bulb wall. The function of the halogen is to set up a reversible chemical reaction with the tungsten evaporating from the filament. In ordinary incandescent lamps, this tungsten is mostly deposited on the bulb. The tungsten-halogen cycle keeps the bulb clean and the light output constant throughout life. At moderate temperatures the halogen reacts with the evaporating tungsten, the halide formed being moved around in the inert gas filling. At some time it will reach higher temperature regions, where it dissociates, releasing tungsten and freeing the halogen to repeat the process. In order for the reaction to operate, the overall bulb temperature must be high. Blackening, or a loss of throughput measured by the QTH Lamp can indicate that the bulb wall is not reaching a high enough temperature and that the tungsten-halogen mix is condensing on the bulb wall.

5.5.2 Analysis

HCL Ignition time is monitored using telemetry from science data packets. For each HCL ignition, the time difference between the leading edge of the voltage ramp and the flow of current is noted. Since HCL voltage and current are sampled at 375 ms rate, and the measured ignition time is on the order of a second. HCL Running voltage is monitored by plotting the voltage over a narrow range to highlight differences in each ignition. This can also be correlated to the lamp throughput.

For the QTH lamp, throughput monitoring can be used to look for signs of lamp blackening. Also, voltage can be monitored as a sign of filament thinning.

5.5.3 Interpretation

5.5.3.1 HCL / Spectral Lamp

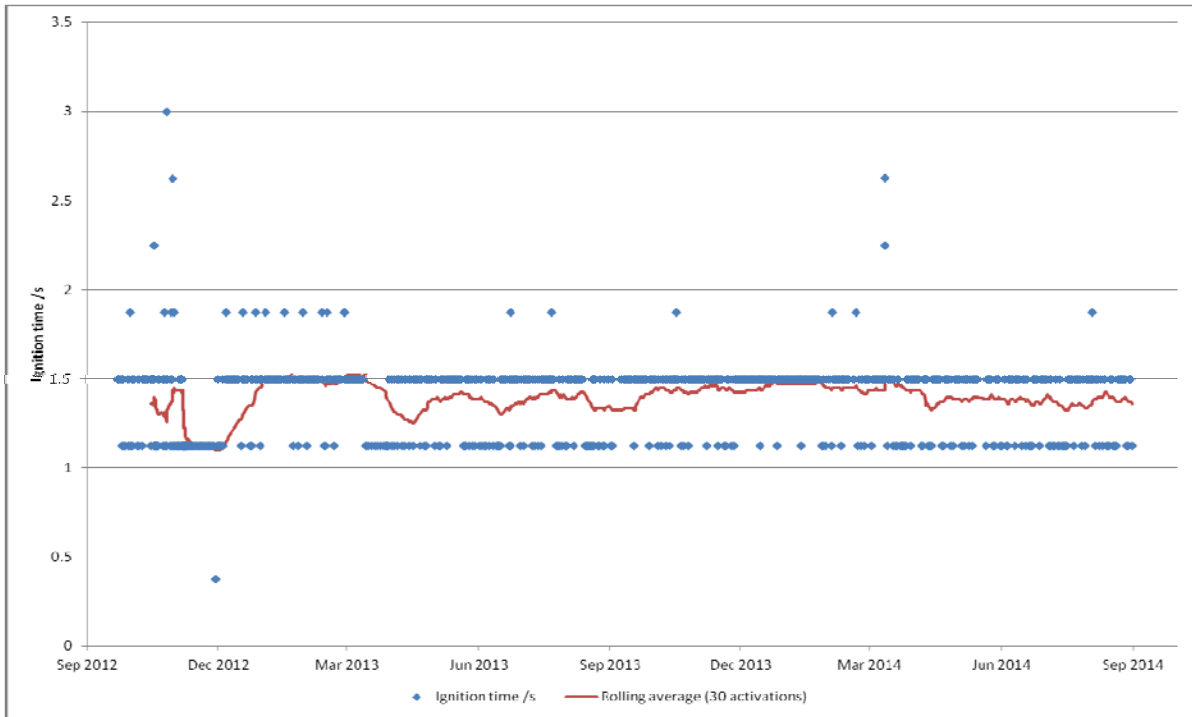


Figure 5-17: GOME HCL Ignition Time since launch

From Figure 5-17, it can be seen that the HCL Ignition time is stable. On Metop-A it appears to follow a cyclic (annual) trend, matching the temperature of the instrument, but no such trend is apparent on Metop-B which exhibits a more consistent ignition time.

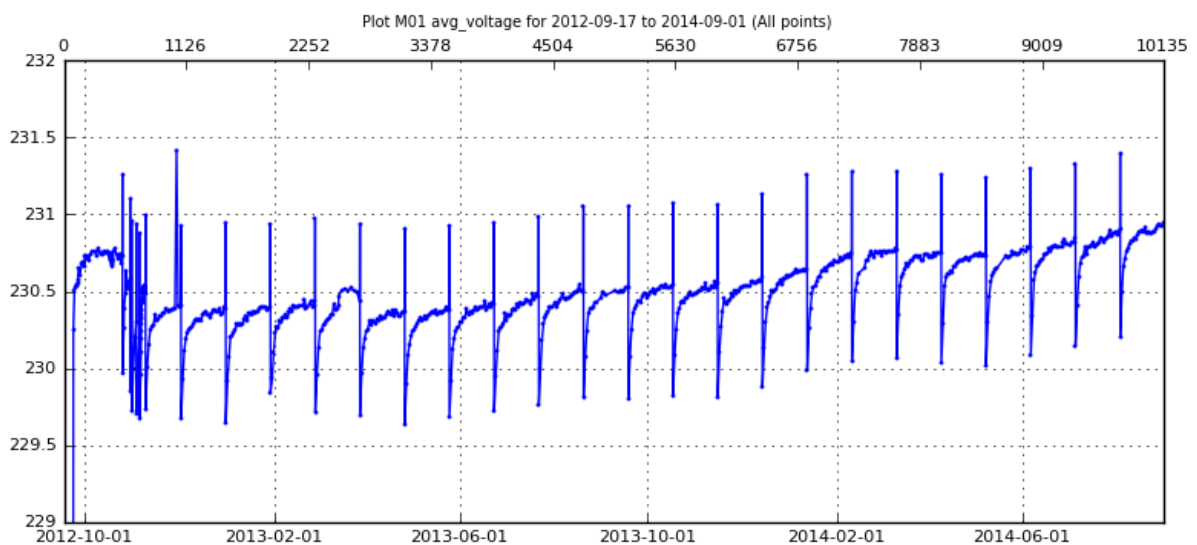


Figure 5-18: GOME HCL Activation Voltages since launch

The 29-day cycle is apparent in the HCL Voltage which is caused by the long DIFCAL (HCL Lamp over diffuser) during the CAL5 timeline.

Figure 5-19 also highlights the 29 day cycle in HCL Lamp throughput, which is the same as aboard Metop-A. This does not cause a problem for the quality of the spectral calibration. However, it does raise some concerns about the quality of the SLS over Diffuser measurements (DIFCAL) used to measure throughput loss of the diffuser.

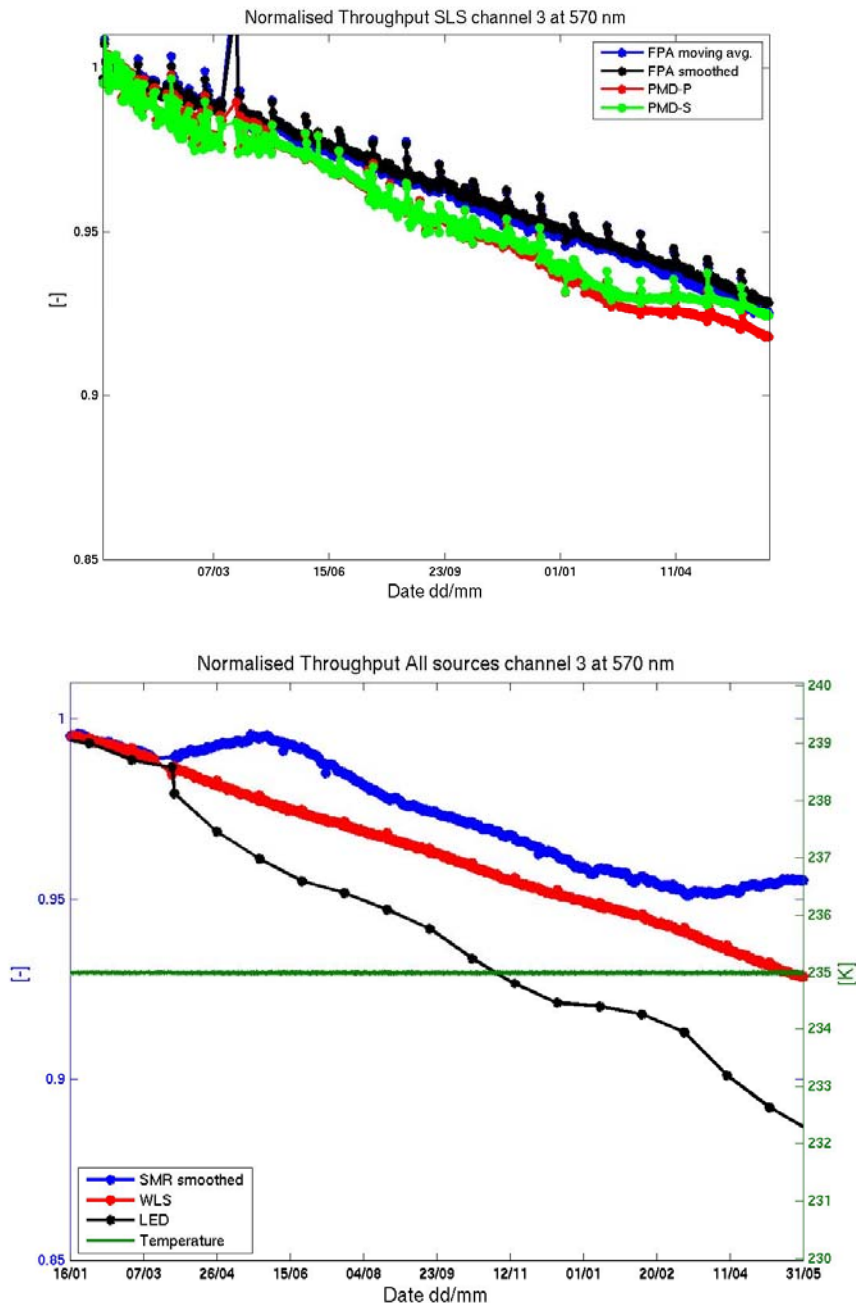


Figure 5-19: Upper panel: Change in instrument throughput around 570 nm for SLS signal. SLS is smoothed with the spectral response function of PMDs in black and with a moving average in blue for main channel data. SLS data for PMD P and S are plotted in red and green respectively. Lower panel: The same but for SMR, WLS and LED.

Ground analysis confirms these observations and also that this instability of the Spectral Lamp voltage can increase or decrease the signal strength of different lines. This means that the DIFCAL can only be used to monitor the diffuser with careful use of the HCL Lamp.

5.5.3.2 WLS / QTH Lamp

Figure 5-20 shows a continuing increase in the QTH Voltage during operation. This is believed to be due to a thinning of the filament, and is in accordance with the behaviour observed on Metop-A.

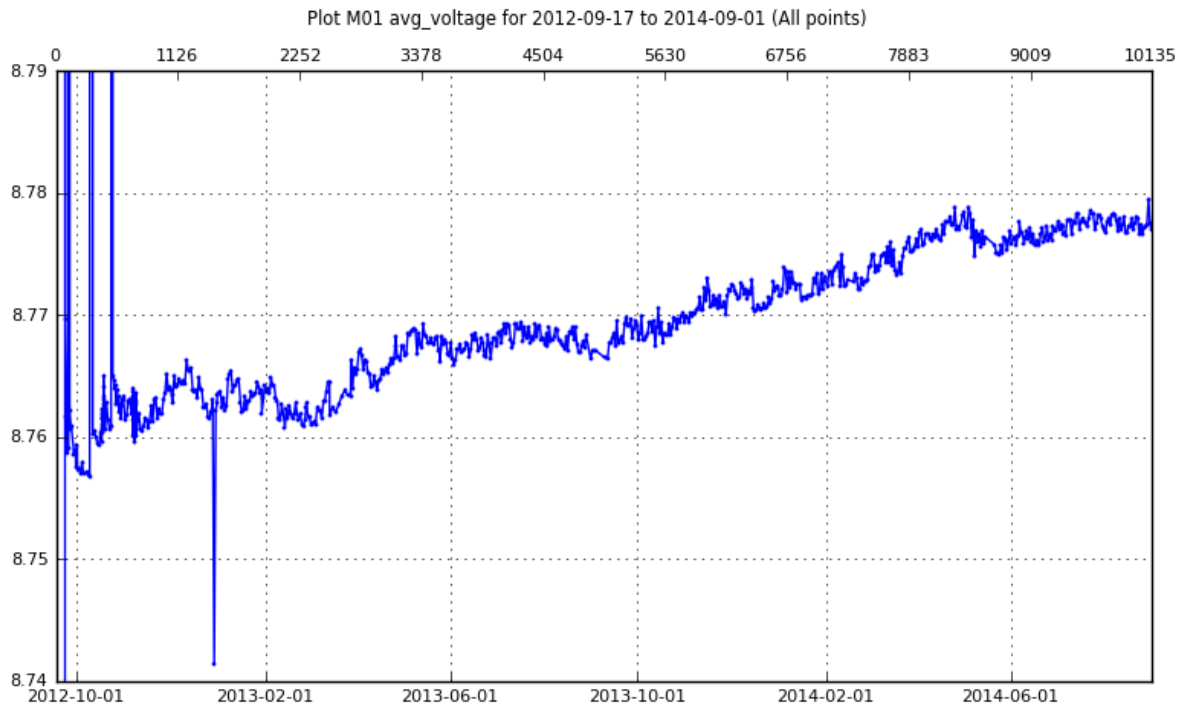
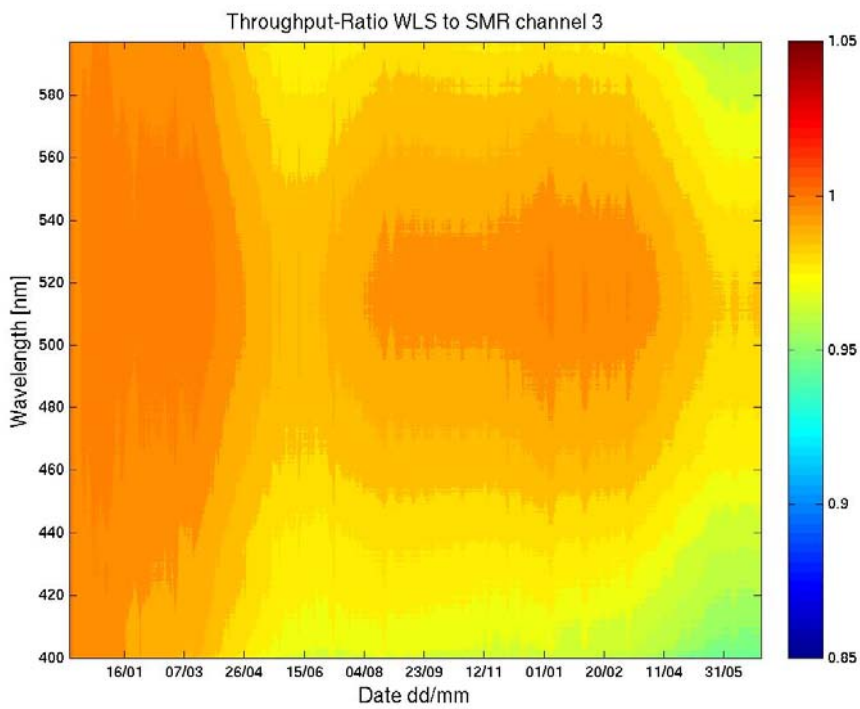
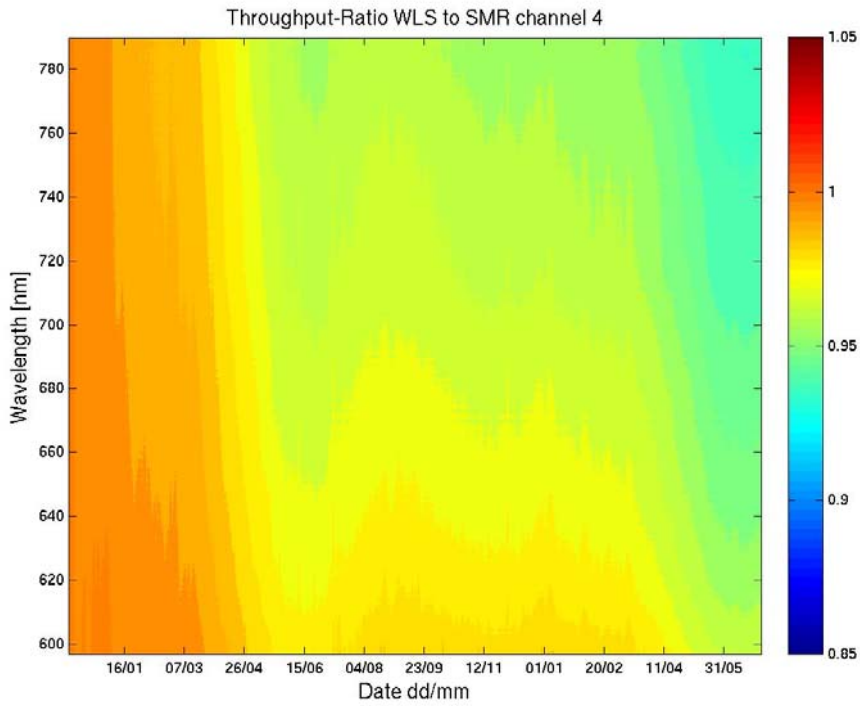


Figure 5-20 GOME QTH Voltage

Figure 5-19 also shows throughput at 570 nm (Channel 3), normalised to 28 Jan 2007. This is approximately the wavelength of light emitted by the LEDs, so puts all sources on a level playing field. From Figure 5-19, it can be seen that throughput as measured by the QTH Lamp is falling more rapidly than that of the SMR measurements, implying there is some lamp blackening. However, for a full picture all wavelengths should be considered.



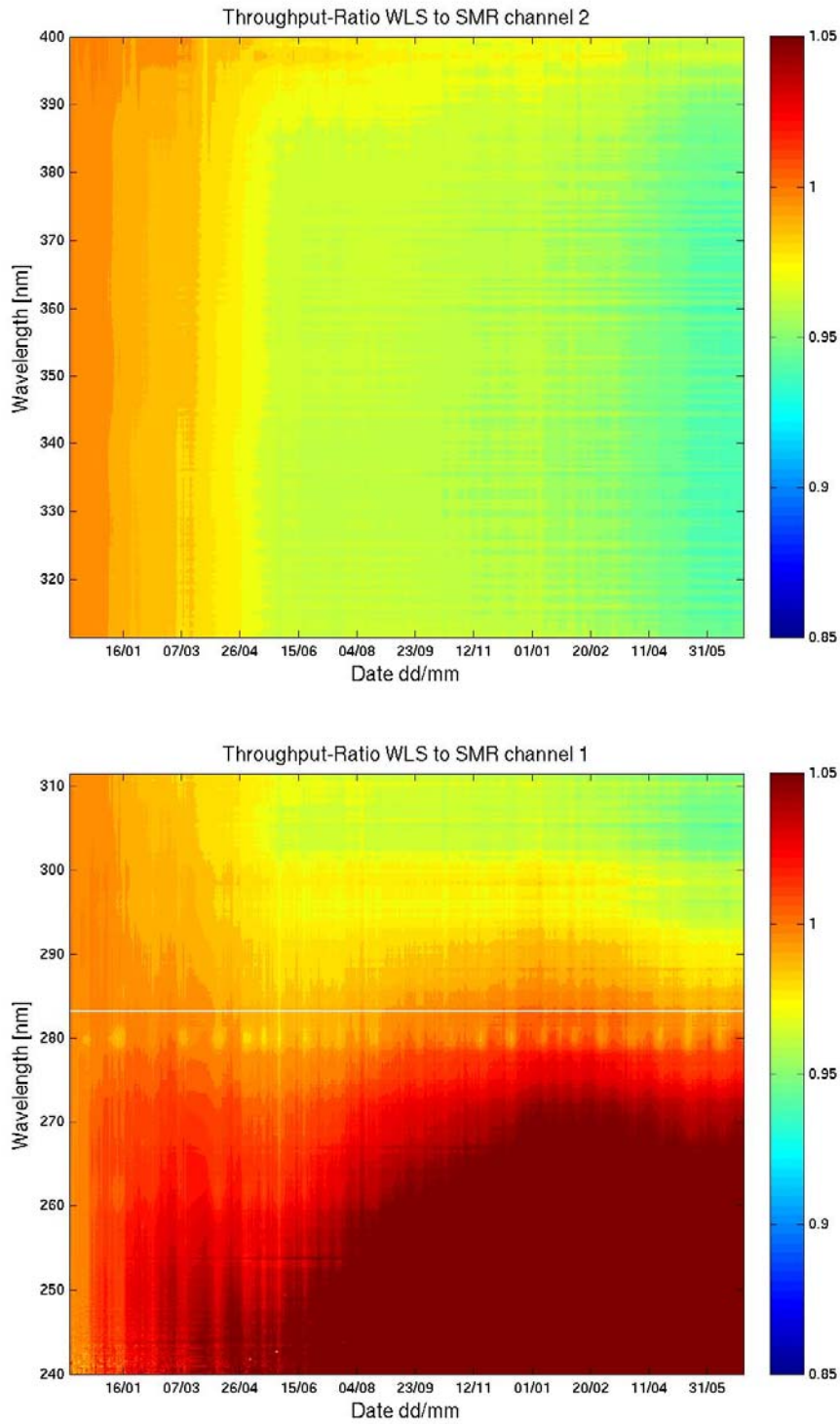


Figure 5-21: GOME WLS to SMR ratio normalised to January 2007 for all Main Channels.

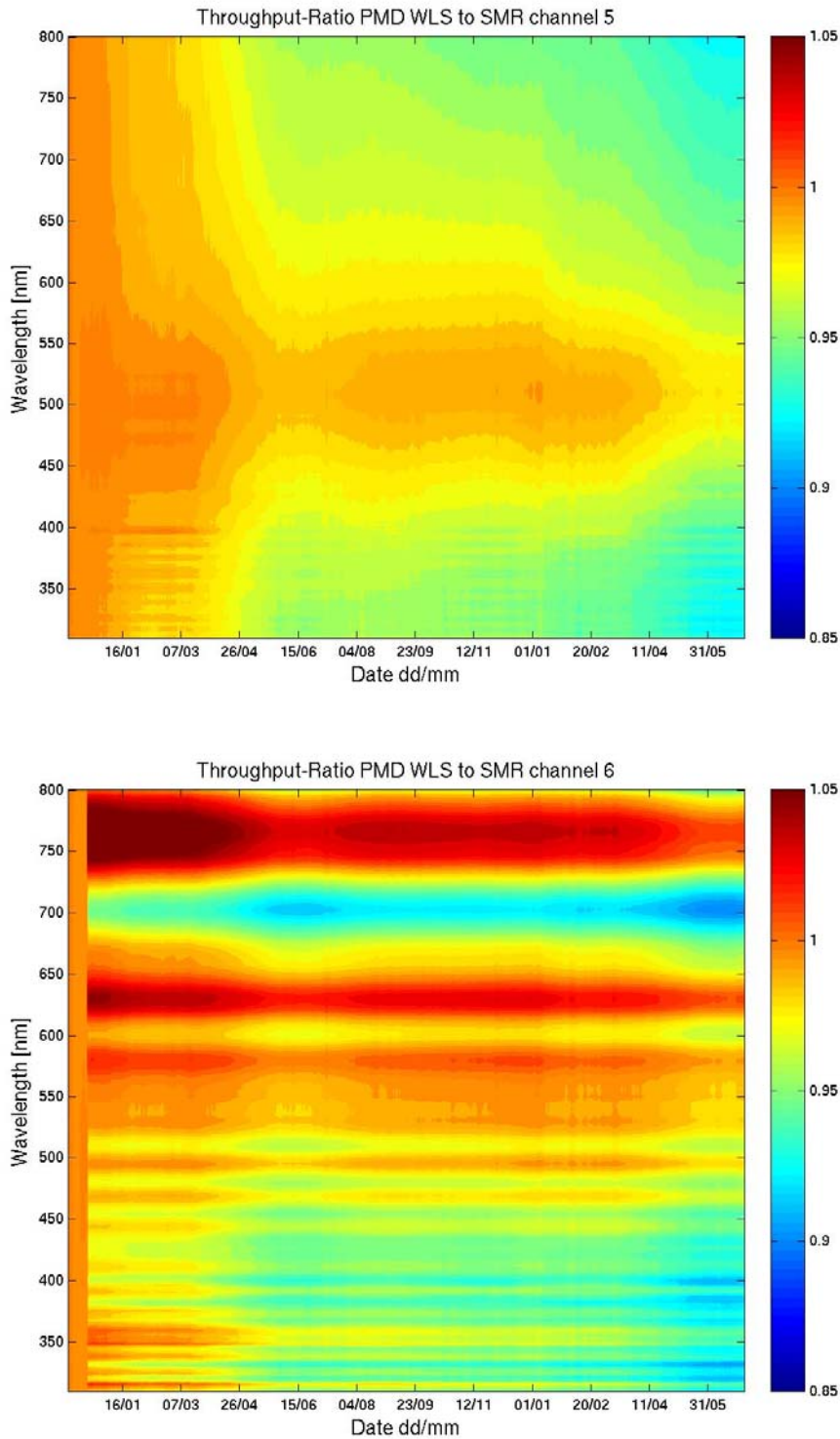


Figure 5-22: GOME WLS v SMR Throughput for PMD Channels (Upper pane PMD-P, lower panel PMD-S).

Note, the etalon structure for PMD-S is an artefact of an anomaly introduced at 28 November 2012 and resolved at the 21 December 2012 in the on-ground processing. It can only be resolved by reprocessing of the full archive.

From Figure 5-21 and Figure 5-22, it can be seen that there is a strong wavelength dependency for the WLS v SMR throughput. In the wavelength range 300-400nm and 700 + nm, the throughput as measured by WLS is as much as 5% lower than that of SMR at an increasing rate. The throughput loss is similar only in the region of 500 nm. In the UV (below 290 nm) the output levels of the WLS are too low with respect to the solar measurements to provide reliable results.

The extra loss of throughput as measured by the QTH Lamp could either be due to some mirror angle / wavelength cross coupling if the source of the throughput loss is the scan mirror surface. However, since the WLS throughput has fallen at the same rate as SMR or quicker (depending on wavelength) it is more likely that the absorption spectra of the tungsten-halide soot is being observed.

The QTH test was performed in August 2009 on Metop-A without conclusive results –there was no increase in throughput. It is now understood that the OMI QTH lamp is operated at 408mA and powered at a higher voltage, consuming 5.32W, much higher than can be achieved on GOME-2.

Signal degradation in itself is not an issue for the instrument since an etalon correction can still be produced in the UV. If the SNR gets too low, options are to increase the integration times or run the lamp at 380mA, however these will only be revisited if and when needed.

Health of the QTH lamp is also confirmed by the Life limited item usage and the very small voltage increase (caused by filament thinning)

5.5.4 Assessment

From analysis of this physical signature, both Lamps appear to be healthy. The HCL ignition time appears to be related to temperature and does not exhibit any additional trend over and above this. There are also no signs of unusual ignition behaviour.

The HCL Voltage and output instability mean that measurements of the diffuser throughput stability are “noisy” and can only be meaningfully interpreted after a couple of years. For details, see Section 5.8.3.

The throughput of the QTH Lamp does appear to be falling faster than that of SMR measurements, indicating Lamp Blackening which is confirmed by the increasing lamp voltage during operation and OMI experience. The extent of blackening which is currently evident is not believed to be a concern for lamp life and in the worst case scenario, longer integration times can be used for Radiometric calibrations.

This observation is very consistent with what has been observed for FM3 over a similar time range.

5.6 GOM04: Detector response stability

5.6.1 Description

LEDs can be used to monitor Pixel to Pixel gain which is used to correct for the pixel to pixel variation of quantum efficiency of the detectors, as well as for identification of hot or dead pixels. Pixel to Pixel gain is measured by using the LEDs mounted directly in front of each detector.

5.6.2 List of Correlated Events

None.

5.6.3 Analysis

LEDs illuminate the detectors uniformly with green light (approximately 550 nm). By comparing the LED measurements with an LED spectrum smoothed over ~5 pixels, an estimate of the pixel-to-pixel gain can be made. We can observe changes in pixel-to-pixel gain changes in the relative behaviour of the quantum efficiency of the detectors. This result must be fed back into other throughput monitoring so that relative changes in pixel performance do not appear as pixel-dependent signatures.

5.6.4 Interpretation

From Figure 5-23 the time series of the standard deviation of Pixel to Pixel gain over each channel of the FPA and PMD detectors remain fairly constant in all main channels and well within expectations.

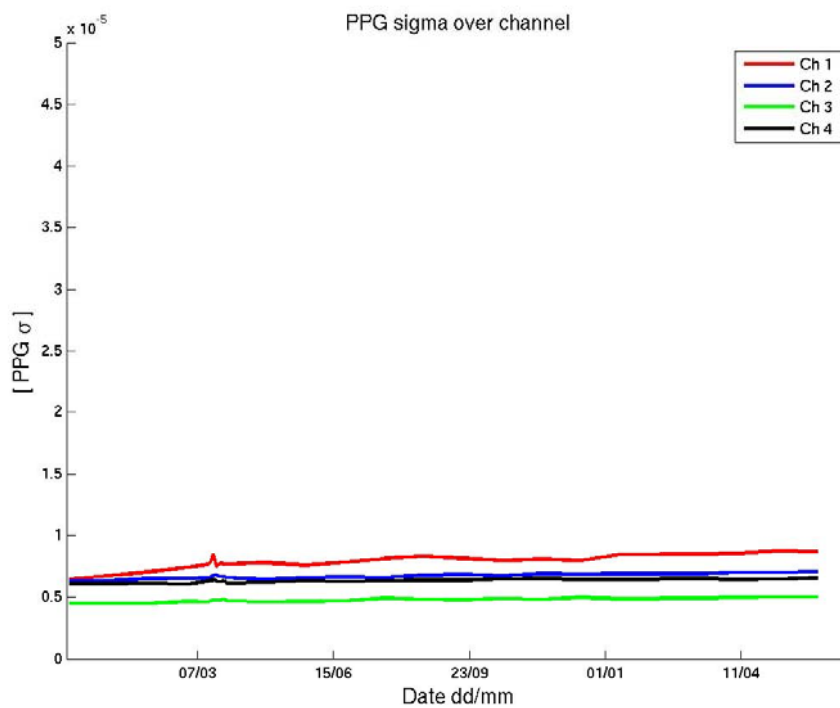


Figure 5-23: Time series of PPG standard deviation over the channel in all four main channels (red: channel 1, blue: channel 2, green: channel 3, black: channel 4)

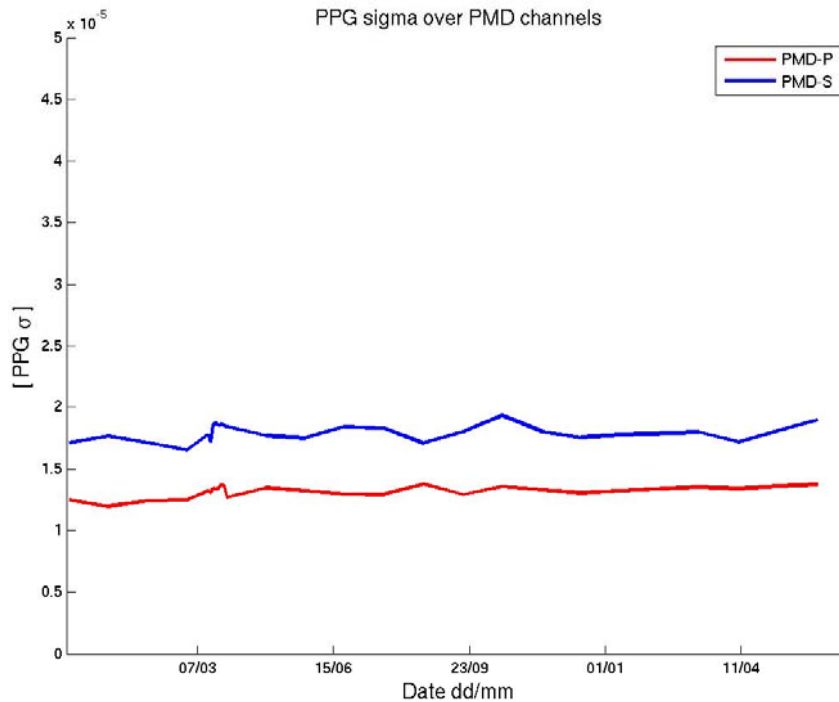


Figure 5-24: Time series of PPG standard deviation over the channel in PMD channels (red: PMD-P, blue: PMD-S)

5.6.5 Assessment

The pixel to pixel gain appears to be quite stable in all channels. Vertical lines in the plots are the results of non-nominal operations conditions like IOV and Darkness test periods.

5.7 GOM05: Spectral Stability

5.7.1 Description

SLS measurements are primarily used for pixel to wavelength mapping and also to monitor the spectral stability of the instrument which is important for the maintenance of product quality. The strength of the measured SLS lines is also an important result that must be used in the throughput monitoring. When the intensity of individual lines falls below specified thresholds they are no longer deemed reliable for use in spectral calibration. SLS measurements are made daily and the positions of spectral lines on the detectors are monitored.

5.7.2 List of Correlated Events

None

5.7.3 Analysis

The plots in Figure 5-25 show the results derived from maximum spectral line signals and daily spectral calibrations at various wavelengths. The wavelength that is being measured by a particular pixel is calculated and that trend is displayed throughout the reporting period.

The wavelength range covered per pixel is given in Table 5-2 below.

<i>Channel</i>	<i>1</i>	<i>1</i>	<i>2</i>	<i>2</i>	<i>3</i>	<i>4</i>	<i>5/6</i>
Band	1A	1B	2A	2B	3	4	PMD P/S
Used Pixels	877/659	147/365	71	953	1024	1024	256
Spectral Range (nm)	240-307/283	307/283-315	290-300	300-412	401-600	590-790	290-790
nm/pixel	0.07	0.07	0.09	0.09	0.2	0.2	2
Predefined dark signal electronic offset (BU)	1501	1501	1503	1503	1495	1492	1503/1499

Table 5-2 GOME Wavelength Range per Pixel for all main channels

5.7.4 Interpretation

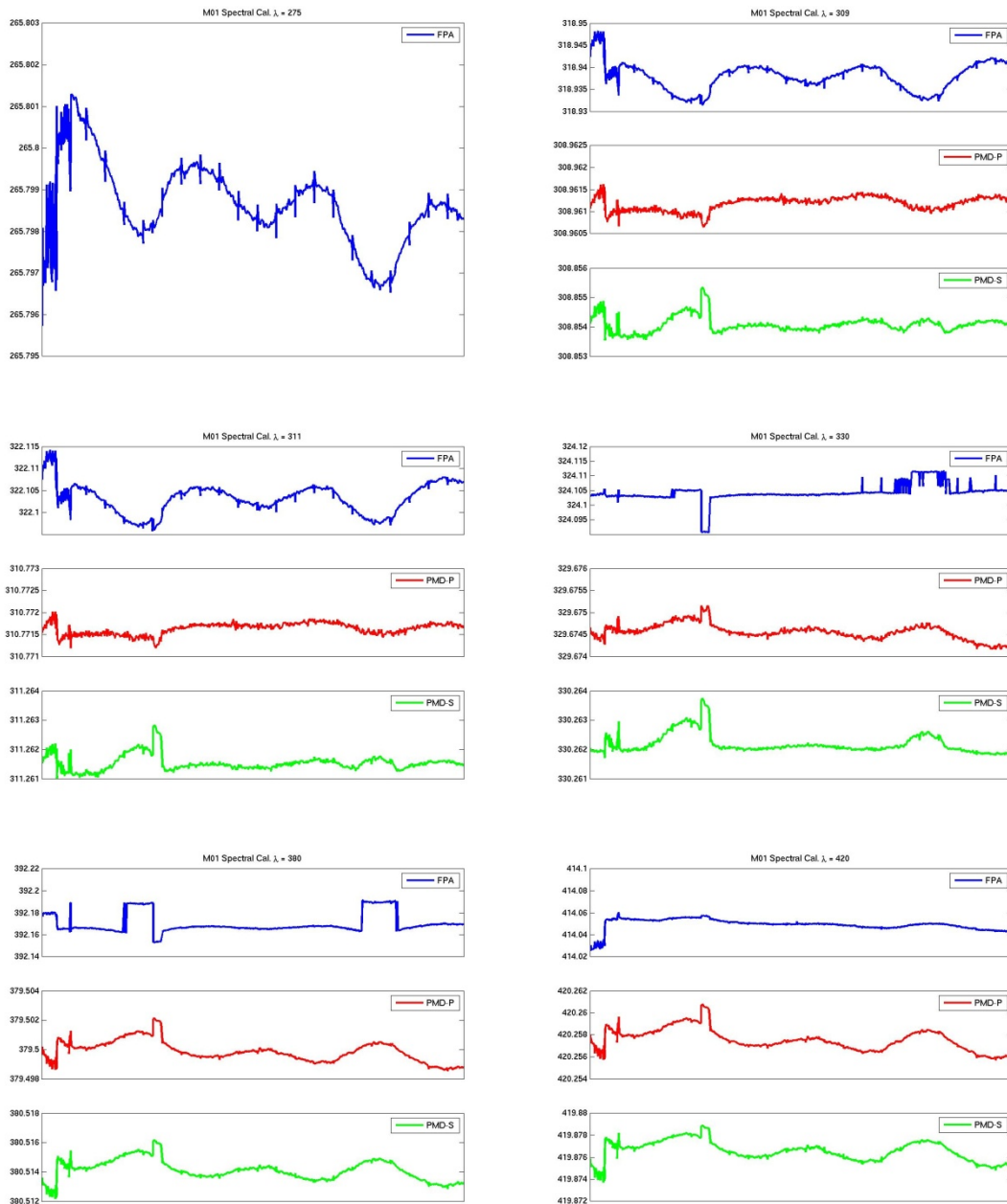


Figure 5-25: Spectral stability at various wavelengths between November 2012 and October 2013 and for main channels and PMD channels at 275, 309, 310, 330, 380 and 420 nm. The initial step functions are due to thermal environment changes during IOV, the second step function during 2 weeks in March 2013 is due to the darkness-test and the slight thermal environment change then. There is a step function visible at the end of channel 2 starting end of January for both 2013 and 2014 at 330 and 380 nm which is due to changing polynomial solutions in different OB regimes.

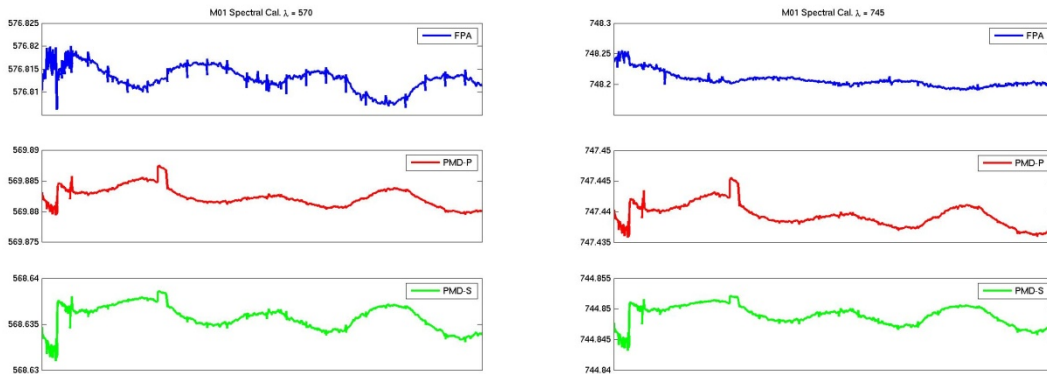


Figure 5-26: Same as Figure 5-25 but at 570 and 745 nm.

From Figure 5-25, it can be seen that spectral stability is quite stable at all wavelengths. Step functions observed can be attributed to the events listed before, which have an effect on the thermal environment (IOV, darkness test) and these are evident in these plots. In addition the polynomial solution for the dispersion in channel 2 changes in January for some period potentially owing to larger-occurring OB temperature regimes during this period (see Figure 5-4) towards lower temperature and coming back by beginning of April (coinciding with the end of the darkness test period). This had a significant effect on the spectral assignment of the detector pixels at the end of channel 2 (approximately 380 nm) and highlights again the very sensitive relationship of OB-temperature and any aspect of spectral dispersion.

Figure 5-27 shows the stability of the spectral co-registration between PMD-P and S in % per detector pixel spectral width. The results demonstrate the strong stability of the co-registration outside the special events regime.

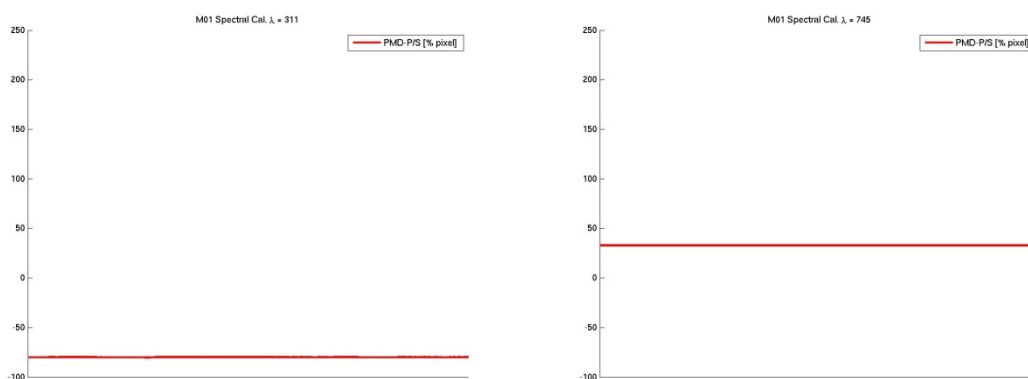


Figure 5-27 Spectral stability of the co-registration between PMD-P and S in percentage of fractional detector pixel around 311 and 745 nm.

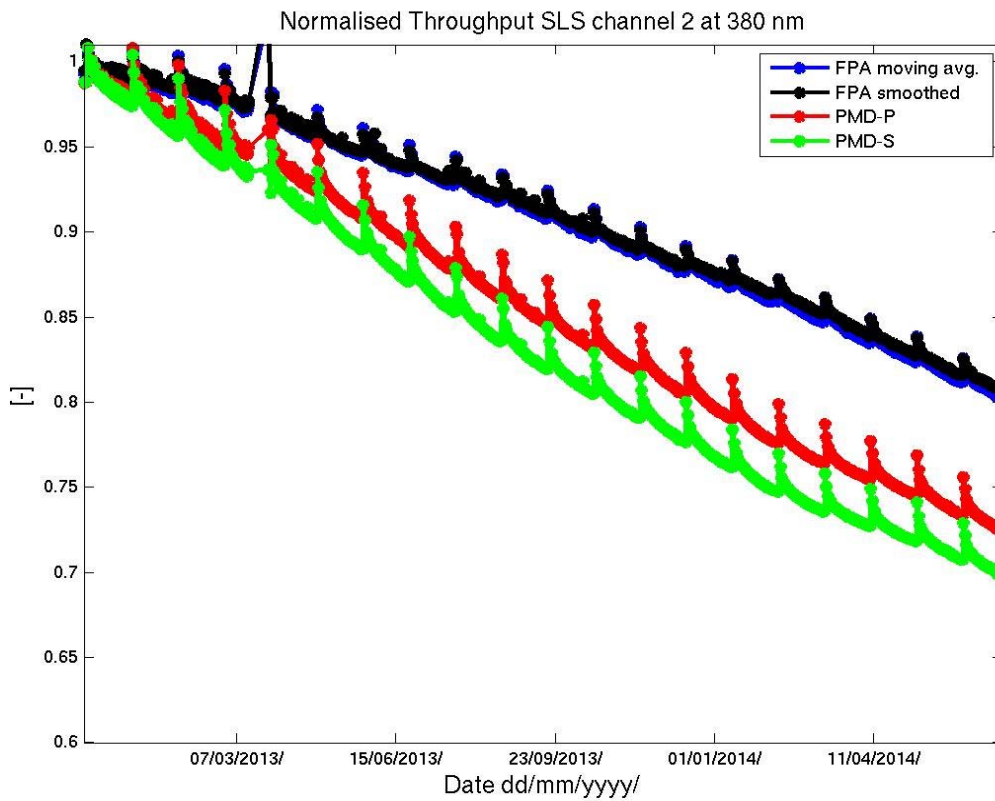


Figure 5-28: Signal strength of 380 nm spectral line.

Figure 5-28 finally shows the signal strength around the 380 nm spectral lines, spectrally smoothed for FPAs. There is no sign that change in signal triggered the observed change in spectral calibration by the end of channel 2 at the beginning of February 2013.

Figure 5-29 shows the variation of the FWHM using a set of distinct SLS lines, which are well separated from their neighbours in order to allow for a stable gaussian shape fitting. Note, that the applied gaussian shape is normal, and no distortion is applied, although the line shape is non to be assymetrical. Nevertheless, in case everything is stable, the derived FWHM should also be stable. However, it has been observed for FM3 that this is not the case and that the change in FWHM follows very closely the in-orbit OB temperature. For FM2 the situation is as follows:

- 1) A spectrally well-ordered pattern (see Figure 5-29) resembling closely the timescale of the degradation during which the FWHM is continously decreasing especially for the lower wavelength range. A similar pattern has been observed by users of level-1 data using solar Fraunhofer lines. The long-term change is well anti-correlated with the optical bench temperature of the instrument over the same time range (see Figure 5-4).
- 2) On top of that, the FWHM varies significantly with the in-orbit change in the thermal environment and therefore following as seasonal pattern. The latter can easily be verified when comparing the seasonal signals with the OB temperature provided in Figure 5-4. The seasonal signal of FWHM changes is corelated with the OB temperature for channel 1, 3 and 4, while channel 2 is anti-corelated.

- 3) The FWHM also changes over the orbit as shown in the FM3 instrument reprot. The FWHM is there derived from Fraunhofer line fitting in the Earthshine spectrum (courtesy A. Richter, IUP Bremen). For the investigated case in channel 3 at 455 nm the signature is correlated with the OB temperatures.

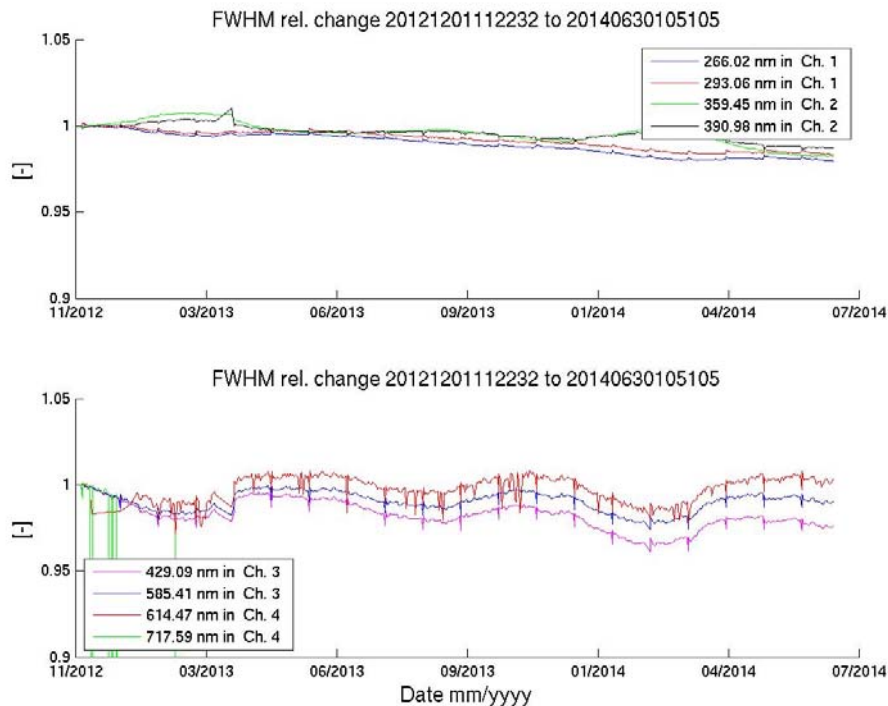


Figure 5-29: FWHM relative change with respect to November 2012 evaluated from a regular Gaussian fitting of well separated SLS lines. Upper panel shows the results in channel 1 and 2. The lower panel results for channel 3 and 4.

Note: A detailed evaluation of the underlying mechanism is provided in the instrument review report for FM3. Note that this issue is a design feature and therefore the analysis as carried out for FM3 is expected to be valid for FM2.

Figure 5-30 shows the difference in the centre line position with respect to November 2012. This variation basically reflects the origin of changes which translate into changes observed in the overall spectral calibration in Figure 5-25 and Figure 5-26. The change in the centre-line position does not exhibit any long term trend and is predominately correlated with seasonal changes (and orbital as known from level-2 retrievals) of the OB temperature.

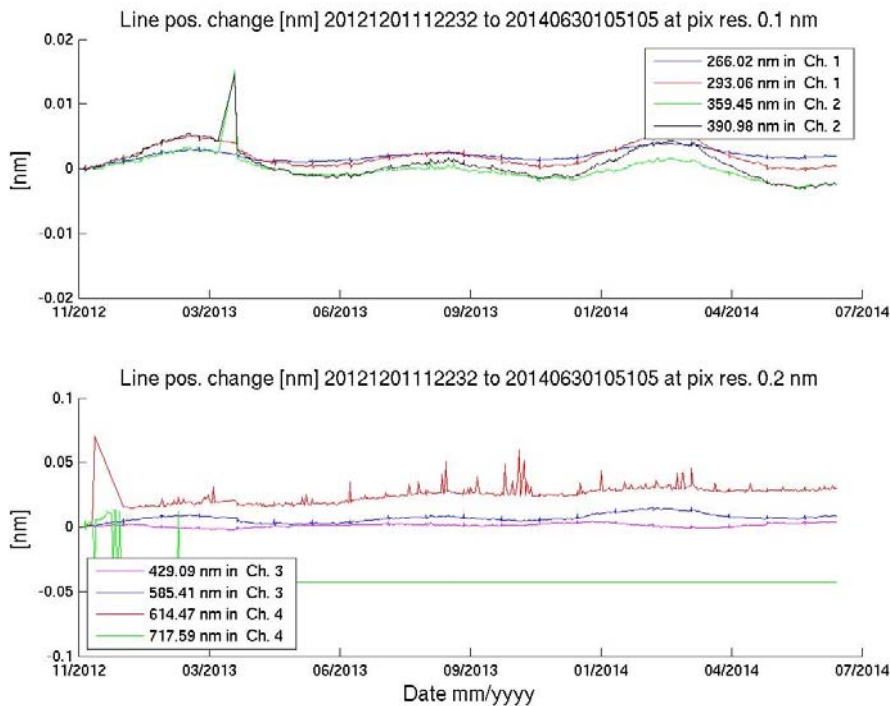


Figure 5-30: Difference of the centre line position with respect to November 2012 evaluated from a regular Gaussian fitting of well separated SLS lines. Upper panel shows the results in channel 1 and 2. The lower panel results for channel 3 and 4.

5.7.5 Assessment

Step functions observed can be attributed to the events listed before, which have an effect on the thermal environment (IOV, darkness test) and these are evident in these plots. In addition the polynomial solution for the dispersion in channel 2 changes in January for some period potentially owing to larger-occurring OB temperature regimes during this period (see Figure 5-4) towards lower temperature and coming back by beginning of April (coinciding with the end of the darkness test period). This had a significant effect on the spectral assignment of the detector pixels at the end of channel 2 (approximately 380 nm) and highlights again the very sensitive relationship of OB-temperature and any aspect of spectral dispersion. This is to be expected since changes in temperature will cause slight movement of the optical components of the instrument.

The FWHM to OB temperature relations as observed for FM3 are also consistently observed for FM2 during its first years in orbit and thanks to the same underlying mechanism: the increased thermal sensitivity due to the defocusing of the instrument in order to increase the spectral oversampling. For details we refer to the FM3 report.

Apart from the seasonal variation in spectral stability, it is also possible to see changes on short timescales due to switch-off events, dedicated test (darkness test in March 2013) and the IOV periods.

Overall, the spectral calibration of the instrument varies well within the sub-detector pixel range since end of November 2013 and the variation in the centre line position is translated in the change in spectral calibration, which in turn is known to be closely related to changes in the seasonal and orbital time-scales of the OB temperature.

5.8 GOM06: Throughput Stability

5.8.1 Description

Throughput measurements are made using a variety of techniques. The use of different techniques allows isolation of various components in the optical path.

5.8.2 List of Correlated Events

None

5.8.3 Analysis

Please note that the results and the impact of the observed long-term degradation and the first and second throughput test on instrument throughput performance are not discussed as part of the main body of this report. However we do note that the observed throughput degradation of FM3 is obviously an essential ‘feature’ of the instrument performance and will very likely continue to be so. In order to streamline the reporting on this issue to various parties and stake-holders we want to focus in the future on updating one dedicated report on the matter only. For earlier analysis of the throughput degradation and on the issuing of the throughput tests and their initial analysis, we refer to [AD.3] [AD.6] and [AD.7].

Results of continuous throughput degradation analysis carried out at EUMETSAT and results of the analysis on the matter by the joint EUMETSAT and ESA assessment team are now documented in a dedicated report issued by the EUMETSAT GOME-2 instrument engineer (version 2 issued in September 2010). This report will replace and supersede the previous reports on the issue and will be updated on a regular basis. For the analysis of the GOME-2 FM3 throughput degradation we therefore refer to this report [AD.8] and to the latest validation report of the reprocessed level 1 dataset release 2 (G2RP-R2) [AD.9]. Also see Investigation on GOME-2 throughput degradation, version 2, (EUM/LEO/REP/09/0732).

Figure 5-31 provides an example of signal degradation for all calibration sources (SLS, WLS, SMR and LED) at 275 nm in channel 1 (LED at approximately 570 nm) until 1st of July 2014. The SMR signal exhibits peculiar variations which we refer to deficiencies in the on-ground key-data for the angular irradiance response (AIRR) characterisation in solar azimuthal direction. The drop in LED output after the dark signal test in March 2013 (as shown in Figure 5-19) is also visible in this time series. Since none of the other sources are experiencing such a drop this may be referred to as being an impact at the LED source/output itself following the test. The drop is visible in all four channels

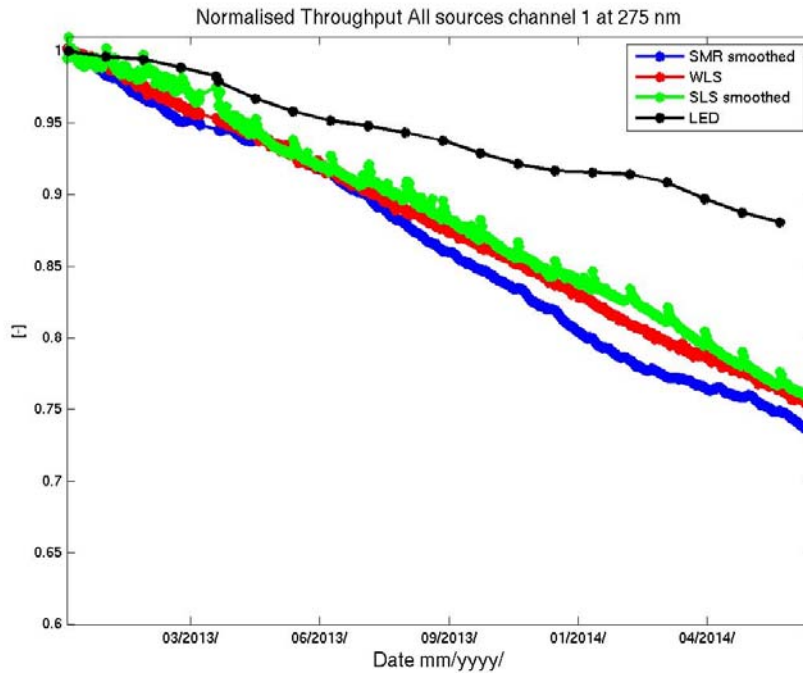


Figure 5-31: Signal degradation of SMR, SLS, WLS and LED sources at 275 nm in channel 1 (LED at approx. 570 nm) normalised to 01 December 2012

Comparisons of signal degradation between FM2 and FM3 on Metop-B and A reveal similar patterns of signal degradations in all channels over a period of 547 days starting after 102 days in orbit for both instruments (see Figure 5-32 and Figure 5-33). Notable differences are however observed in main channel 2 (see Figure 5-32) and for PMD-S for which degradation rates over the observed period seem overall lower and stronger respectively for FM2.

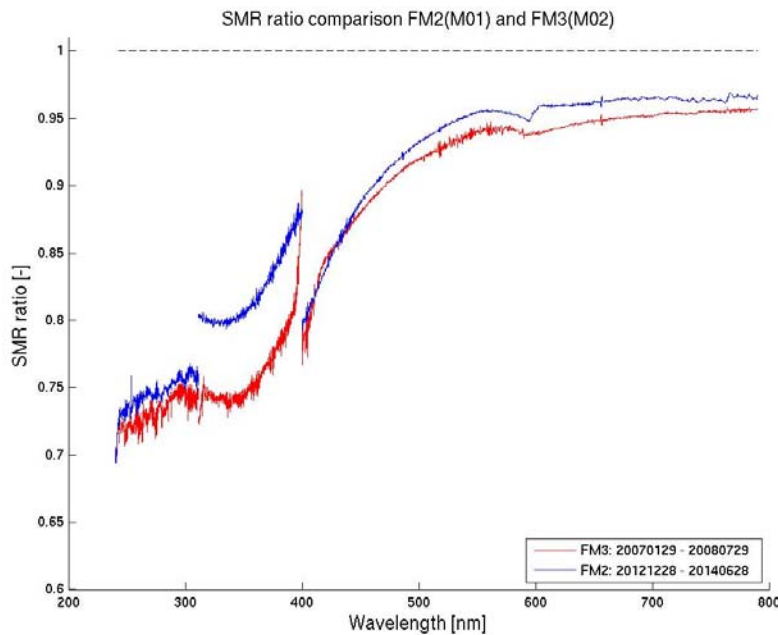


Figure 5-32: Signal degradation (SMR ratio values; see legend) of GOME-2 FM2 (blue line) and FM3 (red line) over a period of 547 days and after both instruments have been in-orbit for 102 days.

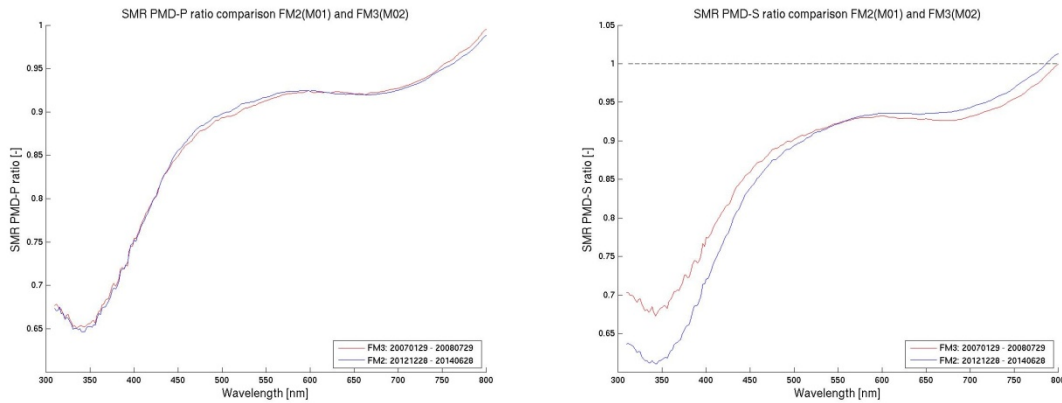


Figure 5-33: Same as Figure 5-32 but for PMD-P (left panel) and PMD-S (right panel) respectively

Figure 5-32 shows the throughput degradation of FM2 Metop-B at 570 nm (channel 3) between 28 November 2012 and 28 June 2014 for solar mean reference (SMR), white light source (WLS) and LED data. The plot is accompanied by a FM3 Metop-A plot covering a similar period in orbit (28 Feb to 29 July 2008). All calibration sources behave very different after the period of the darkness test end of March 2013. WLS and SLS signals behave however as expected with respect to each other. See Section 5.5. The LED signal seems to decrease stronger than the WLS at a wavelength similar to the LED emitted light.

Comparisons for the LED signals between Metop-A and B done in a similar fashion than for the SMR but over the first 500 days period after 102 days in orbit reveal however a very similar picture than observed for SMR.

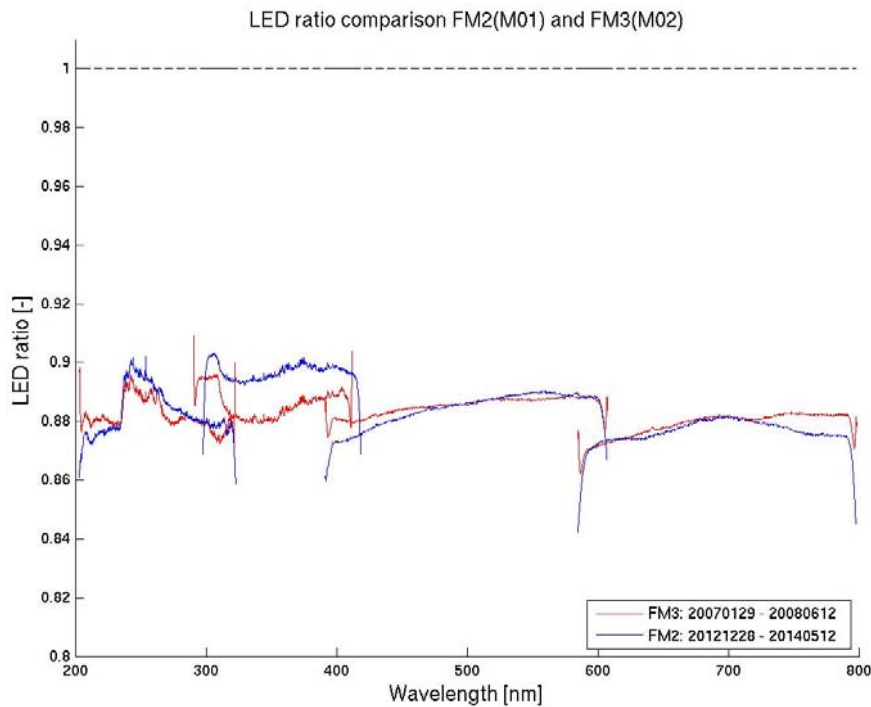


Figure 5-34: Signal degradation for LED (ratio values; see legend) of GOME-2 FM2 (blue line) and FM3 (red line) over a period of 500 days and after both instruments have been in-orbit for 102 days.

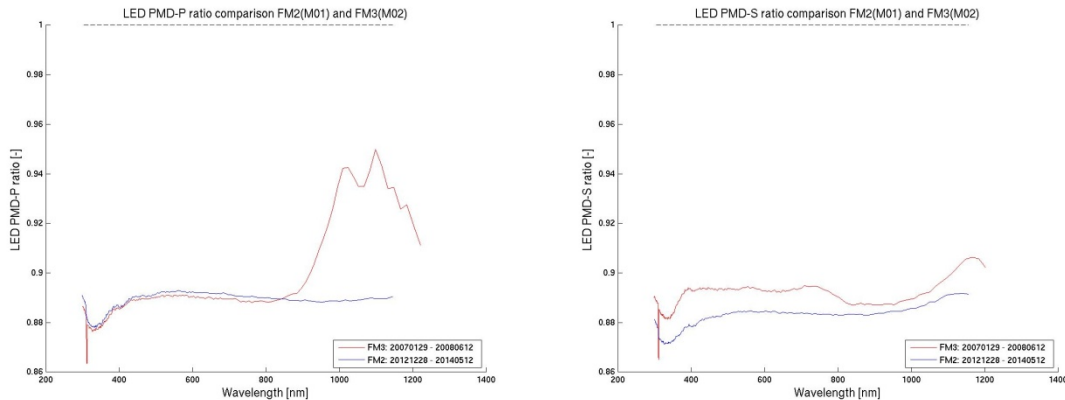


Figure 5-35: Same as Figure 5-34 but for PMD-P (left panel) and PMD-S (right panel) respectively

Figure 5-34 and Figure 5-35 show that relative degradation of LED signals show the same overall consistent behaviour as for SMR, again with the exception of channel 2, where also LED degradation for FM2 is weaker than for FM3. This places the origin of the latter difference at detector level. The same conclusion might be drawn for observed differences in degradation between FM2 and FM3 for PMDs.

Note: Since monthly measurements of diffuser signal are known to be “noisy” the current time period of FM2 in-orbit is not sufficient to draw conclusions on diffuser degradation.

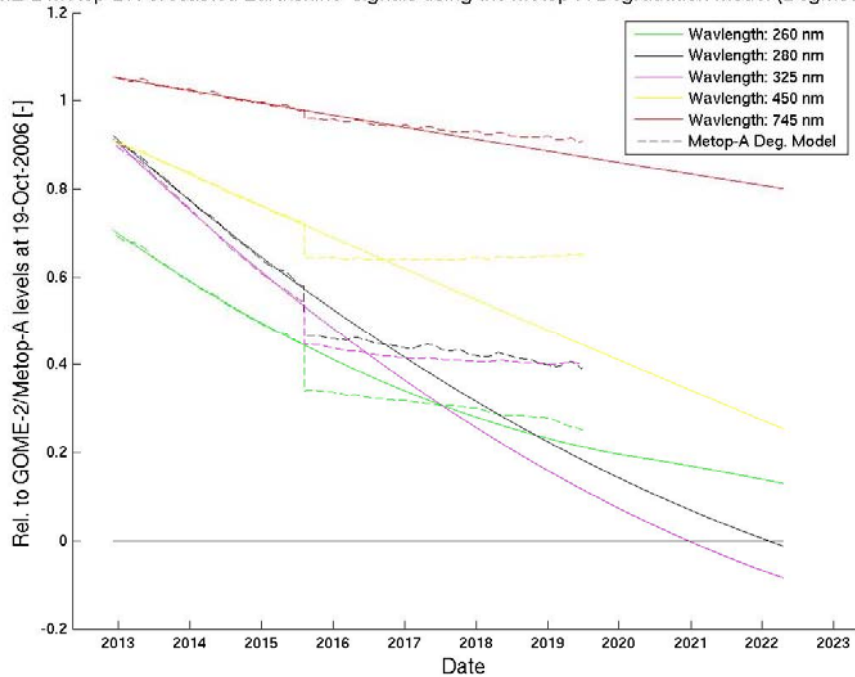
Since the overall signal evolution of GOME-2 / Metop-B is very similar to the one for Metop-A it seems justified that a signal evolution projection might be undertaken based on the signal degradation model version 0.9 meanwhile available for Metop-A (for details see Metop-A report).

This version 0.9 of the GOME-2 /Metop-A degradation model provides us with the possibility to forward project the signal evolution for GOME-2 / Metop-B at various representative wavelengths until the end of commissioning of EPS-SG (end of Metop-B/C tandem operations).

Figure 5-36 shows the evolution of the Earthshine signal averaged over all viewing angles for selected wavelength in all channels. For Metop-B the period before the Second throughput test (TT) is used as basis for the projection (solid line) until the 2022 time frame (launch of EPS-SG). The dashed line shows the underlying model of the Metop-A degradation. In case the signal gradient of the projection based on pre-Second TT times maps the gradients of the post Second TT evolution of Metop-A the latter signal is used as a basis for the projection. This turns out to be however only the case for the lowest wavelength (here 260 nm) where the initial signal evolution is more parabolic than for longer wavelength.

Next to the Earthshine degradation is the solar mean reference signal, shown using the same forecast method.

GOME-2 Metop-B: Forecasted Earthshine signals using the Metop-A Degradation Model (DegModM02ver09)



ME-2 Metop-B: Forecasted Solar Mean Reference signals using the Metop-A Degradation Model (DegModM02)

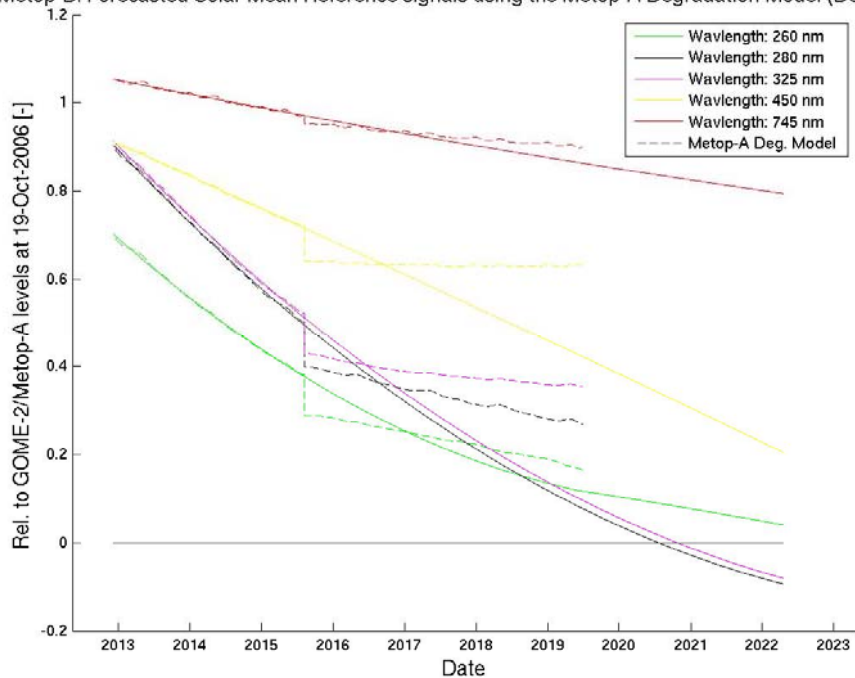


Figure 5-36: Signal evolution for selected wavelength for GOME-2 Metop-B (solid line) based on version 0.9 of the signal degradation model for Metop-A (dashed line). The projection is based on the signal evolution of the pre Second throughput test period of Metop-A. Left panel: Earthshine signal averaged over all viewing directions. Right panel: Solar mean reference signal. For details see text.

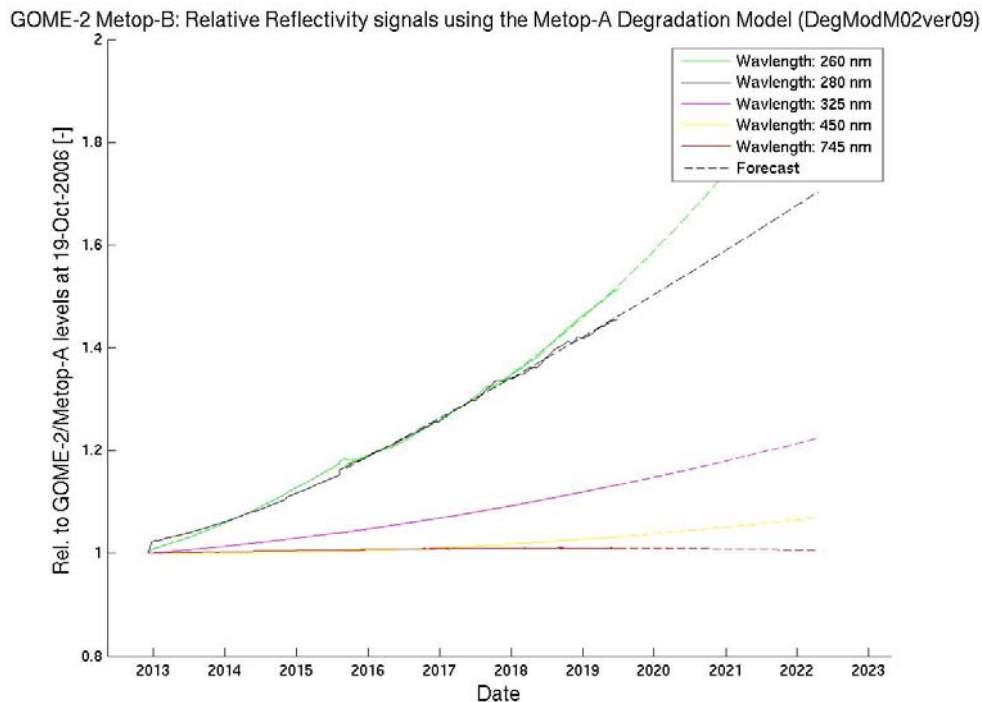


Figure 5-37: Same as Figure 5-36 but for the reflectivity. The dashed line shows the forecasted projection.

Figure 5-37 shows the reflectivity evolution. The reflectivity is the quantity which is commonly used for level-2 retrievals. Since the solar path is degrading faster than the Earthshine path (as discussed in the assessment of the next section) the reflectivity is overall increasing. Decreasing signal levels of radiance and irradiance however lead to larger error bars on the reflectivity values and therefore to larger errors on the retrievals.

5.8.4 Assessment

Comparisons of FM2 and FM3 signal degradation after similar time in-orbit and over the same time-period show similar patterns of degradation in all channels with the exception of main channel 2, for which the intra-channel degradation spectral signature for FM2 resembles the one for FM3 but the overall rates seem to be lower. The same is true for the spectral degradation patterns observed for PMDs, however, there the degradation rates for FM2 seem to be higher especially in the visible to UV region. The same observations can be made when comparing the degradation rates of the LED signals, for which observed differences between FM2 and FM3 are consistent with what is observed for SMR and therefore places the origin of these differences at detector level. The differential degradation leads to increased reflectivity values over time. Based on the pre-Second throughput test signal evolution of Metop-A a projection of signal levels into the future reveals that we can expect still good overall performance of the instrument until the timeframe of EPS-SG commissioning, with however continuous increase in retrieval errors as will be detailed in a forthcoming dedicated study on signal level decrease on GOME-2 Metop-B level-2 product quality.

Currently, it is not possible to derive a meaning full degradation signal for the diffuser because of the noisy nature of the SLS over diffuser measurements (see also FM3 Metop-A instrument report, Section 5.8.3)

5.9 GOM07: Darksignal

5.9.1 Description

The dark signal noise, dark signal offset and leakage are evaluated from dedicated dark measurements at the dark side of the orbit. Dark measurements are taken for different integration times used during calibration and nominal earth scanning measurements and averaged over the valid integration period. The dark signal results are stored in the in-flight calibration file during processing for different temperatures and applied only for the relevant integration time and within a narrow range of the actual temperature.

The dark signal offset and leakage are specified in the PGS to be determined by the level 0 to 1b processor from mean dark signal readouts using a linear fit over integration time. During the analysis of data from the Second throughput test it has been found that this assumption on linearity is valid for the current operational temperatures of the main detectors, but breaks down at temperatures significantly above 280 K and for integration times longer than three seconds. To ensure a robust fit the following analyses have been based on dark measurements with integration times shorter than 3 seconds. The post process of the results from data derived from the operational monitoring database makes sure that results are provided only if a significant amount of measurements is found to ensure a robust fitting result. For band 1A, during parts of the year not enough measurements for a certain integration time are available since they are taken outside of eclipse. Results close to these data gaps are therefore also not trustworthy (because the eclipse might be too shallow at this point in time).

Note : Based on these fitting criteria the only other operations induced change visible in the data is the turning on and off of co-adding in channel 3 (co-adding has been re-introduced at 3 March 2009 with the introduction of new timelines. It had been turned-off earlier in March 2007 shortly after SIOV.

5.9.2 List of Correlated Events

<i>Date</i>	<i>Description</i>	<i>Reference</i>
2013-07-12..2013-08-15	GOME-2 FM2 leakage current increase in band 4 (channel 4)	EUM/OPS/AR/14946
2013-10-28..2014-02-02	leakage current increase in band 4 (channel 4) -Re-occurrence	EUM/OPS/AR/15205
2014-08-20..ongoing	leakage current increase in band 4 (channel 4) -Re-occurrence	EUM/OPS/AR/15205

Table 5-3: List of Correlated Events

5.9.3 Analysis

The following plots show band averaged results for dark signal electronic offset (blue-line) and leakage signal (green line). Note that the dark-signal measurements for different integration times per band are taken at a different part of the orbit and therefore at different SZAs. Even though all dark measurements have so far been assumed to be taken (tagged as “valid”) well within eclipse, recent analysis of the timelines with the new GTL builder tool at EUMETSAT indicate that some of the dark measurements may suffer from (twilight) stray-light, especially when taking the variation of the “shallowness” of the eclipse over the seasonal cycle into account. The latter is likely to cause the observed seasonal cycle in the noise signals, which varies significantly with integration time, which, in turn, are related to different SZA or positions within the eclipse.

The wavelength range covered per band is given in Table 5-4 below.

Channel Number	1	1	2	2	3	4	5/6
Band	1A	1B	2A	2B	3	4	PMD P/S
Band Number	1	2	3	4	5	6	7/8
Used Pixels	877/659	147/365	71	953	1024	1024	256
Spectral Range (nm)	240-307/283	307/283-315	290-300	300-412	401-600	590-790	290-790
nm/pixel	0.07	0.07	0.09	0.09	0.2	0.2	2
Predefined dark signal electronic offset (BU)	1501	1501	1503	1503	1495	1492	1503/1499

Table 5-4 GOME Wavelength Range per Pixel for all main channels

5.9.4 Interpretation

In subsequent graphs, unless otherwise stated, data are presented as follows

- Band-averaged electronic offset signal in BU is in blue on the left axis. Leakage current in BU/sec in green is on the right axis.
- Band-averaged dark signals (for all operationally used integration times) is in blue in BU.

Note: Band 2A data are not reported because the data is outside the valid spectral range.

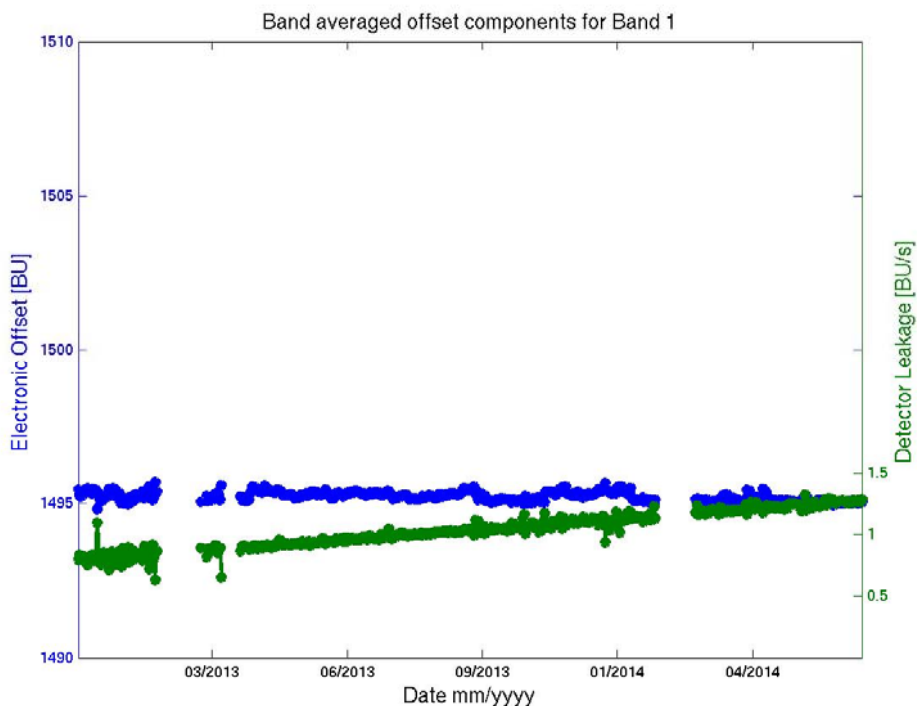


Figure 5-38: Band 1A averaged electronic offset (blue dots) and leakage current (green dots)

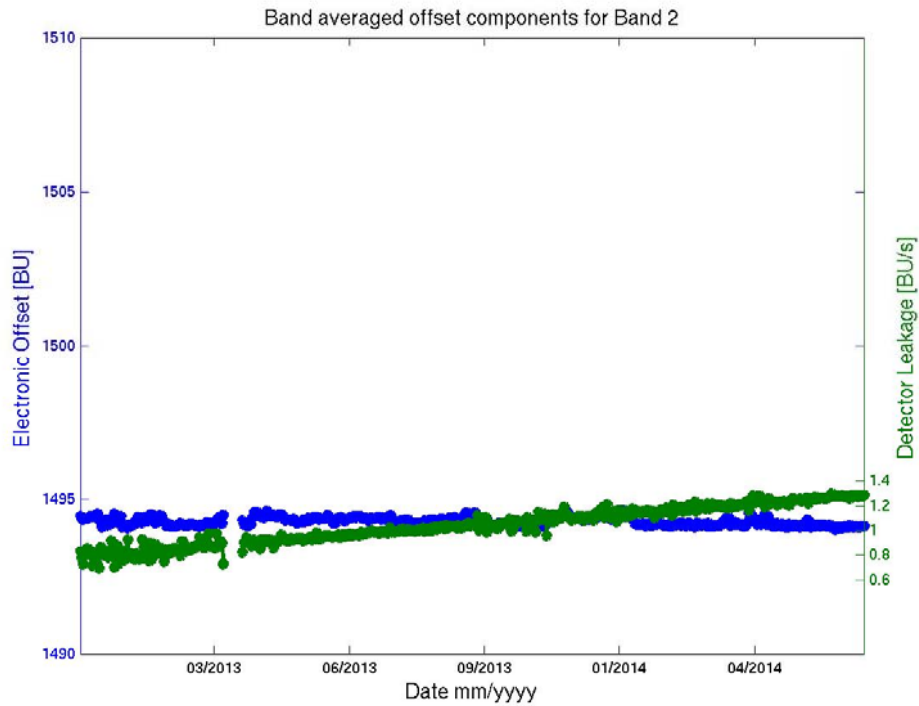


Figure 5-39: Band 1B averaged electronic offset (blue dots) and leakage current (green dots)

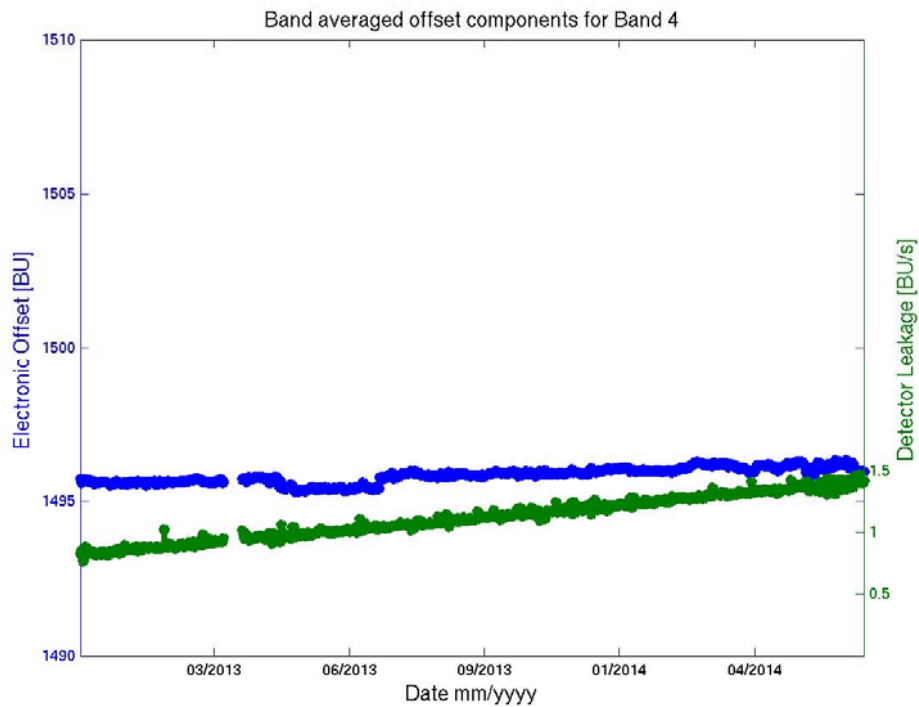


Figure 5-40: Band 2B averaged electronic offset (blue dots) and leakage current (green dots)

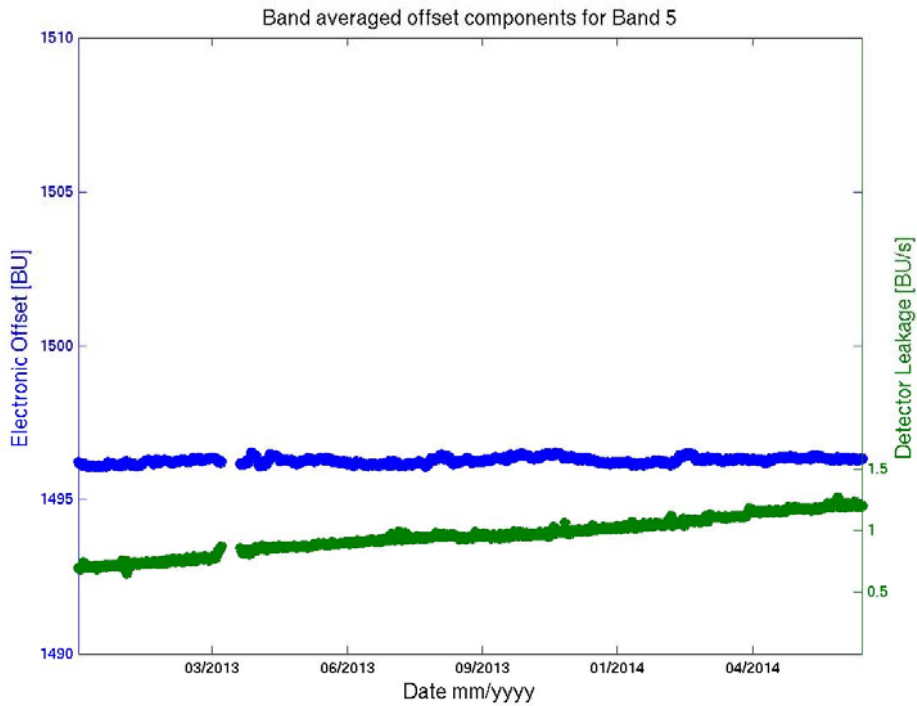


Figure 5-41: Band 3 averaged electronic offset (blue dots) and leakage current (green dots)

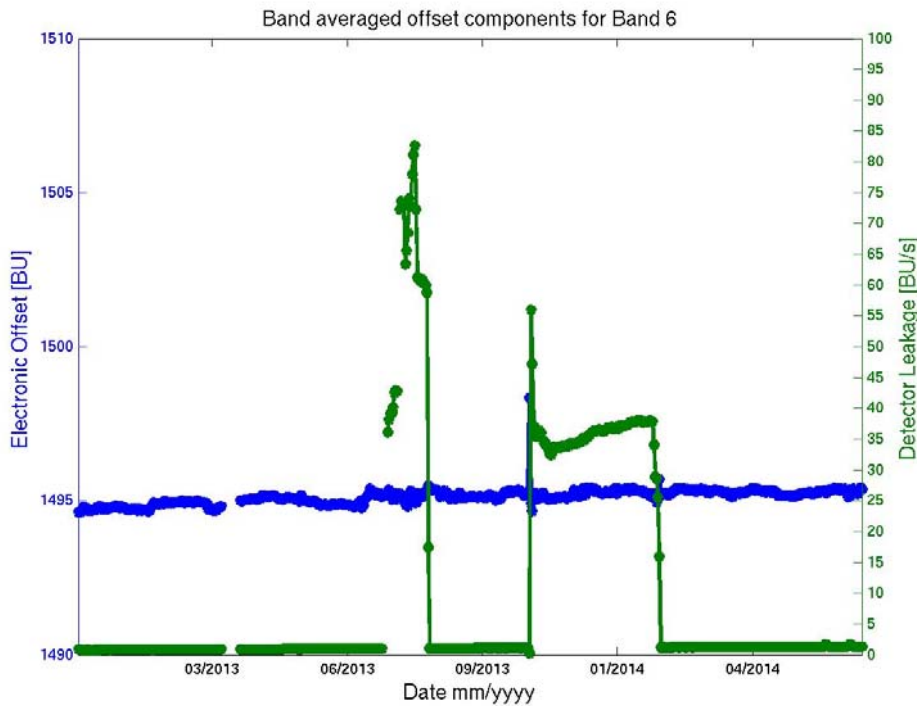


Figure 5-42: Band 4 averaged electronic offset (blue dots) and leakage current (green dots). The sudden increase and recovery during July/August 2013 and November to January 2013/2014 is covered by AD5. Note the difference in Leakage current scale.

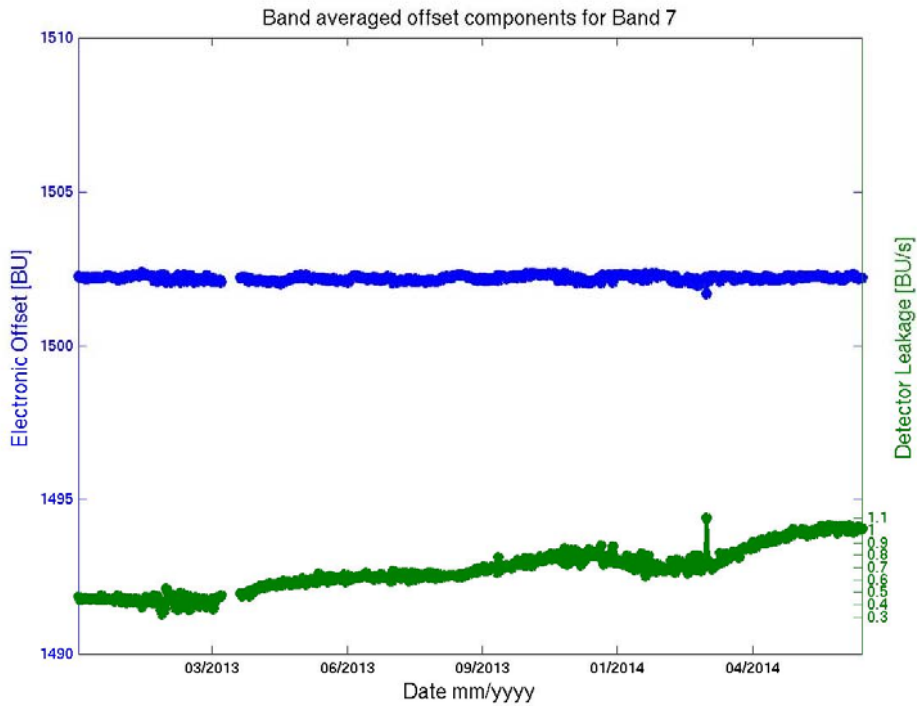


Figure 5-43: PMD-P averaged electronic offset (blue dots) and leakage current (green dots)

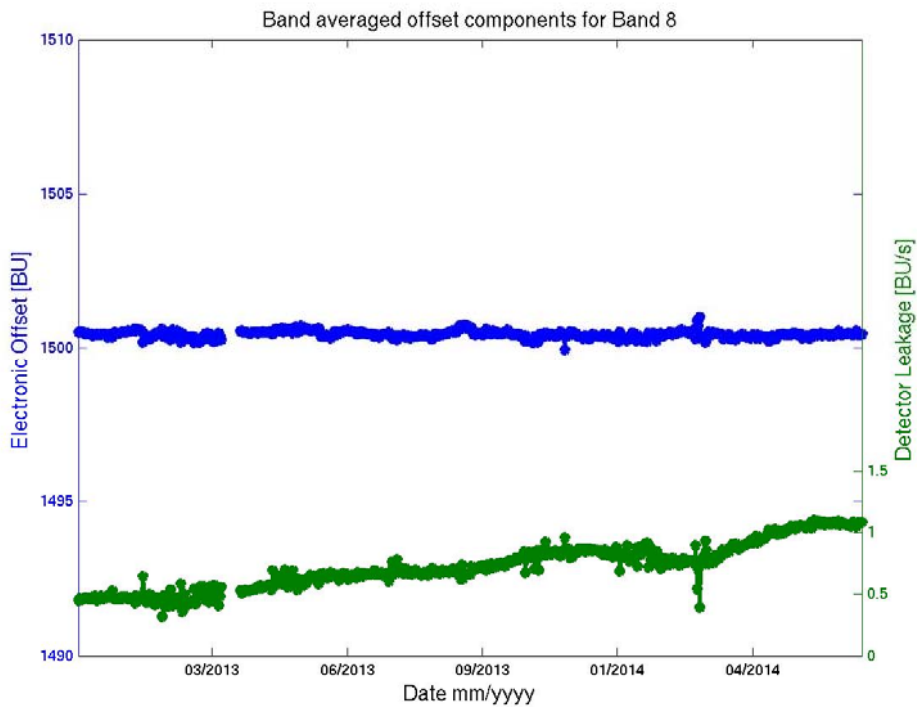


Figure 5-44: PMD-S averaged electronic offset (blue dots) and leakage current (green dots)

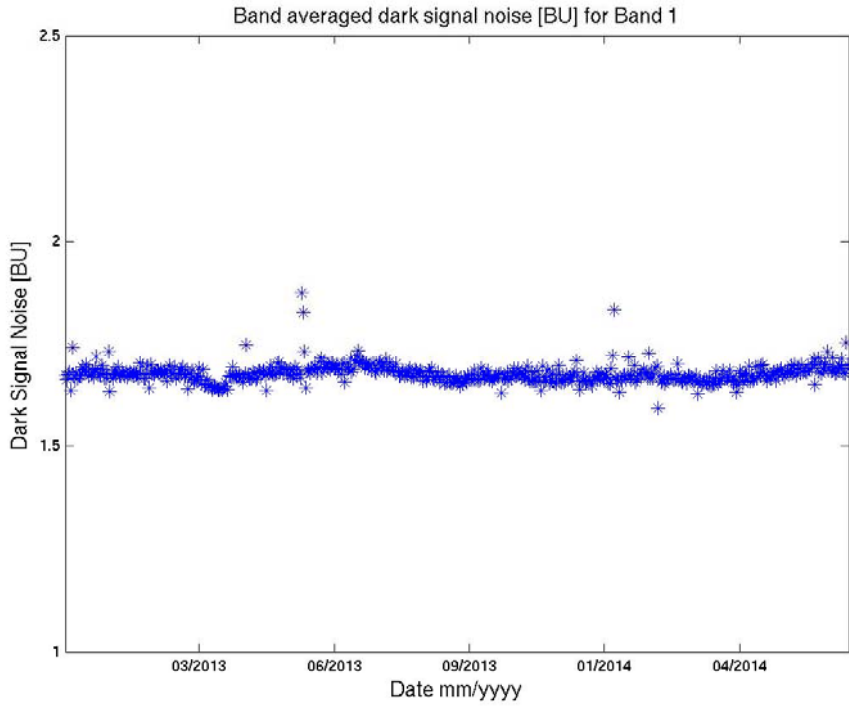


Figure 5-45: Band 1A averaged noise.

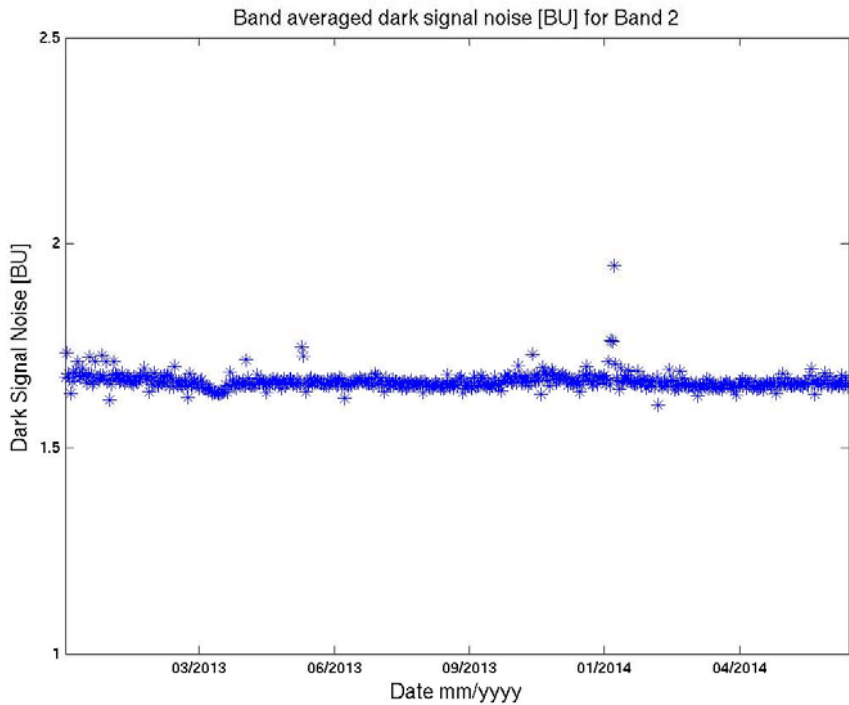


Figure 5-46: Band 1B averaged noise.

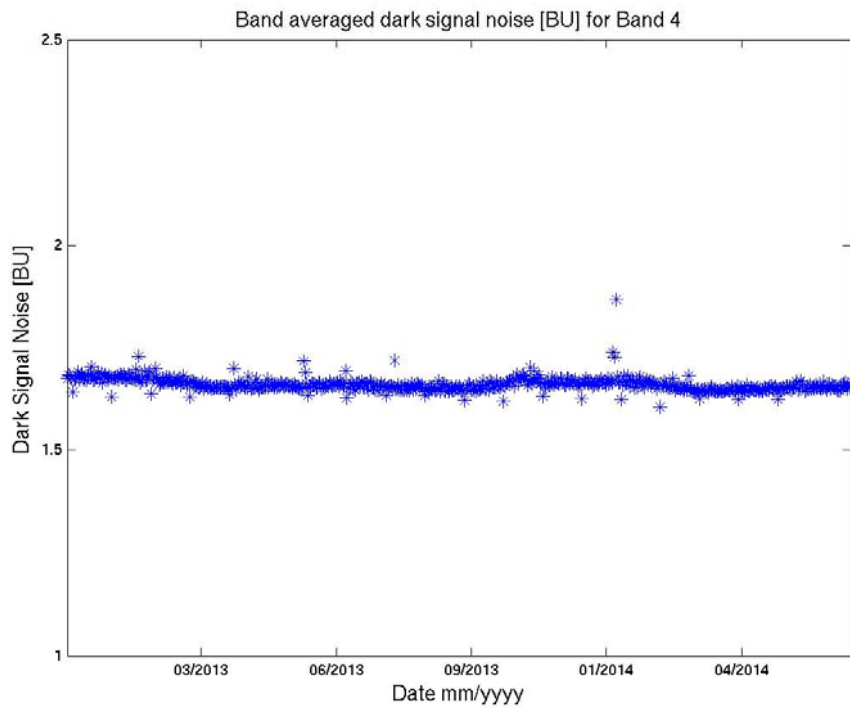


Figure 5-47: Band 2B averaged noise.

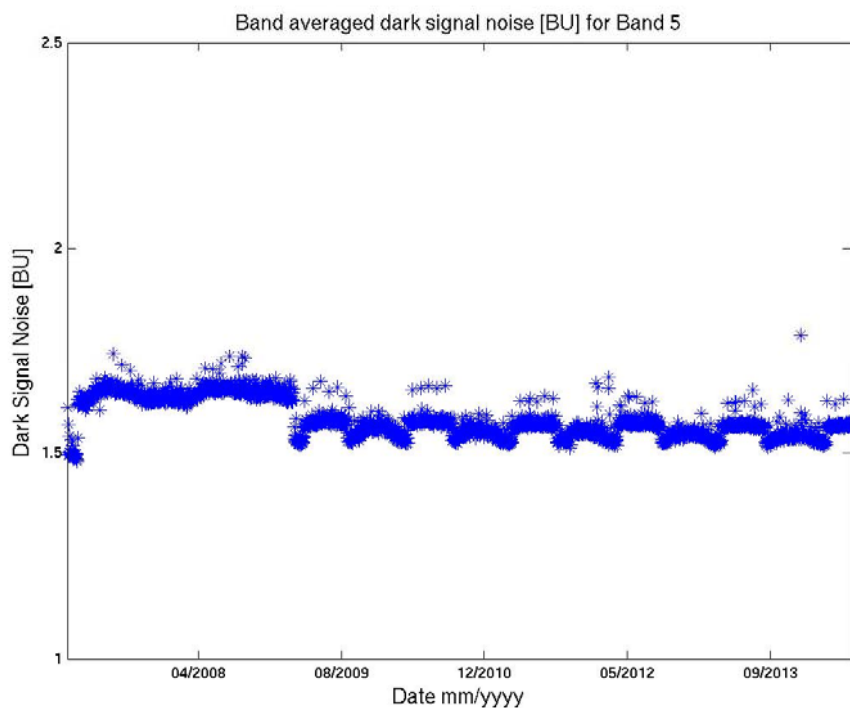


Figure 5-48: Band 3 averaged noise.

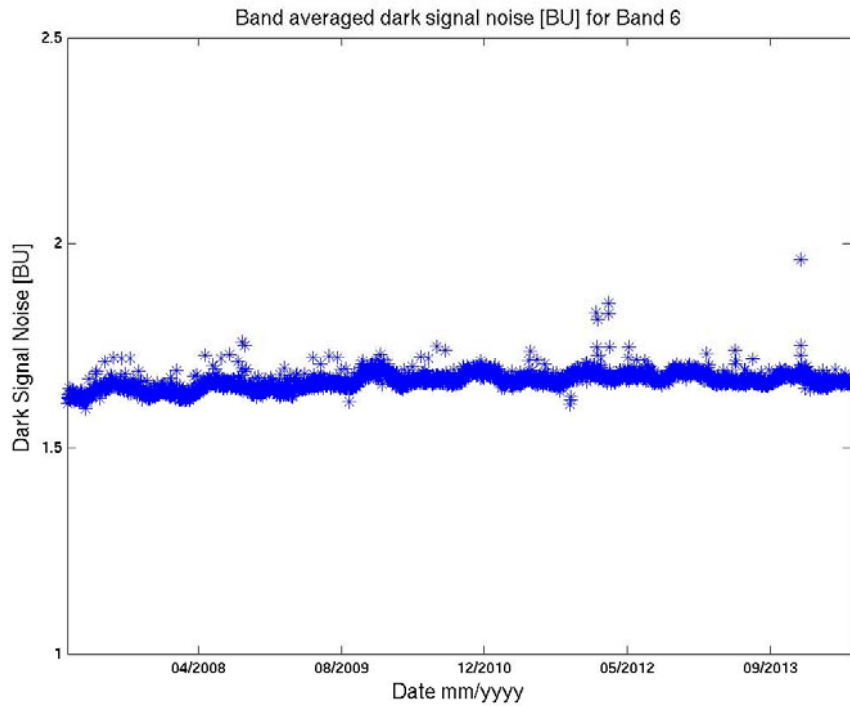


Figure 5-49: Band 4 averaged noise.

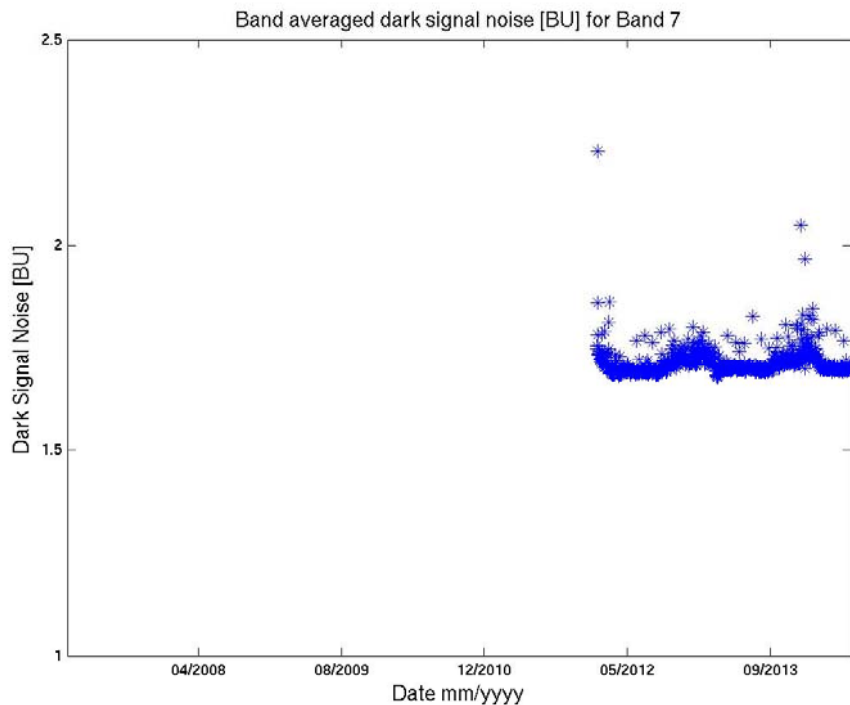


Figure 5-50: PMD-P averaged noise. Due to an ingestion problem in the operational database, noise levels before April 2014 are unfortunately not available for PMDs.

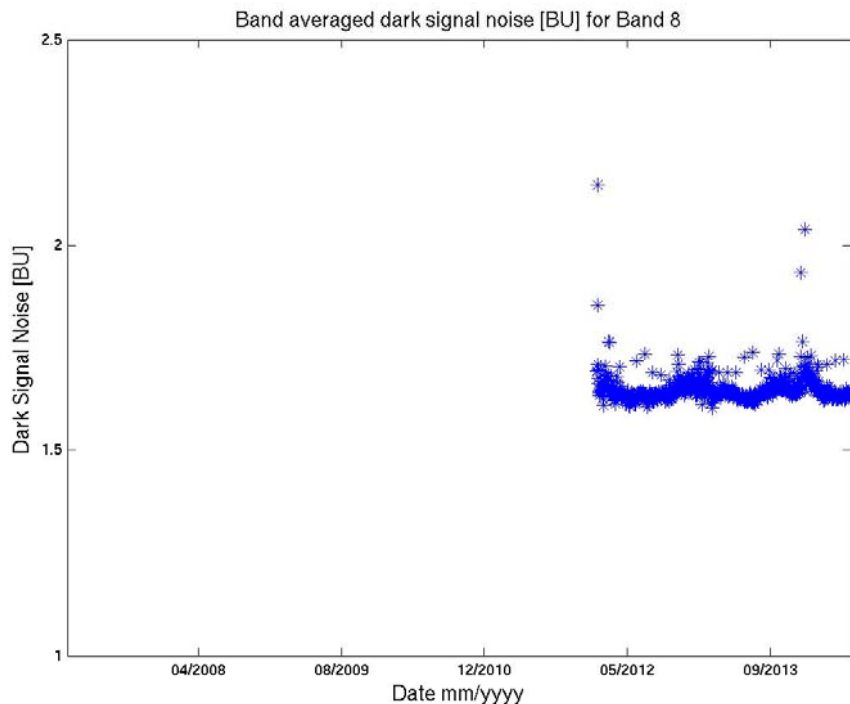


Figure 5-51: PMD-S averaged noise. Due to an ingestion problem in the operational database, noise levels before April 2014 are unfortunately not available for PMDs.

5.9.5 Assessment

There is no increase in the electronic offset baseline visible at this stage of the mission. The leakage current is increasing moderately and at a level significantly less than 0.5 BU/s per year, which is not unexpected for this type of detectors. The exception has been the anomaly in channel 4 of the leakage current during July/August 2013, which is covered in all details in [AD5]. As a result of the investigation and after a recovery to original levels in August the signal re-occurred at the end of November 2013 and lasted until January 2014. Another episode at lower increased signal levels occurred in August 2014. The following has been suggested as rule for operations and the continuous monitoring of the anomaly. See EUM/OPS/AR/15205.8:

The nominal level for the Leakage current in channel 4 is between 1 and 2 BU/sec. In any situation where this value is significantly exceeded (>5BU/sec) the situation has to be monitored at a day to day basis. In principle the latter is done in any case by the operational MPSTAR monitoring system and the on-call team. In case there would be a significant impact on channel 4 level 1 data quality an event/alarm would be raised by the system and taken up by the on-call team. In case we experience a re-occurrence of the anomaly as defined before, any relation with leakage current values and potential channel 4 level-1 quality alarms shall be monitored in addition to the nominal monitoring.

All the previously experienced leakage increases did not have a significant impact on level-1b radiances in channel 4. The largest current so far was 85 BU/sec (August 2013; see Figure 5-42). This may for now be used as an upper limit for a "no -impact" status. All currents above this threshold shall receive increased monitoring attention levels.

Apart from the seasonal cycle contributions depending on SZA (related to specific integration times) within eclipse there is no significant other trending signal visible in the noise pattern. The seasonal cycle is related to the “shallowness” of the SZA within eclipse. Overall, the noise pattern is very stable and slightly below two BU, as expected from pre-flight calibrations.

There is no negative impact from the very small increase in leakage current expected for the near to medium term future, neither on instrument nor on processing level.

5.10 Physical Signatures Conclusion

Overall, the status of the GOME instrument can be considered healthy. Detailed analysis of each physical signature is given in each section.

The main points raised by the analysis and subsequent discussions are as follows:

- HCL Lamp throughput needs to be assessed over a broad spectrum due to apparent instability in throughput which may be caused by a narrow spectral line hovering between two pixels for example. This is handled in the stand-alone throughput document. [AD.8]
- Considering the relationship between HCL throughput, voltage and running time, getting useful data from DIFCAL measurements need is extremely challenging. This is something that needs to be re-considered for Metop-C and/or future missions.
- QTH Lamp Blackening is considered to be a likely cause for differential WLS/SMR throughput loss, however test results and comparison with OMI indicate this is not likely to be curable on GOME-2. Mitigating actions such as increased integration time and running the lamp at a higher current may be considered in future. The impact on lamp life is not considered an issue.
- The FWHM is changing with OB temperature and potentially changing temperature gradients at long-term, seasonal and orbital time scales. The origin is the increased sensitivity of the instrument to thermal changes due to the “defocusing” of the instrument in order to improve spectral oversampling. This phenomenon has to be accepted as a design feature and is similar for FM2 and FM3. This is expected to be similar for FM1.
- The Leakage current increases slightly at below 0.5 BU/s per year. The electronic offset does not show any signs of increase at this point in the mission. An anomalous behaviour of this current is observed in channel 4 (EUM/OPS/AR/15205; [AD5]) but so far did not have an impact on product quality.
- Throughput degradation rates are generally on the order of the ones for FM3 Metop-A covering the same timeframe and at the same mission age. This is also true for their spectral behaviour. The only exception to this are the main channel 2 signals, where degradation rates seem overall lower for FM2 than for FM3, and slightly larger degradation rates for the visible to UV part in PMD-S. The latter differences are very likely originating at detector level since exactly the same signatures are observed when the same analysis is carried out using LED signals.
- GOME scan-unit torque appears to be stable and still has plenty of margin

6 OPERATIONAL CONFIGURATION AND EVOLUTION PLAN

6.1 HW Component Configuration

<i>Component</i>	<i>Description</i>	<i>Routine</i>	<i>Trending</i>	<i>Comments</i>
GEN	General Status	GREEN	→	
CDHU	Control and Data Handling Unit	GREEN	→	
GPDU	GOME Power Distribution Unit	GREEN	→	
CU	Calibration Unit (Including LED's)	GREEN	→	
SU	Scan Unit Electronics and Mechanism	GREEN	→	Torque
OPTICS	All Elements In Optical Path	GREEN	↘	Throughput
PMD	PMD Detectors and Coolers	GREEN	→	
FPA	FPA Detectors and Coolers	GREEN	→	

Table 6-1: HW Component Performance and Configuration

<i>Status Colour</i>	<i>Meaning</i>
GREEN	Fully Operational (or capable of)
YELLOW	Operational with Limitations
ORANGE	Operational with Degraded Performance
RED	Not Operational
BLANK	No Status Reported

<i>Trend Colour</i>	<i>Meaning (with respect to expected behaviour)</i>
→	Stable
↘	Evolution in non-favourable direction
↗	Evolution in favourable direction
BLANK	No Trend Reported

6.2 Lifetime Limited Items

This section lists all those components that have a limited lifetime, indicating the predicted date when the lifetime will expire. For example, a relay that has a limit to the number of on-off switches, a component that has a limited on/off time before expected failure, etc.

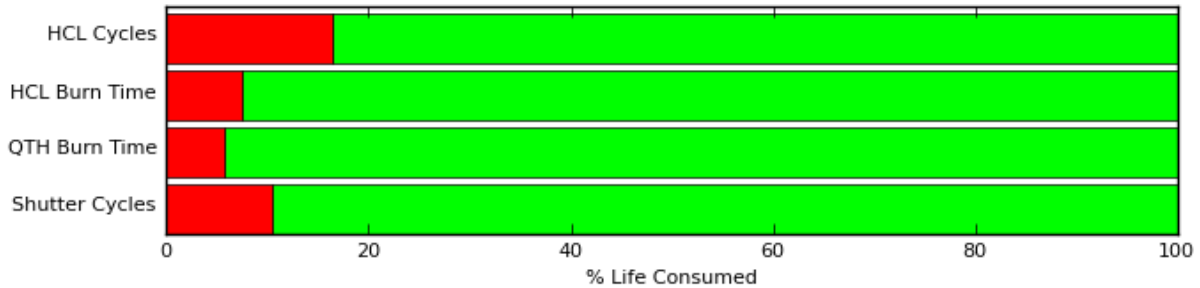


Figure 6-1: Life-limited Item Usage to Sep 2014

Figure 6-1 shows the GOME Life Limited Item usage to Sep 2014. These figures are derived from METOP HK data and are compared to the qualified ratings in section 9 of the GOME IOM.

The main concern is the continued use of the Spectral Lamp at the current rate – this number of cycles will be approaching the qualification limit after ten years in orbit. However, the qualification limits are quite conservative and there is plenty of voltage margin, so this does not cause any concern at present.

6.3 SW Configuration and Evolution Plan

This section provides the current state of the on-board software and tables of the instrument, and any expected evolutions to that software that are expected in the future.

GOME-2 FM2 was launched with software version 2.6.4b, and does not require patching In-Flight with the exception of uploading the latest timeline versions.

There is currently no proposed plan for the software on GOME-2 FM2/Metop-B to evolve. Since the EQSOL (AR.6210) patch is not required for FM1 and 2 due to a hardware fix, version 2.6.4b/c is defined as version 2.6.3a without the AR.6210 patch.

Table 6-2 below shows a summary of actual software versions, bright green being current.

<i>Software Version</i>	<i>Content</i>	<i>Configured as</i>	<i>Full image Available</i>	<i>Note</i>	<i>METOP</i>
2.5	Reference	New Release	Yes	At Launch	A
2.5.1	v2.5 + AR.6210, AR.6674 patches	Patches	No	Patches to ICUuP Only	A
2.6	v2.5 + SCluP reload for AR.7050	New Release	Yes	Evolution of v2.5. Reloading of SCluP only to fix AR.7050. ICUuP patches to fix AR.6210 and AR.6674 not included	A
2.6.1	v2.6 + AR.6210, AR.6674 patches	New Release	Yes	Evolution of 2.5.1	A
2.6.2	v2.6 + AR.6210, AR.6674, AR.6963 and 2.6 bug patches	New Release	Yes	Evolution of v2.6.1	A
2.6.3a	v2.6.2 plus EEPROM default timelines and Metop A identifier	New Release	Yes	Evolution of v2.6.2	A
2.6.4b	v2.6.2 less the AR.6210 patch, plus EEPROM default timelines and Metop B identifier	New Release	Yes	Evolution of v2.6.2	B
2.6.4c	v2.6.2 less the AR.6210 patch, plus EEPROM default timelines and Metop C identifier	New Release	Yes	Evolution of v2.6.2	C

Table 6-2 GOME-2 Software Versioning

6.3.1 Timelines and Onboard Tables

Table 6-3 shows the current status of Software and on-board tables. Note that in future releases, one or more pseudo tables will be defined to cover all DSMs that are not highly dynamic. This will include all DSMs requiring Standby-Idle transition for an update, plus DSMs that are not regularly updated by timelines.

<i>Component</i>	<i>Status</i>	<i>Comments</i>
CDHU ICU SW	Version 2.6.4b	AR.6210 Ghost EQSQL Patch not required due to HW
CDHU SCI SW	Version 2.6.4b	None.
SU SW	Version x.x	None.
GTL	Nominal	GOME_LTL_00_M01_CAL0xxxx02 GOME_LTL_01_M01_CAL4xxxx02 GOME_LTL_02_M01_CAL5xxxx02 GOME_LTL_03_M01_PMDRAWxx02 GOME_LTL_04_M01_CAL6xxxx02 GOME_LTL_05_M01_NOT1920x02 GOME_LTL_10_M01_NADIRxxx02 GOME_LTL_12_M01_MOON1xxx03 GOME_LTL_13_M01_MOON2xxx05 GOME_LTL_14_M01_MOON3xxx04
GTL SEQ	Nominal	V4.0
GTT	Empty	Not Used
Monitoring Parameters	Nominal	MDB_IGO1STM_DEFAULT.dts v1.9 MDB_IGO1RFD_DEFAULT.dts v1.1 MDB_IGO1XAS_DEFAULT.dts v1.1 MDB_IGO1XMN_DEFAULT.dts v1.1
PMD Bands	Nominal	MDB_IGO8PMD_DEFAULT.dts v1.4

Table 6-3: Onboard Tables Configuration

6.4 Operational Documentation Status

The GOME-2 IOM has been updated to v.7 including updates in accordance with APR-AI004 (PROM patching precautions) and APR-AI006 (Shutter powered by the ICU bus).

7 CONCLUSION

Currently, all indicators of GOME health and performance are excellent, with the exception of problems relating to throughput, which is decreasing in a comparable manner to aboard Metop-A. The degradations observed for both the HCL and QTH lamps are just normal signs of aging and do not cause concern within the timeframe until the end of 2024.

The Scan Unit torque appears to be stable, and there is no reason to believe that this will be a limiting factor before the end of the baseline assumption mission duration of 12 years. In the meantime ESA tribology experts will study the bearing design, use of the scan mirror and torque telemetry to determine possible mechanisms for the worsening trend on Metop-A, the projected evolution on Metop-B and recommend any mitigating action which could be taken.

APPENDIX A MAPPING OF PHYSICAL SIGNATURES, INSTRUMENT COMPONENTS AND TM PARAMETERS

		<i>GOM01</i>	<i>GOM02</i>	<i>GOM03</i>	<i>GOM04</i>	<i>GOM05</i>	<i>GOM06</i>
Test Title		HKTLM Stability	SU Bearings Monitoring	HCL, QTH Lamp Monitoring	Spectral Stability	Detector response stability	Throughput
Description		Monitor Stability of HKTLM and Type 14 entries to determine health of Instrument	For each 171 Hz 1920 km swath torque profile, plot the average difference between all points on reference profile, separating for "turn arounds" and the main part of the cycle. Repeat for Mirror position.	Plot current and voltage profiles during operation and ensure they fit within envelope. For HCL Lamp monitor for Low Voltage Mode and Ignition Time in particular. SMR v WLS monitoring may indicate differential loss of throughput which could indicate lamp blackening.	SLS measurements are primarily used for pixel to wavelength mapping and also to monitor the spectral stability of the instrument which is important for the maintenance of product quality. The strength of the measured SLS lines is also an important result that must be used in the throughput monitoring. When the intensity of individual lines falls below specified thresholds they are no longer deemed reliable for use in spectral calibration. SLS measurements are made daily and the positions of spectral lines on the detectors are monitored.	LEDs can be used to monitor Pixel to Pixel gain which is used to correct for the pixel to pixel variation of quantum efficiency of the detectors, as well as for identification of hot or dead pixels. Pixel to Pixel gain is measured by using the LEDs mounted directly in front of each detector. LEDs illuminate the detectors uniformly with green light (ca 550 nm). By comparing the LED measurements with an LED spectrum smoothed over ~5 pixels, an estimate of the pixel-to-pixel gain can be made. By monitoring changes in pixel-to-pixel gain changes in the relative behaviour of the quantum efficiency of the detectors can be observed. This is a result must be fed back into other throughput monitoring so that relative changes in pixel performance do not appear as pixel dependent signatures.	By assessing various Instrument throughputs and comparing in various combinations, it is possible to identify individual components as a source of throughput loss.
Component	Subcomponent						
SU	Bearings	0x11 0x12 0x13 0x14 0x15 0x16 0x64 0xB1, sub 0x7	SU Mode SU Torque (all samples) SU Torque Shift (all samples) SU Position (all samples) Torque Profile Position Profile				
SU	Scan Mirror						Scan Mirror Contamination
CU	HCL	0x70, sub 0xC		HCL Status HCL Voltage HCL Current HCL Ignition Time HCL Low Voltage Mode			HCL Lamp Degradation
CU	QTH	0x70, sub 0xD		Lamp Blackening			QTH Lamp Degradation
CU	SHUTTER	0x70, sub 0xB 0x71					
CU	DIFFUSER						Diffuser Contamination
PMD	COOLERS	0x70, sub 0x0, 0x1 PMD temperatures					
PMD	DETECTORS	0xB1, sub 0x4, 0x5 0xB2, sub 0x4, 0x5 0xB3, sub 0x4, 0x5 PMD temperatures				hot or dead pixels	Detector Contamination
FPA	COOLERS	0x70, sub 0x7, 0x8, 0x9, 0xA, 0x6 0xB1, sub 0x8, 0x9, 0xA, 0xB FPA temperatures Peltier Output V OB temp					

		<i>GOM01</i>	<i>GOM02</i>	<i>GOM03</i>	<i>GOM04</i>	<i>GOM05</i>	<i>GOM06</i>
	Test Title	HKTLM Stability	SU Bearings Monitoring	HCL, QTH Lamp Monitoring	Spectral Stability	Detector response stability	Throughput
	Description	Monitor Stability of HKTLM and Type 14 entries to determine health of Instrument	For each 171 Hz 1920 km swath torque profile, plot the average difference between all points on reference profile, separating for "turn arounds" and the main part of the cycle. Repeat for Mirror position.	Plot current and voltage profiles during operation and ensure they fit within envelope. For HCL Lamp monitor for Low Voltage Mode and Ignition Time in particular. SMR v WLS monitoring may indicate differential loss of throughput which could indicate lamp blackening.	SLS measurements are primarily used for pixel to wavelength mapping and also to monitor the spectral stability of the instrument which is important for the maintenance of product quality. The strength of the measured SLS lines is also an important result that must be used in the throughput monitoring. When the intensity of individual lines falls below specified thresholds they are no longer deemed reliable for use in spectral calibration. SLS measurements are made daily and the positions of spectral lines on the detectors are monitored.	LEDs can be used to monitor Pixel to Pixel gain which is used to correct for the pixel to pixel variation of quantum efficiency of the detectors, as well as for identification of hot or dead pixels. Pixel to Pixel gain is measured by using the LEDs mounted directly in front of each detector. LEDs illuminate the detectors uniformly with green light (ca 550 nm). By comparing the LED measurements with an LED spectrum smoothed over ~5 pixels, an estimate of the pixel-to-pixel gain can be made. By monitoring changes in pixel-to-pixel gain changes in the relative behaviour of the quantum efficiency of the detectors can be observed. This is a result must be fed back into other throughput monitoring so that relative changes in pixel performance do not appear as pixel dependent signatures.	By assessing various Instrument throughputs and comparing in various combinations, it is possible to identify individual components as a source of throughput loss.
FPA	DETECTORS	0x70, sub 0x2, 0x3, 0x4, 0x5 0xB1, sub 0x0, 0x1, 0x2, 0x3 0xB2, sub 0x0, 0x1, 0x2, 0x3 0xB3, sub 0x0, 0x1, 0x2, 0x3 FPA Temps				hot or dead pixels	Detector Contamination
SPEC	TELESCOPE						Telescope contamination
SPEC	PRISMS						
SPEC	MIRRORS						
SPEC	GRATINGS						
SPEC	FOCUSSING OBJECTIVES						
CDHS	CDHU	0x20, 0x21, 0x31, 0x44, 0x45, 0x4F, 0x51, 0x52, 0x55, 0x56, 0x65, 0x66, 0x77, 0x78, 0xB1 sub 0x6, 0xB9, 0xBB, 0xBE CDHU Power V EQ status					
CDHS	GPDU	0x70, sub 0x14 GPDU Power V EQ status					
OB							